U.S. DEPARTMENT OF COMMERCE
National Technical Information Service

PB-281 320

Evaluation of Four Novel Fine Particulate Collection Devices

Air Pollution Technology, Inc, San Diego, Calif

Prepared for

Industrial Environmental Research Lab, Research Triangle Park, N C

Mar 78

PB 281 320

EPA-600/2-78-062
March 1978

Environmental Protection Technology Series

EVALUATION OF FOUR NOVEL FINE PARTICULATE COLLECTION DEVICES

REPRODUCED BY
NATIONAL TECHNICAL
INFORMATION SERVICE
U. S. DEPARTMENT OF COMMERCE
SPRINGFIELD, VA. 22161

RESEARCH REPORTING SERIES

Research reports of the Office of Research and Development, U.S. Environmental Protection Agency, have been grouped into nine series. These nine broad categories were established to facilitate further development and application of environmental technology. Elimination of traditional grouping was consciously planned to foster technology transfer and a maximum interface in related fields. The nine series are:

1. Environmental Health Effects Research
2. Environmental Protection Technology
3. Ecological Research
4. Environmental Monitoring
5. Socioeconomic Environmental Studies
6. Scientific and Technical Assessment Reports (STAR)
7. Interagency Energy-Environment Research and Development
8. "Special" Reports
9. Miscellaneous Reports

This report has been assigned to the ENVIRONMENTAL PROTECTION TECHNOLOGY series. This series describes research performed to develop and demonstrate instrumentation, equipment, and methodology to repair or prevent environmental degradation from point and non-point sources of pollution. This work provides the new or improved technology required for the control and treatment of pollution sources to meet environmental quality standards.

EPA REVIEW NOTICE

This report has been reviewed by the U.S. Environmental Protection Agency, and approved for publication. Approval does not signify that the contents necessarily reflect the views and policy of the Agency, nor does mention of trade names or commercial products constitute endorsement or recommendation for use.

This document is available to the public through the National Technical Information Service, Springfield, Virginia 22161.

TECHNICAL REPORT DATA
(Please read Instructions on the reverse before completing)

1. REPORT NO. EPA-600/2-78-062	2.
3. RECIPIENT'S ACCESSION NO. PB281320	
4. TITLE AND SUBTITLE Evaluation of Four Novel Fine Particulate Collection Devices	5. REPORT DATE March 1978 6. PERFORMING ORGANIZATION CODE
7. AUTHOR(S) S. Calvert, S.C. Yung, H. Barbarika, and R.G. Patterson	8. PERFORMING ORGANIZATION REPORT NO.
9. PERFORMING ORGANIZATION NAME AND ADDRESS Air Pollution Technology, Inc. 4901 Morena Boulevard, Suite 402 San Diego, California 92117	10. PROGRAM ELEMENT NO. 1AB012; ROAP 21ADL-004 11. CONTRACT/GRANT NO. 68-02-1496
12. SPONSORING AGENCY NAME AND ADDRESS EPA, Office of Research and Development Industrial Environmental Research Laboratory Research Triangle Park, NC 27711	13. TYPE OF REPORT AND PERIOD COVERED Final; 7/74-12/77 14. SPONSORING AGENCY CODE EPA/600/13

15. SUPPLEMENTARY NOTES IERL-RTP project officer is Dale L. Harmon, Mail Drop 61, 919/541-2925.

16. ABSTRACT The report gives results of an experimental performance evaluation of four novel fine particulate control devices: the Johns-Manville Cleanable High-Efficiency Air Filtration (CHEAF) System, the APS Electrostatic Scrubber, the APS Electrotube, and the TRW Charged Droplet Scrubber. The evaluations included measurement of inlet and outlet particle size distribution and concentration with cascade impactor and diffusion battery. Fine particle collection efficiencies were computed from the data, as functions of particle size. Mathematical performance models were developed for the CHEAF system and the APS scrubber. The models gave satisfactory predictions.

17. KEY WORDS AND DOCUMENT ANALYSIS

a. DESCRIPTORS	b. IDENTIFIERS/OPEN ENDED TERMS	c. COSATI Field/Group
Air Pollution	Air Pollution Control	13B
Dust Collectors	Stationary Sources	13A
Evaluation	Particulate	
Measurement		14B
Particle Size Distribution		
Mathematical Models		12A

18. DISTRIBUTION STATEMENT Unlimited	19. SECURITY CLASS (*This Report*) Unclassified	21. NO. OF PAGES 121
	20. SECURITY CLASS (*This page*) Unclassified	22. PRICE A06 - A01

EPA Form 2220-1 (9-73)

EPA-600/2-78-062
March 1978

EVALUATION OF FOUR NOVEL FINE PARTICULATE COLLECTION DEVICES

by

S. Calvert, S. C. Yung, H. Barbarika,
and R. G. Patterson

Air Pollution Technology, Inc.
4901 Morena Boulevard, Suite 402
San Diego, California 92117

Contract No. 68-02-1496
ROAP 21ADL-004
Program Element No. 1AB012

EPA Project Officer: Dale L. Harmon

Industrial Environmental Research Laboratory
Office of Energy, Minerals and Industry
Research Triangle Park, N.C. 27711

Prepared for

U.S. ENVIRONMENTAL PROTECTION AGENCY
Office of Research and Development
Washington, D.C. 20460

ABSTRACT

Experimental performance evaluations were conducted on four novel fine particulate control devices. They were the Johns-Manville Cleanable High Efficiency Air Filtration System (CHEAF), the APS Electrostatic Scrubber, the APS Electrotube, and the TRW Charged Droplet Scrubber.

The performance evaluations included the measurements of inlet and outlet particle size distribution and concentration with cascade impactor and diffusion battery. Fine particle collection efficiencies as functions of particle size were computed from the data. Mathematical performance models were developed for the CHEAF and the Electrostatic Scrubber. The models gave satisfactory predictions.

An experiment was carried out in the laboratory to determine the effects of charged particles on cascade impactor data. Results indicated that using the value of impaction parameter determined for uncharged particles will cause overestimation of the size of the charged particles collected.

Preceding page blank

CONTENTS

Abstract iii

Figures v

Tables viii

Abbreviations and Symbols x

Acknowledgement xiv

Sections

1. Introduction 1

2. Summary, Conclusions and Recommendations 2

3. CHEAF 6

4. APS Electrostatic Scrubber 20

5. APS Electro-Tube 37

6. TRW Charged Droplet Scrubber 47

7. Performance Test Method 59

8. Data Reduction and Computation 69

9. Effects of Charged Particles on the Experimental Performance of Electrostatic Devices 87

References 92

Appendix 94

FIGURES

No.		Page
1	Schematic of CHEAF Unit	7
2	Inlet size distributions	10
3	Inlet and outlet size distribution	10
4	Run 18 wet and dry size distributions	11
5	Run 19 wet and dry size distributions	11
6	Penetration versus dry particle diameter for run 10	13
7	Penetration versus dry particle diameter for run 11	13
8	Penetration versus dry particle diameter for run 12	14
9	Experimental grade penetration curve for CHEAF	16
10	Cut diameter versus pressure drop for fibrous bed	18
11	APS Electrostatic Scrubber	21
12	Penetration versus particle diameter for data set A	27
13	Penetration versus particle diameter for data set B	27
14	Penetration versus particle diamter for data set C	28
15	Penetration versus particle diameter for data set A, B, & C	28
16	Penetration versus particle diameter using both diffusion battery and cascade impactor, run 27 (set C, ionizer off)	29
17	Penetration versus particle diameter using both diffusion battery and cascade impactor, run 28 (set C, ionizer off)	29
18	Penetration versus particle diameter using both diffusion battery anc cascade impactor, run 29 (set C, ionizer on)	30

FIGURES (continued)

No.		Page
19	Penetration versus particle diameter suing both diffusion battery and cascade impactor, run 30 (set C, ionizer on)	30
20	Efficiency of single drop versus inertial parameter N_{Red} = 9.6 with N_{FD} as parameter	32
21	Efficiency of a single drop, η, versus N_{FD} with K_p as a parameter (N_{Red} = 9.6)	35
22	Experimental and predicted particle penetration versus particle diameter	36
23	Diagram of APS Electro-Tube	38
24	Penetration versus aerodynamic particle diameter for low gas flow, runs 15, 16, 19	45
25	Penetration versus aerodynamic particle diameter for medium gas flow, runs 7, 10, 12, 13, 14	45
26	Penetration versus aerodynamic particle diameter for high gas flow, runs 3, 4, 5, 18	46
27	TRW Charged Droplet Scrubber schematic	48
28	Particle penetration versus aerodynamic diameter for low electrode voltage and low gas flow rate . .	56
29	Particle penetration versus aerodynamic diameter for high electrode voltage and high gas flow rate .	56
30	Particle penetration versus aerodynamic diameter for high electrode voltage and low gas flow rate. .	57
31	Particle penetration versus aerodynamic diameter for low electrode voltage and high gas flow rate. .	57
32	Modified EPA sampling train with in-stack cascade impactor	62
33	Schematic diagram of diffusion battery system . . .	64
34	Particle diameter versus particle aerodynamic diameter	71
35	Overall penetration fraction versus "d_{pc}/d_{pN}" with "σ_g" as a parameter.	81

FIGURES (continued)

No.		Page
36	Particle penetration through SDB at Q= 4.7 ℓpm . .	82
37	A.P.T. cut/power plot.	84
38	Overall penetration versus cut to mass mean particle ratio for log-normally distributed particles. (Calvert et al. (1972)	86
39	Impaction characteristics with glass fiber filter (0.5 μm PSL).	88
40	Size distribution of particles exiting ESP when $d_{pg_{IN}}$ = 10 μmA, σ_g = 4.0	90
41	Fractional collection efficiencies for a full-scale precipitator on a coal-fired power boiler. (Gooch et al. (1975))	91
A-1	Inlet and outlet size distribution for run 1 . . .	99
A-2	Inlet and outlet size distribution for run 4 . . .	99
A-3	Inlet and outlet size distribution for run 6 . . .	100
A-4	Inlet and outlet size distribution for run 8 . . .	100
A-5	Inlet and outlet size distribution for run 9 . . .	101
A-6	Inlet and outlet size distribution for run 10. . .	101
A-7	Inlet and outlet size distribution for run 13. . .	102
A-8	Inlet and outlet size distribution for run 14. . .	102
A-9	Inlet and outlet size distribution for run 15. . .	103
A-10	Inlet and outlet size distribution for run 16. . .	103
A-11	Inlet and outlet size distribution for run 17. . .	104
A-12	Inlet and outlet size distribution for run 18. . .	104
A-13	Inlet and outlet size distribution for run 19. . .	105
A-14	Diffusion battery data for inlet run 1 & 4	105

TABLES

No.		Page
1	Data Set A. Runs 1-10	25
2	Data Sets B, C, and D, Runs 11-31	25
3	Inlet and Outlet Size Distribution Summary	26
4	Test Run Summary	26
5	Operating Conditions	40
6	Size Distribution, Mass Loading, and Overall Penetration Data	42
7	Total Filter Particle Loading Tests	42
8	Number Basis Size distribution Data for Diffusion Battery Tests	43
9	Operating Conditions	50
10	Test Run Summary	51
11	Cross-Reference to TRW Test Matrix	52
12	Inlet and Outlet Size Distribution Summary	54
A-1	Inlet and Outlet Sample Particle Data for Run 1	95
A-2	Inlet and Outlet Sample Particle Data for Run 4	95
A-3	Inlet and Outlet Sample Particle Data for Run 6	95
A-4	Inlet and Outlet Sample Particle Data for Run 8	95
A-5	Inlet and Outlet Sample Particle Data for Run 9	96
A-6	Inlet and Outlet Sample Particle Data for Run 10	96
A-7	Inlet and Outlet Sample Particle Data for Run 13	96
A-8	Inlet and Outlet Sample Particle Data for Run 14	96
A-9	Inlet and Outlet Sample Particle Data for Run 15	97
A-10	Inlet and Outlet Sample Particle Data for Run 16	97
A-11	Inlet and Outlet Sample Particle Data for Run 17	97

TABLES (continued)

No.		Page
A-12	Inlet and Outlet Sample Particle Data for Run 18. .	97
A-13	Inlet and Outlet Sample Particle Data for Run 19. .	98

LIST OF ABBREVIATIONS AND SYMBOLS

Latin

a_n - Constants, dimensionless

A - Constant

b - Weibull slope

B - Constant

C' - Cunningham correction factor, dimensionless

C_D - Drag coefficient, dimensionless

CDF - Cumulative distribution function, dimensionless

$$= 1 - \exp\left[-\left(\frac{d_p - d_{po}}{\theta - d_{po}}\right)\right]^b$$

C_p - Mass of particles, g

C_{pt} - Total mass of particles, g

C_T - Total mass concentration or loading, g/cm^3

$\overline{d}$ - Symbol for differentiation

d_c - Wire diameter, cm

$\frac{\overline{d}\, C_p}{\overline{d}(d_p)}$ - Slope of the cumulative mass versus particle diameter curve at d_p, dimensionless

d_d - Drop diameter, cm

d_f - Fiber diameter, cm

d_j - Jet diameter, cm

d_p - Actual particle diameter, cm or μm

d_{pa} - Aerodynamic particle diameter, μmA

d_{pac} - Aerodynamic cut diameter, μmA

d_{pc} - Cut diameter, μm

d_{pg} - Mass median diameter, μmA

d_{pi} - Specific particle size, μm

d_{pN} - Number median particle diameter, μm

d_{po} - Minimum particle diameter, μm

E - Field strength, kV/cm

E_o - Charging electric field strength, kV/cm

f - An empirical constant, dimensionless

f_a - Initial value of f ≃ 0.5, dimensionless

K_p - Impaction parameter, dimensionless

ℓ - Fiber pad thickness, cm

m_p - Mass of particles in the infinitesimal size range $(\bar{d}_p + \bar{d}\, d_p)$, g

M_{pi} - Cumulative mass concentration of particles smaller than d_{pi}, g/cm^3

N - Total number of particles, dimensionless

n - number of particles, dimensionless

N_{FD} - Flux deposition number =

$$\frac{u_F}{u_o}, \text{ dimensionless}$$

N_p - Cumulative number concentration of particles smaller than d_p, $no./cm^3$

N_{pt} - Total number concentration of particles, $no./cm^3$

$Pt(d_p)$ - Penetration as a function of particle size, fraction

$\overline{Pt}$ - Overall particle penetration, fraction

Pt_i - Particle penetration for particle size "i", fraction

$P(x) = \frac{W}{W_t}$ = Cumulative mass fraction of sizes smaller than "d_{pa}"

Q_G - Volumetric flow rate of gas, m^3/min

Q_L - Volumetric flow rate of liquid, m^3/min

Q_p - Electrical charge carried by the particle, coulomb

S - Solidity, dimensionless

u_F - Particle drift velocity, cm/s

u_G - Superficial gas velocity, cm/s

u_{Gt} - Venturi throat gas velocity, cm/s

u_j - Jet velocity, cm/s

u_o - Fluid velocity passing the drop, cm/s

W - Mass concentration, g/cm^3

W_{cum} - Cumulative mass concentration, g/cm^3

W_t - Total mass concentration, g/cm^3

$x = \frac{\ln d_{pa} - \ln d_{pg}}{\ln \sigma_g}$

$z = \frac{\ln d_p - \ln d_{pn}}{2 \ln \sigma_g}$

Greek

ε - Porosity, dimensionless

ε_o - 8.86×10^{-14} coulomb cm/cm^2 - Volt

ε_p - Dielectric constant of the particle

η = Single fiber efficiency or single drop collection efficiency, fraction

ℓ - Fiber length, cm

μ_G - Gas viscosity, poise

ρ_G - Gas density, gm/cm^3

ρ_L - Liquid density, g/cm^3

ρ_p - Particle density, gm/cm^3

σ_g - Standard deviation, dimensionless

θ - Characteristic diameter, μm

ΔP - Pressure drop cm W.C.

Abbreviations

ACFM - Actual cubic feet per minute

CDF - Cumulative distribution function

CFM - Cubic feet per minute

GPM - Gallons per minute

SDB - Screen diffusion battery

W.C. - Water column

ACKNOWLEDGEMENT

A.P.T., Inc. wishes to express its appreciation for excellent technical coordination and for very helpful assistance in support of our technical effort to Mr. Dale L. Harmon, EPA Project Officer.

SECTION 1

INTRODUCTION

Air Pollution Technology, Inc. (A.P.T.), in accordance with EPA Contract 68-02-1496, Experimental Tests of Novel Fine Particulate Control Devices, conducted performance evaluations of four novel fine particulate control devices. They were the Johns-Manville Cleanable High Efficiency Air Filtration system (CHEAF), the Air Pollution Systems Electrostatic Scrubber and Electro-Tube, and the TRW Charged Droplet Scrubber.

The performance evaluations included inlet and outlet particle sampling measurements with cascade impactors and the A.P.T. Screen Diffusion Battery. Mathematical performance models were developed for the CHEAF and the Electrostatic Scrubber. The results of the performance evaluations are presented in the text.

The effects of charged particles on cascade impactor data were established as part of this contract because several of the performance evaluations involved sampling charged particles. The charged particle experiments will be covered in detail in a separate report.

SECTION 2

SUMMARY, CONCLUSIONS, AND RECOMMENDATIONS

Field measurements on four control devices were carried out to determine the collection efficiency as a function of particle diameter. A summary of the performance tests is given in the tabulation below.

Control Device	Source	Pressure Drop cm W.C.	Performance Cut Dia. μmA
CHEAF (Johns-Manville)	Diatomaceous earth calciner and dryer	48-53	0.8
Electrostatic Scrubber (A.P.S.)	TiO_2 test aerosol	40	0.35
Electrotube (A.P.S.)	TiO_2 test aerosol	3	<0.1
Charged Droplet (T.R.W.)	Coke oven	10	0.35

Mathematical models were developed for the CHEAF and for the electrostatic scrubber. The models give reasonable performance predictions. The electro-tube is similar to a wetted wall electrostatic precipitator, for which a model is available in the literature. TRW has developed a model for their own scrubber.

CONCLUSIONS

The program achieved the principal objective of obtaining reliable performance data for four novel devices. Based on the data obtained, the following conclusions can be drawn.

1. The CHEAF appears to be a reasonably efficient device for fine particulate control of saturated emissions from a diatomaceous earth calcining and drying process. Particle growth occurring in the pre-cleaner prior to the CHEAF is beneficial to the fine particle collection efficiency of the system.

The CHEAF, with an approximate actual (wet) cut diameter of 0.8 μmA and a pressure drop of 50 centimeters W.C., is comparable to a venturi with a pressure drop of 20 centimeters W.C.

2. Experimental test results for a TiO_2 test aerosol, which has a dispersed mass median diameter of approximately 1.0 μmA and a standard deviation of 2.2, for the Air Pollution Systems electrostatic scrubber show overall collection efficiencies ranging from 86% to 97% (average 92%) with the ionizer on for a pressure drop across the system of 43 cm W.C. With the ionizer off, the electrostatic scrubber becomes a conventional venturi with efficiencies from 66% to 90% (avg 82%), 45cmW.C.

Using the experimental data and the average overall penetrations, effective cut diameters (i.e., the cut diameter for a conventional high energy scrubber with the same overall penetration) for the scrubber with the ionizer on and off were determined. The effective cut diameter computed for the ionizer on ranged from 0.23 to 0.54 μmA and from 0.42 to 0.66 μmA for the ionizer off.

3. Experimental tests of the A.P.S. Electro-Tube were done with TiO_2 aerosol which had a mass median aerodynamic diameter of 1.2 μmA and a standard deviation of 2.2. Overall collection efficiencies ranged from 96.9% for high gas flow rates (22.9 Am^3/min) to 99.3% for low gas flow rates (16.9 Am^3/min).

Experimentally determined penetrations of 0.5 μmA aerodynamic diameter particles were 8.6%, 3.7%, and 1.1% for high, medium, and low gas flow rates, respectively. For 1.0 μmA aerodynamic diameter particles the penetrations were 4.3%, 2.3%, and 0.68% for high, medium, and low gas flow rates, respectively. For 2.0 μmA aerodynamic diameter particles

the penetrations were 0.22%, 0.39%, and 0.38% for high, medium, and low gas flow rates, respectively.

The Electro-Tube performance was found to be similar to that which can be achieved in small wet electrostatic precipitators with the same ratio of plate area to volumetric flow rate.

4. Experimental test results on the TRW Charged Droplet Scrubber showed overall collection efficiencies of 94.1% for low gas velocity and low electrode voltage, 88.2% for high gas velocity and high electrode voltage, 88.3% for high gas velocity and low electrode voltage, and 94.9% for low gas velocity and high electrode voltage.

The TRW Charged Droplet Scrubber was compared to a conventional venturi type scrubber operating at the same overall efficiency for the same inlet particle dust mean diameter (d_{pg}) and standard deviation (σ_g). The power consumption for the TRW Charged Droplet Scrubber was between 17.0 and 25.9 W/(m^3/min) for the electrical section and 33.3 W/(m^3/min) for the fan power based on a fan and motor efficiency of 50% and a system pressure drop of 10.1 cm W.C. The power consumption for a conventional venturi type scrubber at the same overall efficiency as the TRW system was between 354 and 714 W(m^3/min) for a 50% fan and motor efficiency. Therefore, based on power consumption the TRW Charged Droplet Scrubber has an advantage over a conventional venturi type scrubber.

Based on 8,000 hours operation per year and a cost of 3¢/kWH the TRW Charged Droplet Scrubber operating cost savings for a 2,830 m^3/min (100,000 CFM) unit would be between $203,000/yr and $435,000/yr.

5. The section on "Effects of Charged Particles on Experimental Performance of Electrostatic Control Devices" shows that using cascade impactors to measure the size distribution of charged particles may lead to overestimating the particle size distribution. This leads to an underestimation of the collection efficiency for particles greater than several microns in diameter and an overestimation of the collection efficiency of

submicron particles.

Three of the devices tested, the APS Electrostatic Scrubber and Electro-Tube and the TRW Charged Droplet Scrubber, had charged particles at the exit. Therefore, the performance data obtained are expected to differ somewhat from those based on theoretical cascade impactor performance.

RECOMMENDATIONS

The primary goal of this work was to make performance evaluations of several novel devices for controlling fine particulate emissions.

Several of the novel devices tested showed a savings in power consumption for a given level of control. The capital costs for the equipment is not well documented at this time since the devices tested were either in the laboratory or pilot plant stage. The choice of a control device for removing fine particulates depends on the following:

1. Size distribution and chemical composition of the particulate.
2. Gas flow rate, temperature, and composition.
3. Annualized cost of the control equipment which meets the performance requirement.

The performance characteristics of the control devices reported here are only for one type of particulate in a laboratory or pilot plant system. The fourth scrubber was used on a process where solution-induced condensation could augment its efficiency. Therefore the information contained in this report can only be used as a guide in considering any of these devices. It is recommended that more information pertinent to the case at hand be obtained and perhaps a pilot scale test be run before final selection of any of these novel devices for removing submicron particulates from stack gases.

SECTION 3

CHEAF

SOURCE AND SCRUBBER

The CHEAF (Cleanable High Efficiency Air Filter) is primarily a wetted fibrous bed system. It consists of water sprays to wet and clean the filter medium, a rotary drum containing a fibrous "sponge" filter medium and a water bath reservoir for cleaning the rotary filter. Particle collection is accomplished by filtration mechanisms in the rotary filter.

The CHEAF unit tested is installed on a diatomaceous earth calciner and dryer. Figure 1 is a schematic drawing of this system. Prior to the CHEAF, there is a cyclonic pre-cleaner with water sprays for removing large particles in the inlet stream. Emissions enter the pre-cleaner, saturated at a temperature of approximately 75°C, where they are acted upon by water sprays and centrifugal forces which collect the large particles in the stream. The gas exiting the pre-cleaner, saturated at 63°C, then enters the CHEAF. Water sprays again contact the gas as it is drawn through the rotating filter drum where the final cleansing action takes place.

The gas then leaves through the end of the drum while the particles are washed from the filter media as the drum rotates into the water bath reservoir. With the help of two blowers, the gas is forced up the stack and flows into the atmosphere as a saturated plume at approximately 60°C. The particle laden water in the reservoir is periodically drained into the plant's main water purification system and then refilled.

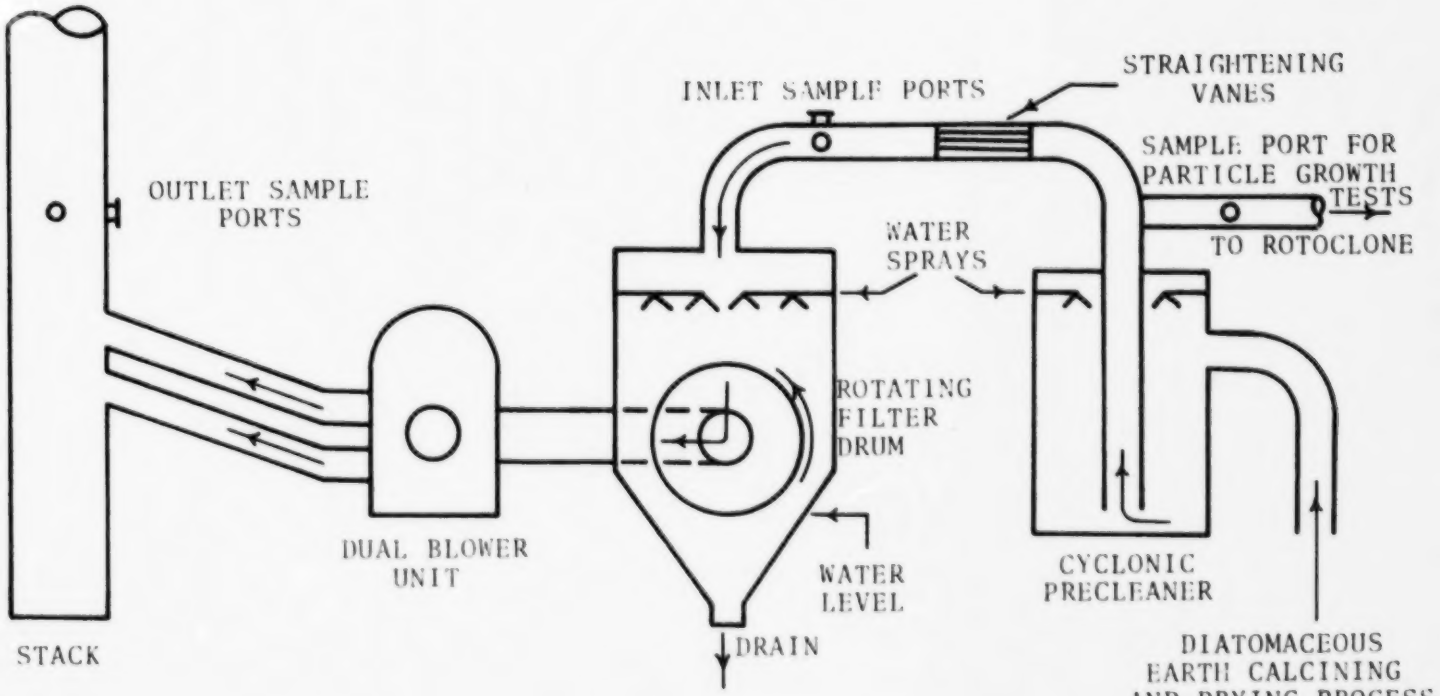

Figure 1. Schematic of CHEAF unit.

TEST METHOD

The performance characteristic of the CHEAF was determined by measuring the particle size distribution and mass loading of the inlet and outlet gas sample simultaneously.

The performance tests consisted of two test series and are reported in greater detail by Calvert et al. (1975). The first series were performed in November 1974. Investigation of particle growth in the cyclonic pre-cleaner was the objective of the second test series during March 1975.

OPERATING CONDITIONS

The CHEAF operating conditions during the first test period were as follow:

1. Gas flow rates and related parameters as shown in tabulation below:

DUCT	INLET	OUTLET
Temperature	63°C	60°C
Velocity	12.2 m/s	5.8 m/s
Am^3/min	710	Same as inlet
ACFM	25,000	Same as inlet
DN m^3/min @ 0°C	480	Same as inlet
DCFM @ 70°F	18,300	Same as inlet
Vol. $\%H_2O$ vapor	17	17
Pressure	-7.6 cm W.C.	0.2 cm W.C.

2. Water flow rate to the CHEAF system was reported as approximately 0.053 m^3/min (14 GPM).

3. Pressure drop through the CHEAF system was approximately 48-53 cm W.C. (19-21 in. W.C.) during the test period.

4. The L/G ratio during the test period was approximately 0.11 ℓ/m^3.

DATA

Particle Data

A total of 14 simultaneous inlet and outlet sampling runs were conducted during the first series of tests on the CHEAF

system. One-point sampling was employed for all runs except Runs 13 and 14, which were EPA Method 5 tests.

The data were grouped into four data sets. The first two data sets (runs 4 and 5 and runs 6, 7, and 8) were obtained at identical one-point sampling locations and identical plant conditions. The third set of data points (runs 9 through 12) was obtained at the previous sample locations but the plant was switched from an oil-fired to a gas-fired drying process. Finally, the fourth data set was obtained from two EPA Method 5 tests (runs 13 and 14). These data sets are presented in detail by Calvert et al. (1975).

As seen in Figures 2 and 3 the following aerodynamic mass median diameters and standard deviations were found:

RUN NO.	INLET		OUTLET	
	d_{pg}, μmA	σ_g	d_{pg}, μmA	σ_g
6, 7, 8	0.82	4.2	--	--
9, 10, 11, 12	0.82	3.9	0.82	3.9

Particle Growth

Size distributions for particle growth, runs 18 and 19, are given in Figures 4 and 5 , in which the particle size (wet or dry) is plotted against the cumulative mass percentage of dry solids. The amount of particle growth is then related to the difference between the two curves at each mass percent solids. These figures show that the small particles grow proportionately more than the large ones, as would be the case if the particles acted as condensation nuclei with a small fraction of soluble material in a super-saturated gas. The aerodynamic mass median diameter of the dry particle size is almost doubled after particle growth occurs. Aerodynamic mass median diameters and standard deviations for runs 18 and 19 are given below:

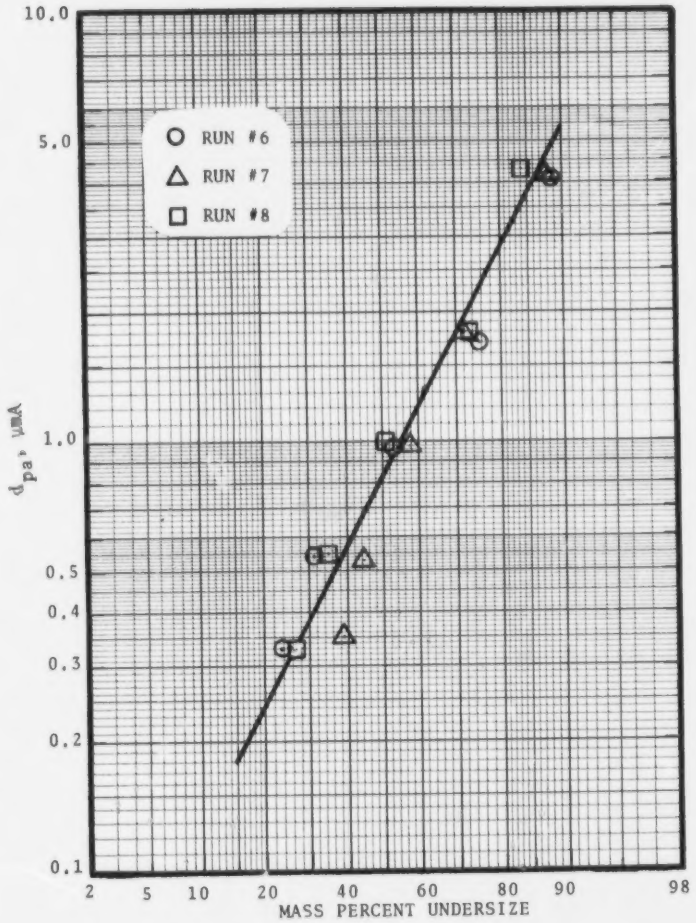

Figure 2. Inlet size distributions.

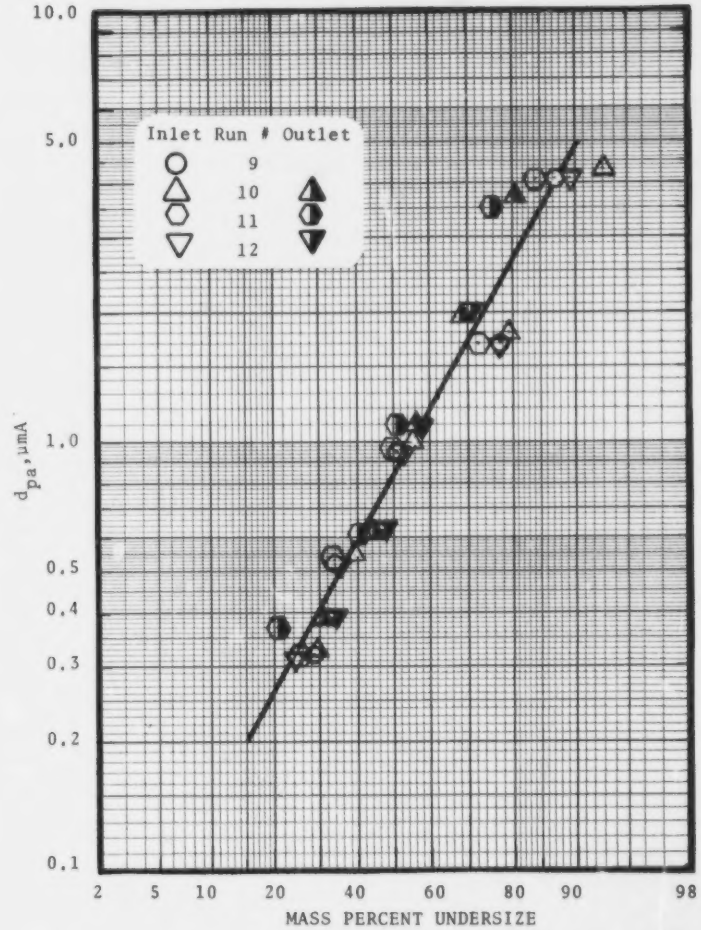

Figure 3. Inlet and outlet size distributions.

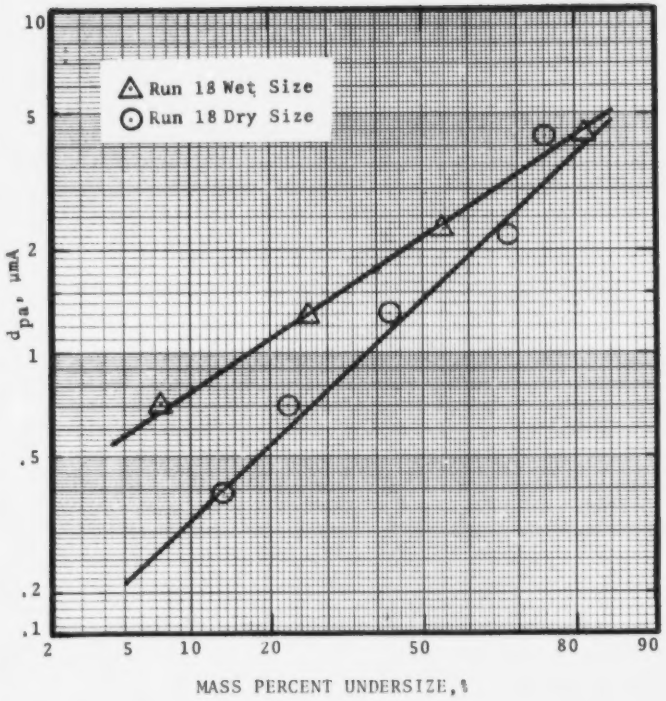

Figure 4. Run 18 wet and dry size distributions.

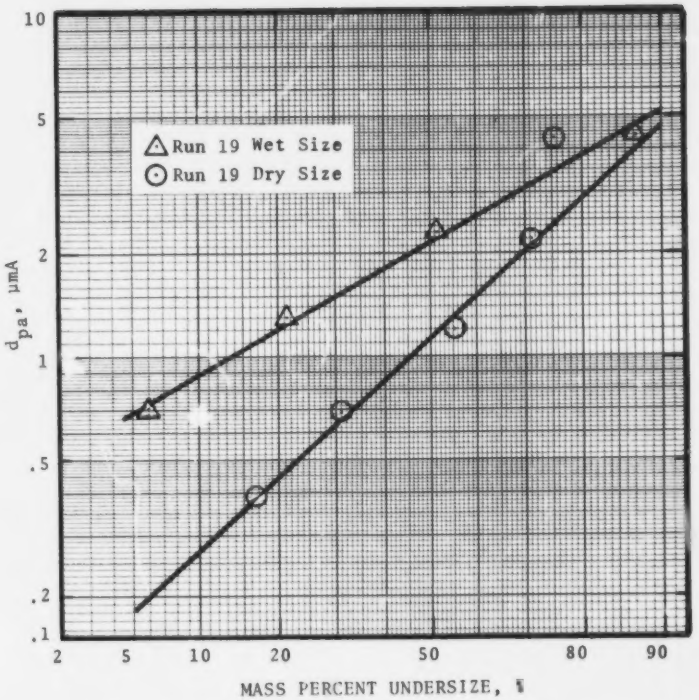

Figure 5. Run 19 wet and dry size distributions.

RUN NO.	DRY PARTICLE SIZE		WET PARTICLE SIZE	
	d_{pg}, μmA	σ_g	d_{pg}, μmA	σ_g
18	1.4	3.2	2.2	2.3
19	1.1	3.1	2.1	2.0

Opacity

Plume opacity of the CHEAF system averaged 10% during the test period. The visual observation method was used for all opacity measurements which were taken by a Johns-Manville employee who was a certified observer trained in a California Air Resources Board "Smoke School". According to the observer, visible measurements were taken on a hill above the stack approximately fifteen meters away. A detached plume enabled the observer to read opacity at the stack.

PARTICLE PENETRATION

Particle penetration versus particle aerodynamic diameter was calculated from simultaneous cascade impactor runs. Since the cascade impactors were heated, the particle diameter measured was that of a dry particle.

Particle penetration versus dry particle for runs 10, 11, and 12 is plotted in Figures 6, 7, and 8. The penetration curves are flat and show a relatively constant penetration of 5% for all particle sizes.

In the scrubber, the particles are wet which gives the submicron particles a larger aerodynamic diameter than their physical size would. The wet particle size was not measured during the first test period.

During the second test period, the CHEAF unit was shut down. Therefore, it was impossible to measure the wet particle diameter in the scrubber inlet and outlet simultaneously. However, the wet and dry particle size distributions were determined at the CHEAF inlet by means of simultaneous heated and unheated cascade impactor sampling runs. The solution induced particle

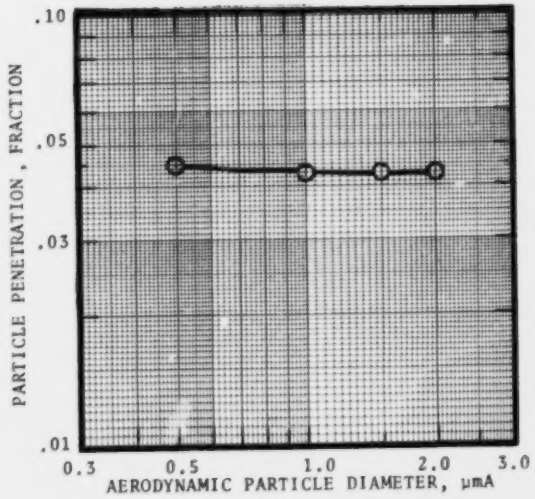

Figure 6. Penetration versus dry particle diameter for Run 10.

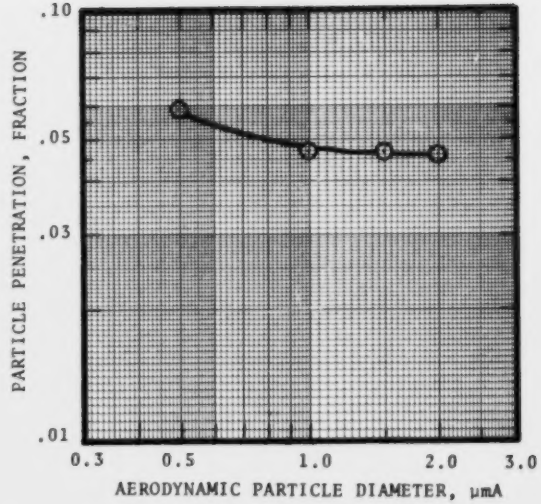

Figure 7. Penetration versus dry particle diameter for Run 11.

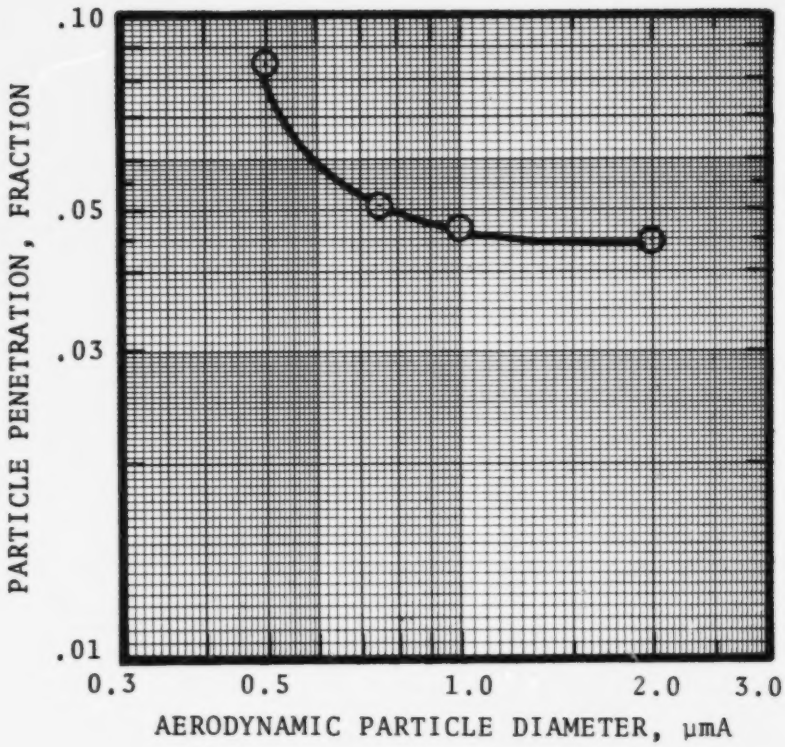

Figure 8. Penetration versus dry particle diameter for Run 12.

growth can be determined from the wet and dry particle size distribution data.

The inlet dry particle size distribtuions are comparable for the first and second test periods. Therefore, by assuming the outlet is also comparable and the extent of particle growth in the outlet is the same as inlet, we can calculate the grade penetration curve for wet particles from the dry particle penetration curve and from the relation between wet and dry particle size distribution curves. The result is shown in Figure 9.

Particle growth appears to have a beneficial effect on particle penetration, especially in the submicron range. Particles in this range grow to as much as 3 times their original diameter. They, in turn, are more easily captured by inertial impaction and thus a lower particle penetration occurs. Instead of particle penetration increasing for submicron particles, it remains constant due to the particle growth and thus the penetration curves appear flat.

The performance cut diameter of the CHEAF calculated by equivalent cut diameter method is 0.8 μmA wet.

MATHEMATICAL MODELING

The prediction of particle penetration for the CHEAF required the development of mathematical models because none were available from the literature. We can mathematically represent the filter as a fiber bed consisting of an array of equally spaced cylinders. The "Scrubber Handbook" (Calvert et al. 1972) gives the following equation for the prediction of particle penetration of a clean fibrous bed:

$$Pt(d_p) = \exp\left[-S\,\eta\right] = \exp\left[-\frac{4\,\ell(1-\varepsilon)}{\pi\, d_f}\,\eta\right] \qquad (1)$$

where "η" is the effective collection efficiency of a single fiber in the bed for all collection mechanisms.

By assuming negligible interaction among fibers, the collection efficiency of a fiber in a bed can be approximated by the collection efficiency of an isolated fiber. This assumption might slightly underestimate the fiber efficiency but

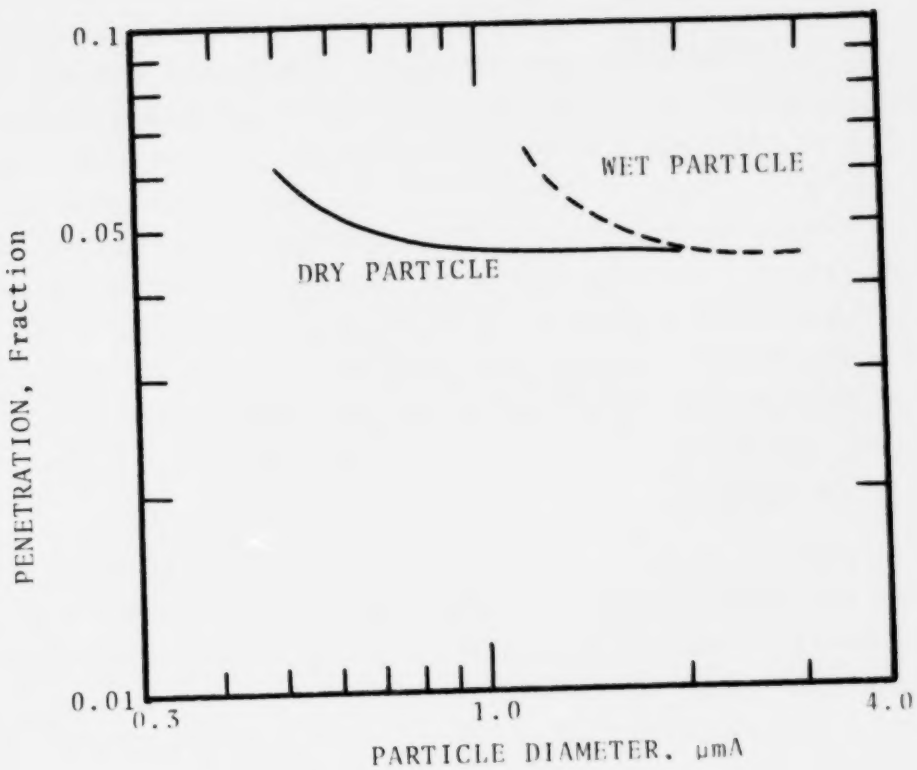

Figure 9. Experimental grade penetration curve for CHEAF.

the fibers are not all oriented normally to the gas flow direction and this will lower the collection efficiency.

The pressure drop across the fiber bed is the sum of the drag losses of all fibers. We used the drag coefficient for an isolated cylinder, as is consistent with the assumption of negligible interaction among fibers.

$$\Delta P = 6.5 \times 10^{-4} \frac{\ell(1-\varepsilon)\ \rho_G\ C_D\ u_G^2}{d_f} \qquad (2)$$

Equations (1) and (2) were used to predict the performance of the CHEAF. The result is shown in Figure 10, a plot of cut diameter versus pressure drop for various fiber diameters. The cut diameter versus pressure drop relation is highly dependent on the diameter of the fiber but not much on the solidity factor. The circle in the figure represents the data we determined experimentally. The fiber diameter and the porosity of the filter medium of the scrubber were not disclosed as they are proprietary. Therefore, it was not possible to determine how well the model predicts the performance.

It is possible to compare our model with the data of Rei and Cooper (1976) for tests on a pilot scale unit of the CHEAF. They reported the volume fraction void of the filter medium to be 97% and the fiber diameters to be 64 μm, 44 μm, and 36 μm for foams with 18, 26, and 33 pores per cm. They also reported the measured cut diameter was somewhere below 0.5 μmA for pressure drops, ranging from 40 to 90 cm W.C. The dashed line in Figure 10 shows their data, which are consistent with our predictions.

ECONOMICS AND OPERATING PROBLEMS

Cost data for the CHEAF were not provided by the manufacturer. According to the manufacturer, the technology is not yet sufficiently well established to provide reliable capital and operating costs.

The CHEAF, although a temporary installation, operated very smoothly during the testing period; however, plant

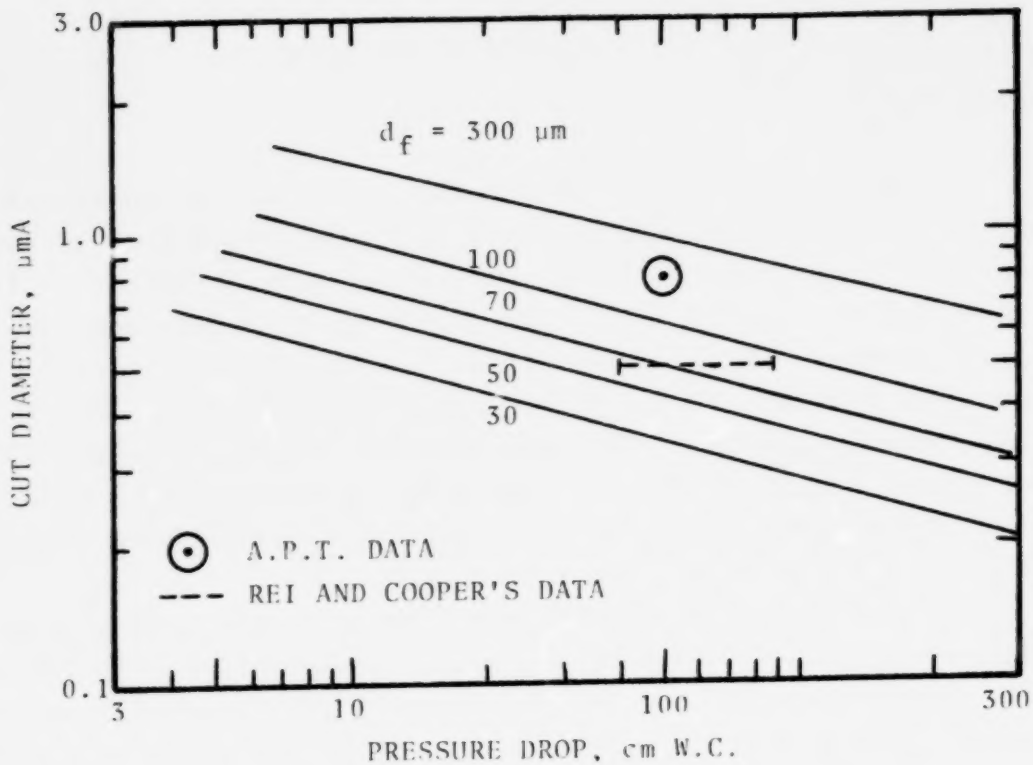

Figure 10. Cut diameter versus pressure drop for fibrous bed.

process shutdowns delayed testing on schedule. The major problem in this CHEAF installation is operating under a corrosive atmosphere. Residual chlorides from the diatomaceous earth process and sulfates from the oil-fired furnace, together with a saturated gas stream, tend to accelerate corrosion on the internal parts of the CHEAF.

Carbon steel fans in both of the blowers were gradually eroding, causing an imbalance in the units. This, in turn, caused considerable vibrational problems and excessive wear on the motors' main shaft bearings.

CONCLUSIONS

The CHEAF appears to be a reasonably efficient device for fine particulate control of saturated emissions from a diatomaceous earth calcining and drying process. Particle growth occurring in the pre-cleaner prior to the CHEAF is beneficial to the fine particle collection efficiency of the system to a certain extent.

According to the test results obtained on the CHEAF (Cleanable High Efficiency Air Filter) system, particle penetration is relatively independent of dry particle size. Penetration is approximately 5% with the mean dry particle diameter equal to 0.82 μmA (1.5 μmA wet). The performance of the CHEAF, with an approximate actual (wet) cut diameter of 0.8 μmA and a pressure drop of 50 centimeters W.C., is comparable to a venturi with a pressure drop of 20 centimeters W.C. However, according to the manufacturer the initial capital investment for the CHEAF is much less.

SECTION 4

A.P.S. ELECTROSTATIC SCRUBBER

SOURCE AND CONTROL SYSTEM

The pilot scale "Electrostatic Scrubber" of Air Pollution Systems is basically an electrostatic charger (or ionizer) followed by a venturi scrubber. Figure 11 is a schematic diagram of the pilot system. An electrode is placed upstream of the venturi to charge the inlet particles, which then enter the venturi throat. The gas stream atomizes the central water spray in the venturi throat and the charged particles, according to A.P.S., are then attracted and collected by the highly polarized water molecules.

The charged particles are also collected on the walls of the ionizer section prior to the throat of the venturi. A thin film of water is run down the inclined surfaces to keep the walls clear and prevent high voltage arcing. The particle laden water droplets are then collected by a cyclonic separator and sent into a settling tank (clarifier). The water can then be recycled back into the scrubber system. However, during the test program, fresh water was used.

The ionizer consists of an electrode supported in the inlet of the venturi section. According to Air Pollution Systems, a stable electrical discharge of high intensity is maintained across the venturi throat between the center electrode and the wall. A.P.S. claims that the average field that can be maintained across the electrode gap (space between the electrode probe and the wall) is substantially higher, 14-16 kV/cm, than that of a standard electrostatic precipitator, 4 kV/cm.

The pilot scrubber had a maximum capacity of 28 Am^3/min (1,000 ACFM) at 16°C. Under testing conditions the scrubber

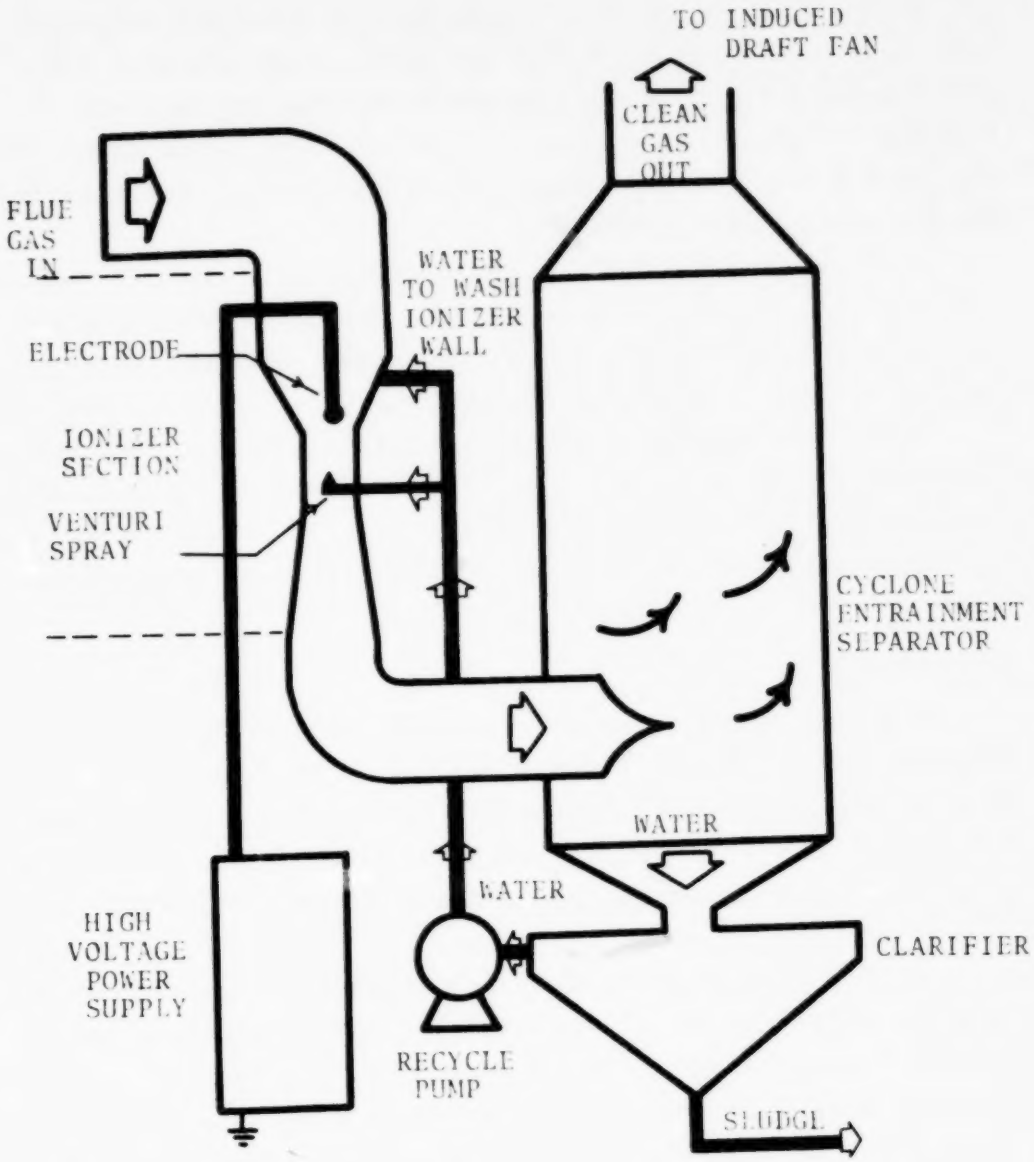

Figure 11. APS electrostatic scrubber.

was operated at 21.0 Am^3/min (740 ACFM) @16°C and at 22.7 Am^3/min (800 ACFM) @ 16°C. Liquid flow rates (total) were set at 30.3 ℓ/min and 41.7 ℓ/min during the test program. L/G ratios were 1.4 $ℓ/m^3$ and 1.8 $ℓ/m^3$, respectively, for the above flow rates. Electrode probe cooling air was introduced at a rate of 1.1 m^3/min (40 CFM). The addition of the cooling air was accounted for as dilution air in the outlet sample calculations.

A 3-horsepower induced draft fan with a capacity of 28 Am^3/min at a pressure of 45 cm W.C. was located downstream of the outlet sample ports. Gas flow rates were adjusted through a damper upstream of the fan.

The test aerosol used during this study was titanium dioxide, TiO_2, which has a density of about 3.0 g/cm^3, as dispersed. The mass median diameter of TiO_2 aerosol was approximately 1.0 microns aerodynamic, μmA, as dispersed, with a standard deviation of 2.2.

TEST METHOD

The performance tests were completed during two test periods. For the first tests performed in June 1975, the University of Washington Mark III (U.W.) cascade impactors were used for particle measurements above 0.3 μmA in diameter. Measurements were conducted simultaneously in the inlet and outlet ducts.

An Air Pollution Technology portable screen diffusion battery (A.P.T.- SDB) was used for particle measurements from 0.1 μm to 0.01 μm (actual). During an impactor run, several inlet and outlet fine particle size measurements were taken alternately with the portable diffusion battery. Since the system remained fairly constant during each run, alternate inlet and outlet SDB measurements were considered to approximate simultaneous sampling.

Additional tests were performed in July 1975 to determine whether static charges carried by the particles was affecting the particle classification of the cascade impactor. Polonium

210 charge neutralizers (Staticmaster, Ionizing Unit Model No. 2U500) were connected prior to the impactors on both the inlet and the outlet.

In the first tests, particles form the particle generator were not neutralized. In order to check the possibility that particle charge might affect scrubber performance when the ionizer is off, a charge neutralizer was added to the dust disperser. A two foot glass tube containing six Staticmasters was placed on the end of the particle generator during the second tests.

OPERATING CONDITIONS

A total of thirty-one simultaneous inlet and outlet sample runs were performed on the electrostatic scrubber. The data are grouped into four data sets.

During the first three series of tests (data sets A, B, and C) the scrubber was tested with the ionizer on and off and during the fourth series (data set D) with the ionizer on.

The scrubber was tested at 21 Am^3/min (740 ACFM) at 16°C for the first series of tests (runs 1-10, data set A). The pressure drop across the venturi was 40 cm W.C. with liquid flow rates to the ionizer wall wash and the venturi throat set at 7.6 ℓ/min and 22.7 ℓ/min, respectively.

The second series of tests (runs 11-26 , data set B) were run at 22.7 Am^3/min (800 ACFM) at 16°C with the same pressure drop across the venturi of 40 cm W.C. The liquid flow rate was increased to 34.1 ℓ/min at the venturi throat and the ionizer wall wash remained the same at 7.6 ℓ/min. An overhanging gasket and water feed tube were removed from the scrubber throat between sets "A" and "B".

The third series of tests (runs 27-30, data set C) were run at identical operating conditions as the second series. These runs were taken to determine the effect of the static charge induced by the aerosol generator. A cross-shaped baffle was introduced into the test aerosol mixing duct prior to set "C", in order to cause better mixing of air and the

aerosol stream from the dust blower.

Finally the last series of runs attempted, used alumina as a test aerosol instead of titanium dioxide. Because of particle generator plugging, run 31 (data set D) was the only test performed on this aerosol.

Gas flow rates, water flow rates and other related operating parameters are tabulated for each data set and are given in the Tables 1 and 2.

DATA

Cascade Impactor and Diffusion Battery Data

The inlet and outlet size distributions obtained during the performance tests are given in Table 3 . These were determined from cascade impactor and diffusion battery runs which are explained in greater detail by Calvert et al. (1976a). A summary of the mass loadings and overall penetrations is given in Table 4 .

PARTICLE PENETRATION

Particle penetration versus particle size was plotted for the data obtained from the electrostatic scrubber. A composite of the runs in data set "A" is represented in Figure 12, which shows the effect of the ionizer on penetration. Penetrations for the individual runs in sets "B" and "C" are shown in Figures 13 and 14. Figure 15 shows composite curves for sets "A" "B", and "C" for overall comparison.

As can be seen in Figures 12 through 15 the ionizer does improve the scrubber performance in all cases. However, the amount of improvement is least in data set "C", where the most precautions were taken to neutralize and mix the test aerosol entering the scrubber.

The penetrations determined from diffusion battery data are presented in Figures 16 through 19 along with the individual penetrations for the cascade impactor runs of data set "C". Particle density variation and loading fluctuation account for discrepancies between impactor and D.B. penetrations.

TABLE 1. DATA SET A, RUNS 1-10

CONDITION	INLET	OUTLET
Temperature	15-21°C	14-20°C
Velocity	8.4 m/s(27.6 ft/s	5.1 m/s (16.7 ft/s)
Am^3/min @16°C	21.0	22.1
ACFM @16°C	740.0	780.0
DNm^3/min @ 0°C	19.6	19.7
DSCFM @21°C	745.0	748.2
Vol. % H_2O vapor	1.1	1.6
Static Pressure	-0.6 cm W.C.	-43.2 cm W.C.
Pressure drop across venturi		40.0 cm W.C.
Pressure drop across separator		2.5 cm W.C.
Ionizer wall wash flow rate		7.6 ℓ/min
Venturi water flow rate		22.7 ℓ/min
*Electrode cooling air		1.1 m^3/min(40 CFM)
L/G ratio		1.4 ℓ/m^3

*Electrode cooling air introduced into system and accounted for as dilution air.

TABLE 2. DATA SETS B, C AND D, RUNS 11-31

CONDITION	INLET	OUTLET
Temperature	15-21°C	14-20°C
Velocity	7.5m/s (24.5 ft/s	5.4m/s (17.8 ft/s
Am^3/min @16°C	22.7	23.8
ACFM @16°C	800.0	840.0
DNm^3/min @0°C	21.2	21.2
DSCFM @21°C	805.0	806.0
Vol. % H_2O vapor	1.1	1.6
Static Pressure	-0.6 cm W.C.	-43.2 cm W.C.
Pressure drop across venturi		40.0 cm W.C.
Pressure drop across separator		2.5 cm W.C.
Ionizer wall wash flow rate		7.6 ℓ/min
Venturi water flow rate		34.1 ℓ/min
*Electrode cooling air		1.1 m^3/min (40 CFM)
L/G ratio		1.8 ℓ/m^3

*Electrode cooling air introduced into system and accounted for as dilution air.

TABLE 3. INLET AND OUTLET SIZE DISTRIBUTION SUMMARY

Run Set No.	Ionizer	INLET		OUTLET	
		d_{pg}, μmA	σ_g	d_{pg}, μmA	σ_g
2 A	ON	0.95	2.2	0.90	1.7
3	ON	0.95	2.2	0.90	1.7
4	ON	0.95	2.2	0.90	1.7
5	OFF	1.1	2.3	1.0	1.9
6	OFF	1.1	2.3	1.0	1.9
11 B	ON	0.90	2.0	0.83	1.6
13	ON	0.90	2.0	0.83	1.6
14	OFF	1.0	2.3	0.95	1.8
16	OFF	1.2	2.3	0.95	1.8
18	ON	1.2	2.3	0.90	1.7
20	ON	1.1	1.9	0.90	1.7
21	ON	0.94	1.9	--------	--------
22	ON	0.94	1.9	--------	--------
23	ON	0.94	1.9	--------	--------
24	ON	0.97	2.2	1.1	1.8
25	OFF	--------	--------	0.92	1.8
26	OFF	1.2	2.1	--------	--------
27 C	OFF	1.5	2.0	1.3	1.8
28	OFF	1.4	1.8	1.1	1.9
29	ON	1.8	1.9	1.1	1.5
30	ON	2.1	2.1	1.4	1.5
31 D	ON	1.9	2.5	1.2	2.1

TABLE 4. TEST RUN SUMMARY

DATE	RUN NO.	SAMPLE DEVICE(1)		IONIZER	MASS LOADING mg/DNm³	
		Inlet	Outlet		Inlet	Outlet
6/17	1(set A)	F(2)	B	ON	-----	1.0
6/18	2 "	I	I	ON	146.5	12.8
6/18	3 "	I	I	ON	156.1	12.0
6/18	4 "	I	I	ON	188.5	16.1
6/19	5 "	I	I	OFF	524.6	75.2
6/19	6 "	I	I	OFF	396.1	62.1
6/19	7 "	F	F	OFF	185.1	62.4
6/20	8 "	F	F	OFF	927.9	108.2
6/20	9 "	F	F	ON	1081.2	37.7
6/20	10 "	F	B	OFF	218.7	41.8
6/23	11(set B)	I	I	ON	152.7	10.3
6/23	12 "	F	B	ON	132.0	13.8
6/23	13 "	I	I	ON	153.4	11.4
6/24	14 "	I	I	OFF	216.9	40.8
6/24	15 "	F	F	OFF	594.2	79.2
6/24	16 "	I	I	OFF	516.9	65.1
6/25	17 "	F	F	ON	472.4	24.2
6/25	18 "	I	I	ON	495.9	18.4
6/25	19 "	F,D	B	ON	69.4	8.4
6/25	20 "	I	I	ON	192.2	12.5
6/26	21 "	I,D	F	ON	48.1	8.1
6/26	22 "	I,D	F	ON	53.7	7.6
6/26	23 "	I,D	F	ON	100.1	10.3
6/27	24 "	I	I,D	ON	85.1	12.7
6/27	25 "	F	I,D	OFF	153.9	31.8
6/27	26 "	I,D	F	OFF	102.6	21.3
7/17	27(set C)	I,D (3)	I,D	OFF	301.8	30.6
7/17	28 "	I,D	I,D	OFF	161.1	24.0
7/17	29 "	I,D	I,D	ON	257.0	7.9
7/17	30 "	I,D	I,D	ON	91.0	5.0
7/18	31(set D)	I(4)	I	ON	183.7	10.9

Notes:

(1) I = Impactor run F = Total filter run
B = Blank impactor run D = Diffusion battery run

(2) Faulty filter holder, no inlet data obtained

(3) Runs 27-31, charge neutralizers connected prior to impactors and also connected on the dust feeder. A cross was installed downstream of the dust feeder to promote mixing.

(4) Alumina used as test aerosol

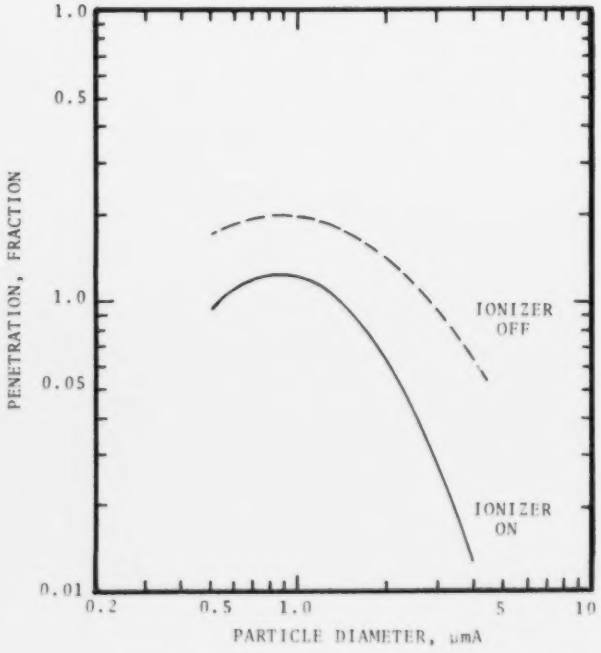

Figure 12. Penetration vs. particle diameter for data set A.

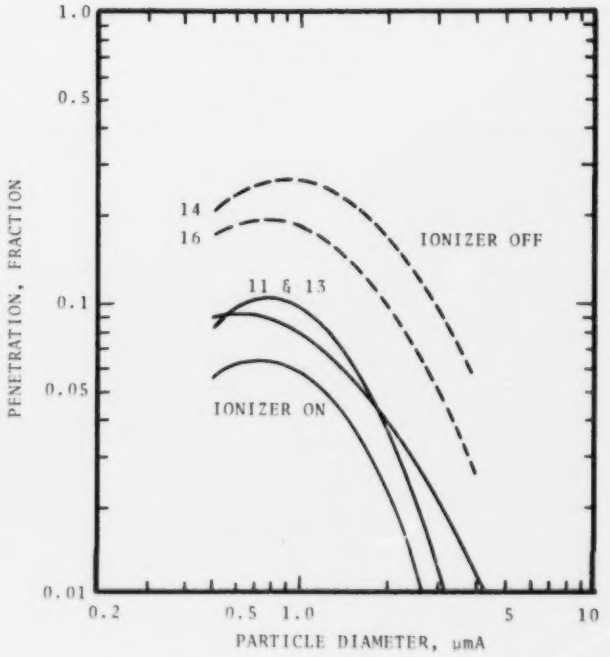

Figure 13. Penetration vs. particle diameter for data set B.

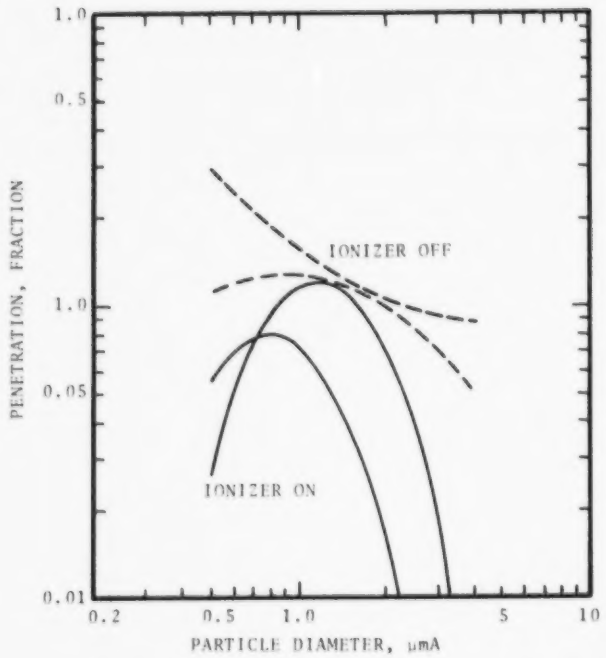

Figure 14. Penetration vs. particle diameter for data set C.

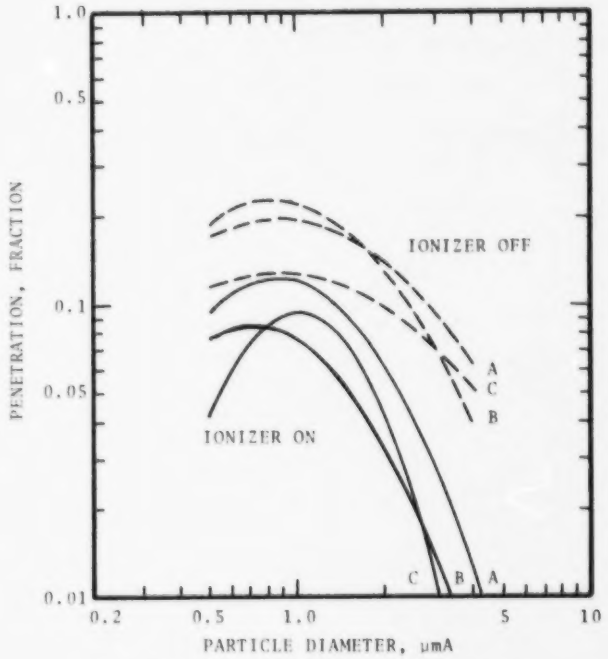

Figure 15. Penetration vs. particle diameter for data sets A, B, & C.

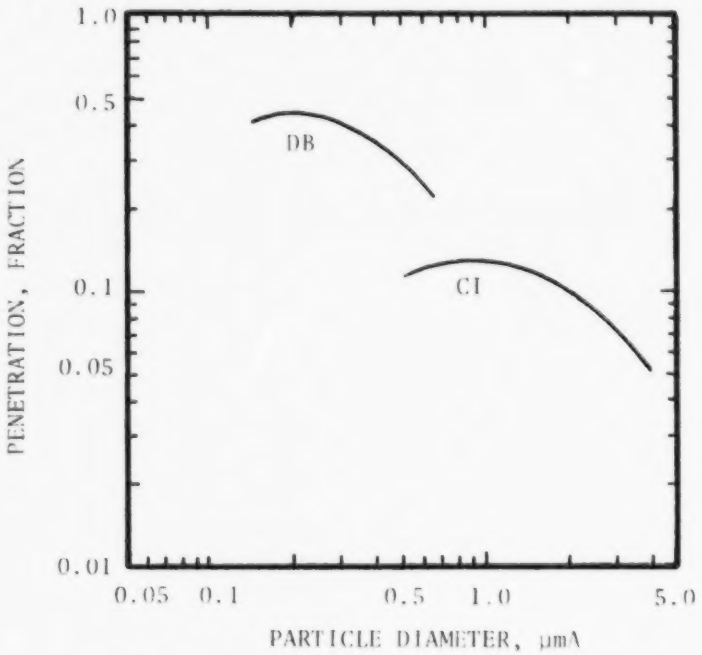

Figure 16. Penetration vs. particle diameter using both diffusion battery and cascade impactor, run 27 (set C, ionizer off)

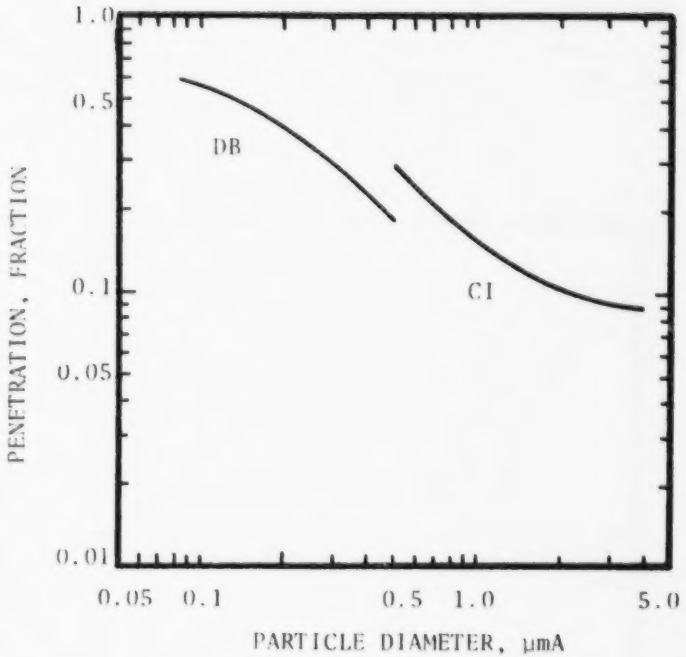

Figure 17. Penetration vs. particle diameter using both diffusion battery and cascade impactor, run 28 (set C, ionizer off)

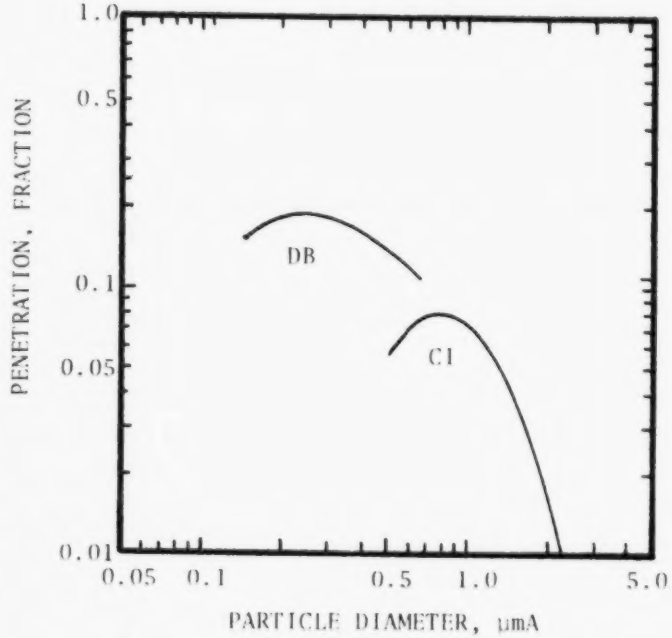

Figure 18. Penetration vs. particle diameter using both diffusion battery and cascade impactor, run 29. (set C, ionizer on)

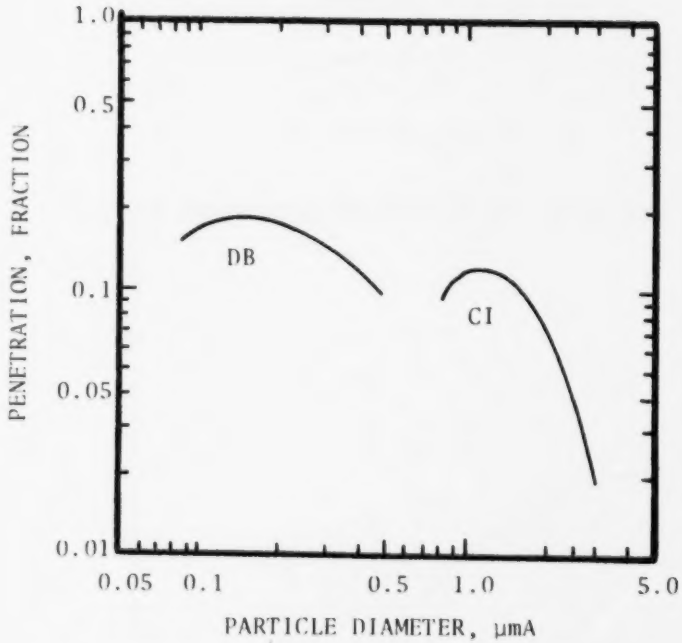

Figure 19. Penetration vs. particle diameter using both diffusion battery and cascade impactor, run 30. (set C, ionizer on)

The penetration curves indicate an increase in efficiency for particles smaller than the 0.1 to 0.2 μmA range. From these results and published literature, it is evident that smaller, more highly diffusive particles experience increased collection efficiency.

MATHEMATICAL MODEL

The prediction of particle penetration for the A.P.S. Electrostatic Scrubber required the development of a mathematical model because none was available from either A.P.S. or the literature. The following section presents the derivation of a predictive model by means of the unit mechanism approach. While the form of the equation is the consequence of theoretical relationships, an empirical constant, f, is included and its value was assumed to be the same as for non-charged venturi scrubbers.

In a venturi scrubber the most important unit mechanism responsible for particle collection is the collection by drops and the predominant collection phenomenon is inertial impaction. When particles are charged, then in addition to the inertial force, electrostatic forces are present that force the particle towards the drop, i.e., increase the collection efficiency of the drop.

Calvert et al. (1973) calculated the theoretical increase in collection efficiency by flux forces. They relate the single drop collection efficiency to the inertial parameter as shown in Figure 20 with flux deposition number, N_{FD}, as parameter. Inertial impaction parameter and flux deposition number, N_{FD}, are defined by the following equations:

$$K_p = \frac{C'\rho_p u_o d_p^2}{9\mu_G d_d} \qquad (3)$$

where:

$$N_{FD} = \frac{u_F}{u_o} = \frac{\text{Particle electrostatic deposition velocity}}{\text{Fluid velocity past sphere}}$$

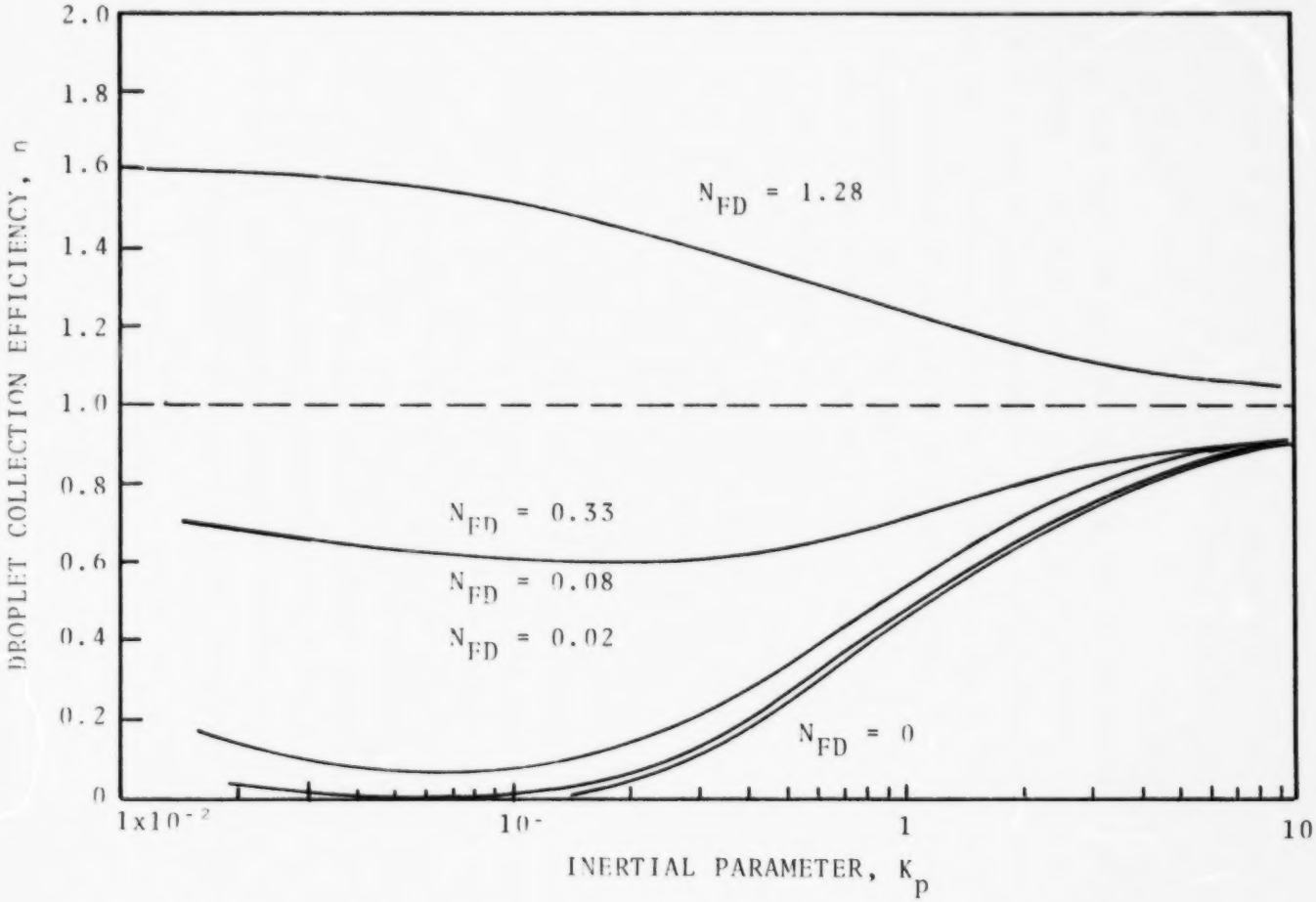

Figure 20. Efficiency of single drop versus inertial parameter N_{Red} = 9.6 with N_{FD} as parameter

K_p = inertial impaction parameter, dimensionless
C' = Cunningham slip factor, dimensionless
ρ_p = particle density, g/cm^3
d_p = particle diameter, cm
μ_G = gas viscosity, poise
d_d = drop diameter, cm
u_o = fluid or gas velocity passing the drop, cm/s

From Stokes' law, the particle drift velocity is given by:

$$u_F = \frac{C' Q_p E}{3\pi \mu_G d_p} \tag{4}$$

where E = field strength, kV/cm
Q_p = electrical charge carried by the particle, coulomb

It is assumed that aerosol particles are charged to saturation after the particles pass through the corona discharge section. If diffusional charge is neglected (this will give conservative results), then according to Oglesby and Nichols (1970), the saturation charge can be calculated from the following equation:

$$Q_p = 3 \frac{\epsilon_p}{\epsilon_p + 2} \pi \epsilon_0 d_p^2 E_0 \tag{5}$$

where ϵ_p = dielectric constant of the particle
$\epsilon_0 = 8.86 \times 10^{-14}$ coulomb cm/cm^2-volt
E_0 = charging electric field strength, kV/cm

The atomized drop diameter in a venturi is assumed to be the Sauter mean diameter, which is predicted by means of the Nukiyama and Tanasawa correlation

$$d_d = \frac{50}{u_G} + 91.8 \left(\frac{Q_L}{Q_G} \right)^{1.5} \tag{6}$$

where Q_L = volumetric flow rate of liquid, m^3/min
Q_G = volumetric flow rate of gas, m^3/min
u_G = gas velocity, cm/s

Once 'N_{FD}' and 'K_p' are calculated, single drop collection efficiency can be read from Figure 21 or from Figure 22. Single drop collection efficiency 'η' is then related to penetration based on an equation given by Calvert (1968) for a venturi,

$$Pt_d = \frac{2\ Q_L\ \rho_L\ d_d\ u_{Gt}}{55\ Q_G\ \mu_G} \int_{f_a}^{o} \eta\ df \qquad (7)$$

where Pt_d = particle penetration for particle size "d_p"
u_{Gt} = venturi throat gas velocity, cm/s
f = an empirical constant
f_a = initial value of $f \approx 0.5$
ρ_L = liquid density, g/cm^3
η = single drop collection, fraction

This model was applied to predict the collection efficiency of the A.P.S. scrubber both with the ionizer on and with the ionizer off. Since the calculation of particle drift velocity (equation (4) involves the determination of field strength distribution, which is unknown, a constant value equal to the field strength at the gap was used. This assumption will lead to an optimistic drift velocity.

Figure 22 shows the predicted A.P.S. scrubber performance along with experimental curves. As can be seen, the model agrees fairly well with experimental values for large particles but deviates for small particles. This deviation may be caused by omission of the diffusion collection mechanism in the theoretical model.

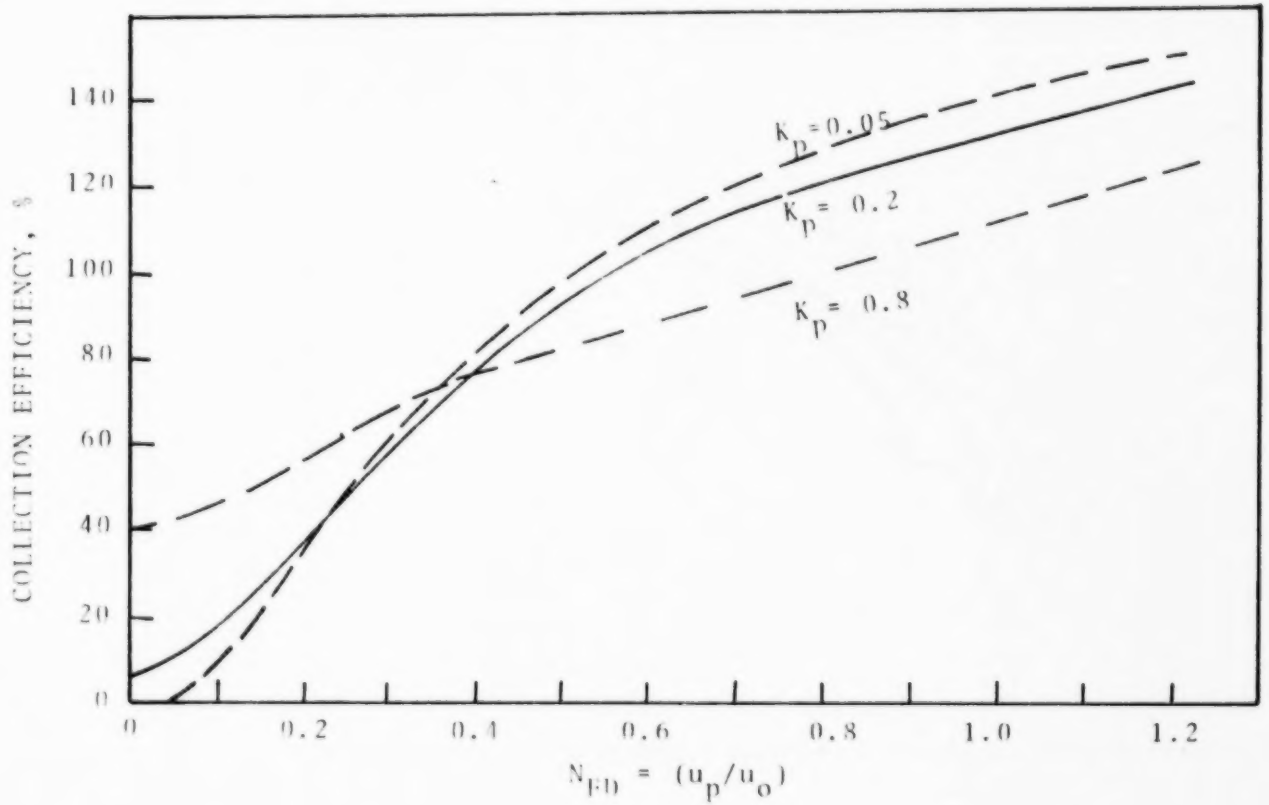

Figure 21. Efficiency of a single drop, η, versus N_{FD} with K_p as a parameter ($N_{Red} = 9.6$)

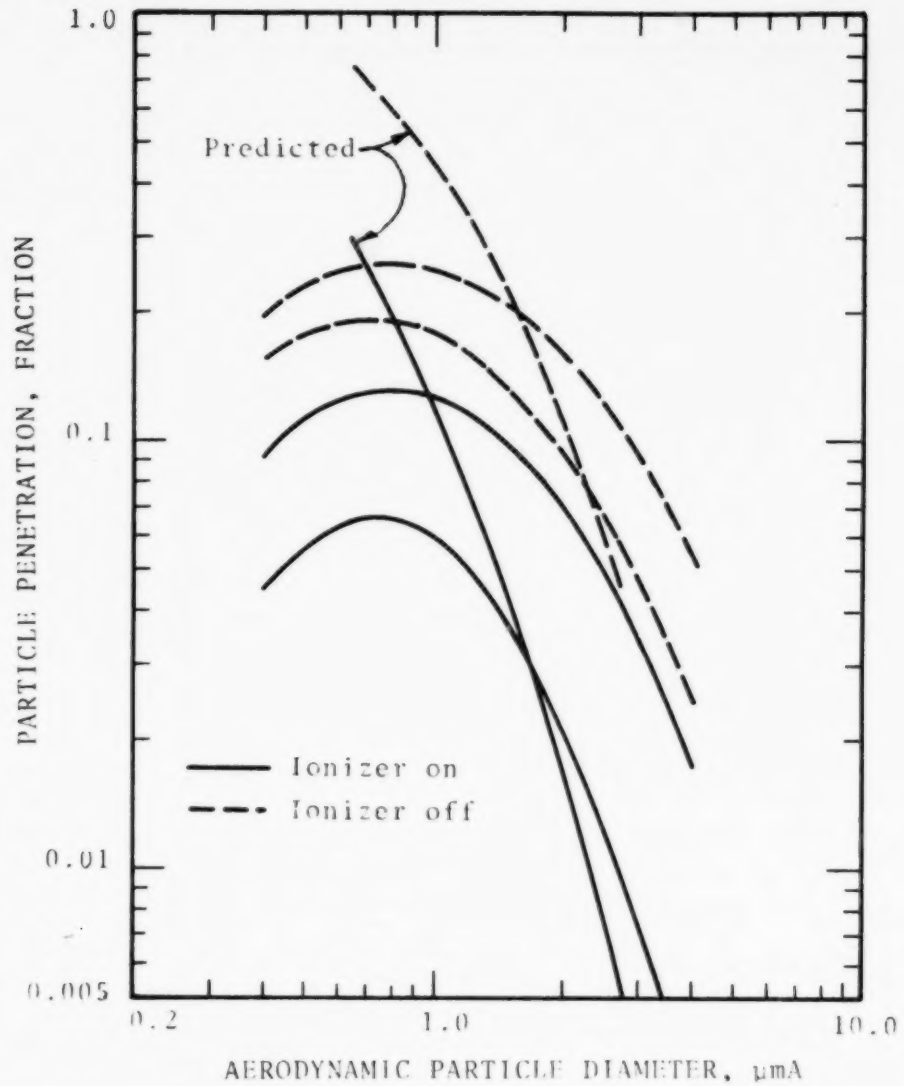

Figure 22. Experimental and predicted particle penetration versus particle diameter.

SECTION 5

A.P.S. ELECTRO-TUBE

SOURCE AND CONTROL SYSTEM

The pilot scale Electro-Tube of Air Pollution Systems (A.P.S.) is basically a tube electrostatic precipitator with a central rod electrode and wetted wall collector. Figure 23 is a schematic diagram of the pilot system. The inlet particles are charged in a high energy field (12 kV/cm) by a high intensity ionizer at the base of the electrode. The charged particles then migrate to the wetted wall in the body of the device in a field of 5-10 kV/cm. A.P.S. indicates that initial saturation charge on the particles is higher than the usual 4-5 kV/cm for a conventional ESP (electrostatic precipitator) and facilitates increased migration in the collecting electric field.

The Electro-Tube tested was a laboratory pilot scale unit. Under testing conditions the Electro-Tube was operated at gas flow rates of 16.9, 18.9, and 22.9 Am^3/min (596, 668, and 808 ACFM, respectively) at 20°C. Liquid flow rates could range from 1.7 to 6.4 ℓ/min according to the manufacturer's specifications, but the liquid flow was held constant at 3.8 ℓ/min during the entire test period. The tube diameter was 30.5 cm (12 in.).

The test aerosol for this study was titanium dioxide (TiO_2) which had a single particle density of 4.1 g/cm^3. The mass median aerodynamic diameter of the dispersed aerosol was about 1.2 μmA, geometric standard deviation 2.2, and agglomerate density about 3.0 g/cm^3.

The particle generator used during the test consists of a feed auger, intermediate blower, deagglomeration orifice

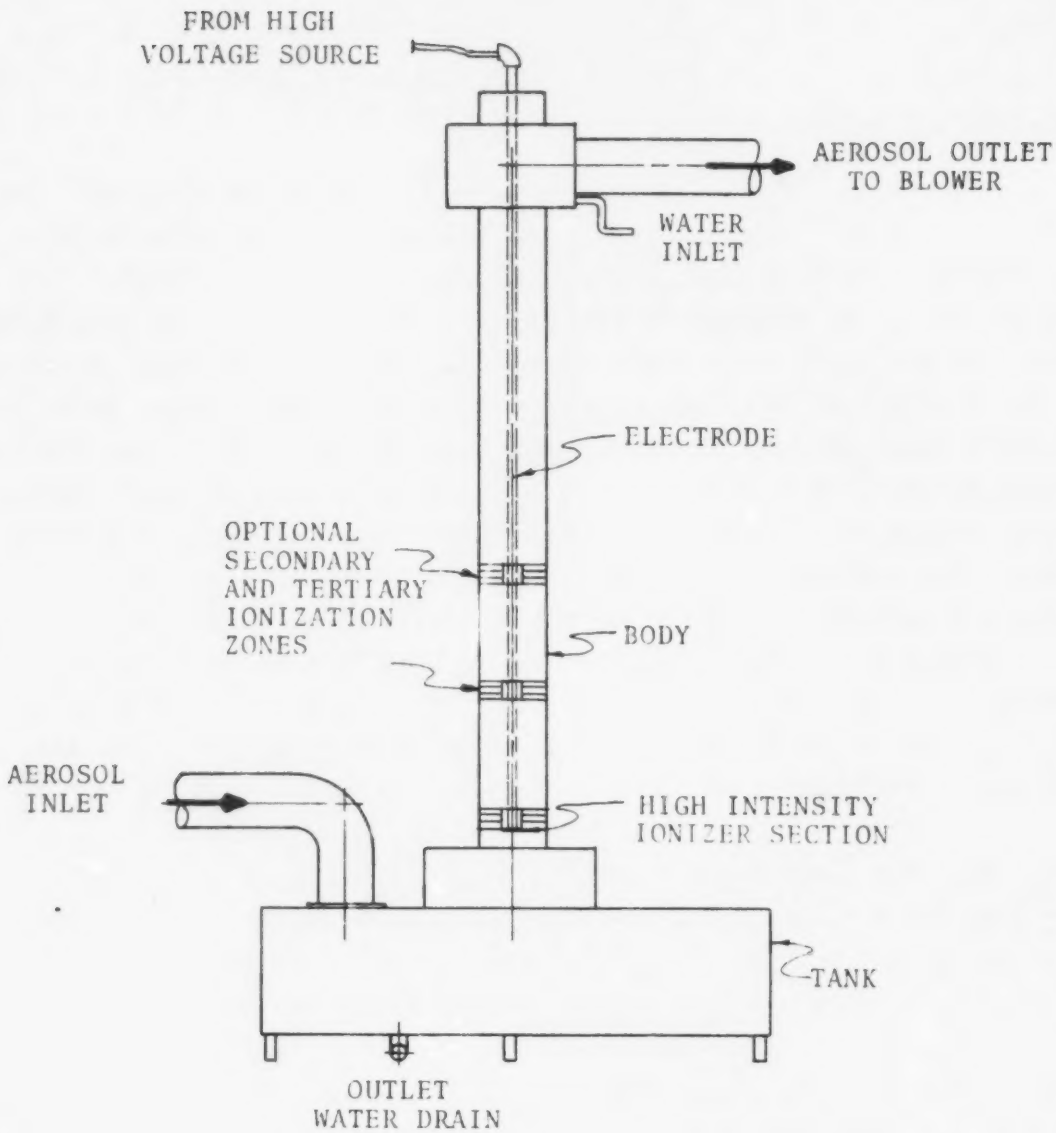

Figure 23. Diagram of A.P.S. Electro-Tube.

chamber, and main blower. A cross-shaped baffle was placed at the system inlet to ensure adequate mixing of the aerosol with the incoming ambient air.

TEST METHOD

All tests were performed using modified EPA type sampling trains with in-stack University of Washington Mark III (U.W.) cascade impactors. Greased aluminum substrates were used in the impactors to prevent particle bounce and minimize wall losses.

The Air Pollution Technology portable screen diffusion battery (A.P.T. - SDB) was used for particle measurements from 0.01 μm to 0.1 μm (actual).

During an impactor run, several inlet and outlet fine particle size measurements were taken alternately with the portable diffusion battery. Since the system remained fairly constant during each run, alternate inlet and outlet SDB measurements were considered to approximate simultaneous sampling.

In-stack filter samples were also taken to obtain total particulate loadings and overall collection efficiencies of the system.

Blank impactor runs were performed periodically to ensure that the greased aluminum substrates did not react with the stack gases. A blank impactor run consisted of an impactor preceded by two glass fiber filters run at identical sample conditions as the actual sampling runs. Total filter loadings were also obtained during the blank impactor run to furnish simultaneously inlet and outlet mass concentrations and overall collection efficiency data.

OPERATING CONDITIONS

The operating conditions for the A.P.S. Electro-Tube are tabulated in Table 5.

TABLE 5. OPERATING CONDITIONS

Condition	Inlet	Outlet
Temperature	18-27°C	18-27°C
Velocity in Electro-Tube	4.3-5.8 m/s (14.1-19.1 fps)	4.4-6.0 m/s (14.5-19.9 fps)
Am^3/min @ 22.5°C	16.9-22.9	17.4-23.8
ACFM @ 22.5°C	596.0-808.2	615.0-841.0
DNm^3/min @ 0°C	15.4-20.9	15.9-21.7
DSCFM @ 21°C (70°F)	585.0-794.0	605.0-826.0
Vol % H_2O Vapor	1.3-2.4	1.3-2.4
Static Pressure at Sample Ports	-0.5 to -1.5 cm W.C.	-2.5 to -4.6 cm W.C.
Pressure drop across Electro-Tube: 0.53 (low flow) to 0.64 (high flow) cm W.C.		
Ionizer wall water wash rate: 3.8 ℓ/min (1 GPM)		

DATA

Cascade Impactor Data

Data sets for three gas flow rates were obtained for the A.P.S. Electro-Tube. As the gas flow was fully developed one-point sample locations were used for all data points.

Table 6 is a summary of the size distribution of inlet and outlet mass loading, and overall penetration data for the various runs made. Table 7 summarizes the total filter loading tests. The original data obtained during the performance test is described in greater detail in a report by Calvert et al. (1976b).

Diffusion Battery Data

Diffusion battery data were taken during the last three days of testing. The runs were made simultaneously with cascade impactors and numbered accordingly. Runs 14 and 16 were preliminary tests to determine count and flow adjustment techniques; therefore, they were not included in the data set.

Performances for runs 17, 18, and 19 were determined by statistical conversion of inlet-outlet size distribution to cumulative number concentration and calculating the particle penetrations in the same manner as the cascade impactor analysis. Calculations were performed by a computerized FORTRAN program.

Table 8 contains the size distribution summary of the diffusion battery tests. Note that the sizes given are actual rather than aerodynamic as with cascade impactor analysis. This is necessary when reducing data from the diffusion battery as this instrument classifies particles according to their physical size. Conversion to aerodynamic diameter for comparison with impactor analysis requires knowledge of the density.

The titanium dioxide powder used had a density of 4.1 g/cm^3 as measured by a pycnometer. This value agreed closely with published data for TiO_2. The solid unitary particles would have this value for their density. However, the batch of TiO_2 that was used consisted of many agglomerated as well as single particles. Most of the single particles and the detectible units

TABLE 6. SIZE DISTRIBUTION, MASS LOADING, AND OVERALL PENETRATION DATA*

Run No.	INLET			OUTLET			Overall Penetration (%)
	d_{pg}, μmA	σ_g	mg/DNm³	d_{pg}, μmA	σ_g	mg/DNm³	
1	Filter		177	Filter		8.7	4.9
2	Filter		242	Filter		11.0	4.6
3	1.02	2.1	185	0.69	1.4	8.5	4.6
4	1.15	2.1	248	0.71	1.5	8.7	3.5
5	1.47	2.4	571	0.70	1.5	13.0	2.3
6	Filter		775	Filter		14.5	1.9
7	1.55	2.4	1080	0.68	1.5	13.7	1.3
8	Filter		606	Filter		19.0	3.1
9	Filter		662	Filter		9.1	1.4
10	1.30	2.2	364	0.82	1.7	5.0	1.4
12	0.87	2.0	167	0.69	1.6	4.1	2.5
13	1.27	2.1	389	0.75	1.9	7.0	1.8
14	1.11	2.2	248	0.74	1.4	4.2	1.7
15	1.05	2.0	375	0.68	1.8	2.5	0.7
16	1.20	2.5	738	0.79	1.8	5.8	0.8
18	1.25	2.2	274	0.66	1.5	7.8	2.9
19	1.20	1.9	240	1.00	2.2	1.2	0.5

*d_{pg} is the geometric mass mean aerodynamic particle diameter in this table

TABLE 7. TOTAL FILTER PARTICLE LOADING TESTS

Run No.	INLET		OUTLET	
	M_{cum} (mg/DNm³)	DNm³	M_{cum} (mg/DNm³)	DNm³
1	177	0.25	8.7	0.94
2	242	0.28	11.0	1.01
6	775	0.12	14.5	1.23
8	606	0.11	19.0	1.02
9	662	0.067	9.1	0.83

of the agglomerates had diameters in the range of 0.1 to 0.3 μm as measured from scanning electron micrographs. Therefore, particles larger than about 0.3 μm were mainly agglomerates and, because of their irregular shape and possible voids, had a density less than 4.1 g/cm^3. The density of the larger particles was estimated to be about 3 g/cm^3.

TABLE 8. NUMBER BASIS SIZE DISTRIBUTION DATA FOR DIFFUSION BATTERY TESTS*

Run No.	INLET		OUTLET	
	d_{pN}, μm	σ_g	d_{pN}, μm	σ_g
17	0.37	7.8	0.12	7.6
18	0.14	7.2	0.035	4.3
19	0.34	7.9	0.19	7.5

*d_{pN} is the geometric number (count) mean particle diameter in this table.

PARTICLE PENETRATION

The overall penetration summary is presented in Table 6 Total mass loadings were taken by cascade impactors or total filter samples. Overall penetrations tended to decrease with decreasing volumetric gas flow rates.

Average overall penetrations for the Electro-Tube were 3.1% for 22.9 Am^3/min, 1.8% for 18.9 Am^3/min, and 0.7% for 16.9 Am^3/min. The average aerosol "d_{pg}" was 1.2 μmA with a geometric standard deviation of 2.2.

Particle penetration versus particle size were plotted for the data obtained from the Electro-Tube and appear in

Figures 24, 25, and 26. The data have been plotted together according to the gas flow rate in the device. The penetrations calculated from the diffusion battery data were converted to penetrations corresponding to aerodynamic diameter using both 3 g/cm^3 and the 4.1 g/cm^3 densities, and are also shown in Figures 24, 25, and 26. The lower density results in 5 to 15% lower particle penetration for the three sets of runs shown.

MATHEMATICAL MODEL

The APS Electro-Tube is essentially a wetted wall ESP. The mathematical model presented by Gooch and Francis (1975) for predicting the performance of an ESP is applicable

ECONOMICS

No data were available for determining the annualized costs associated with operating the APS Electro-Tube. It is expected that the costs would be comparable to those of a conventional wetted wall ESP.

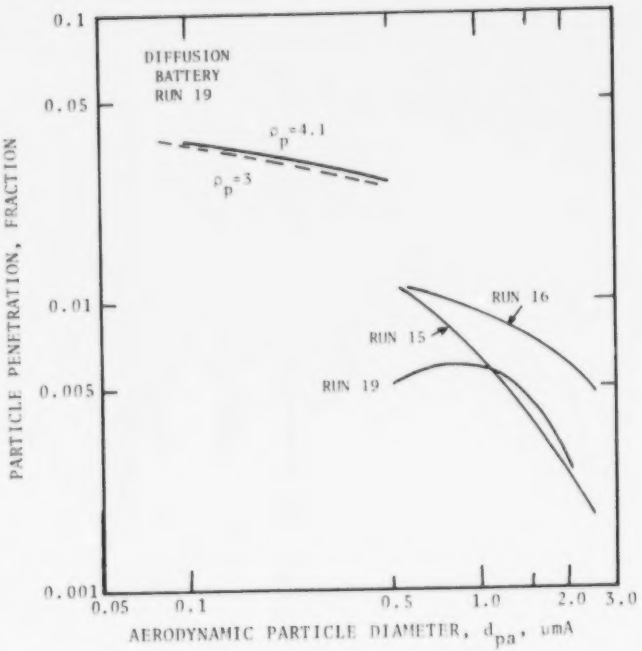

Figure 24. Penetration versus aerodynamic particle djameter for low gas flow, Runs 15, 16, 19

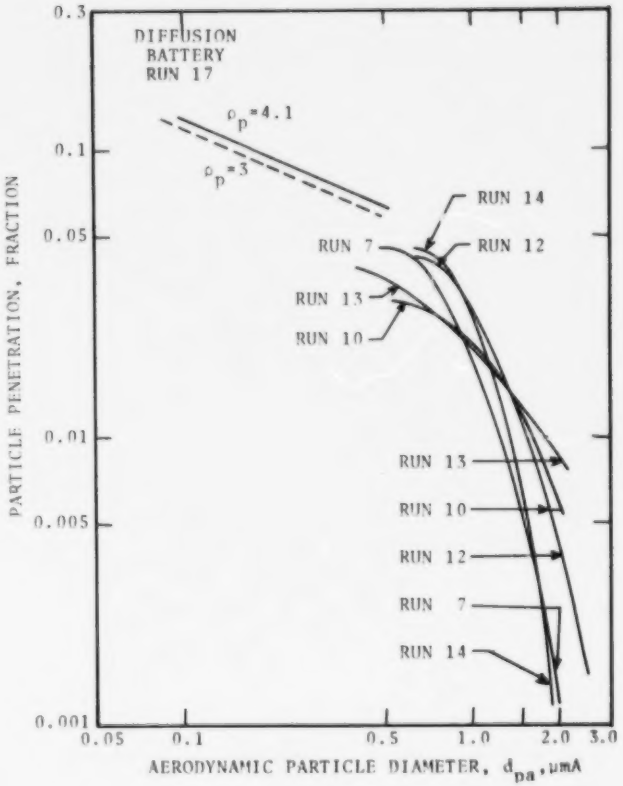

Figure 25. Penetration versus aerodynamic particle diameter for medium gas flow, Runs 7, 10, 12, 13, 14.

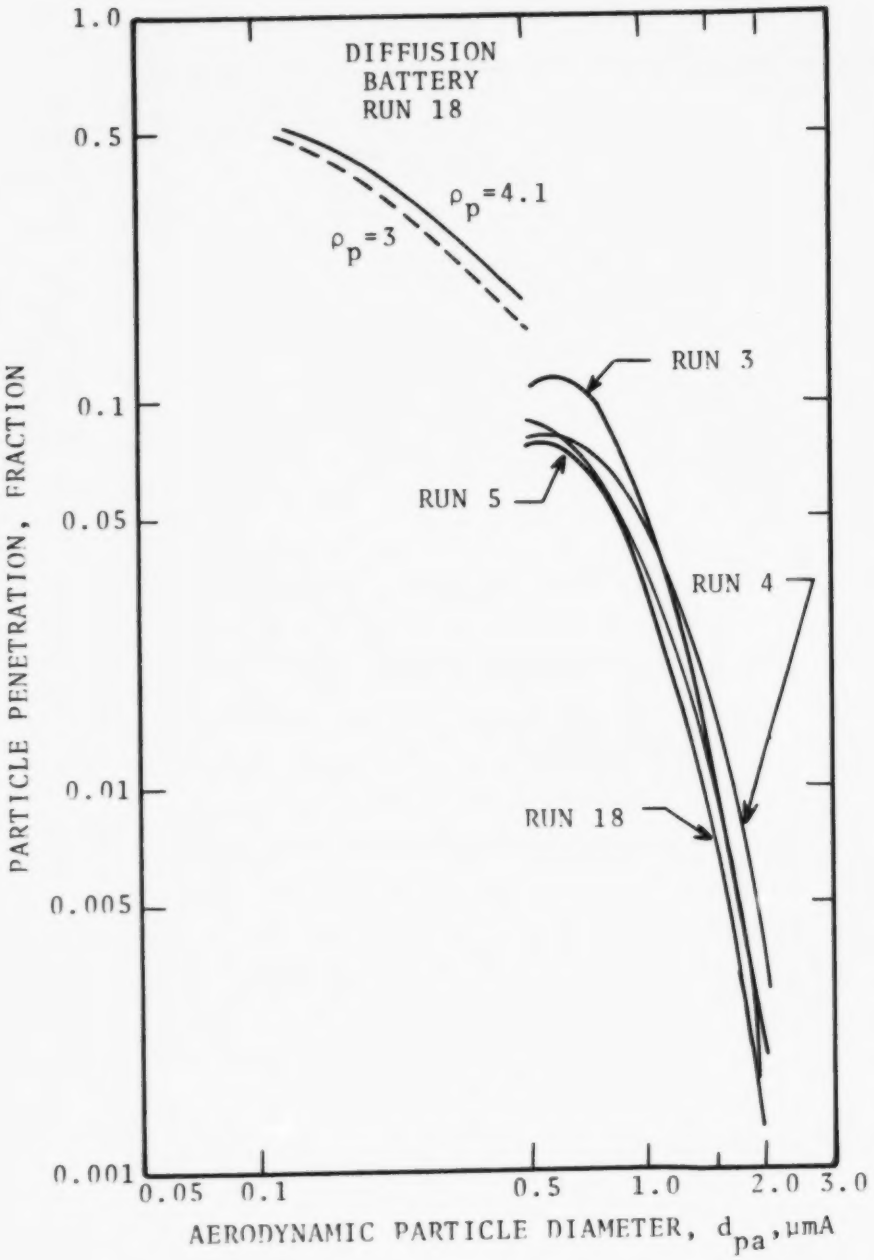

Figure 26. Penetration versus aerodynamic particle diameter for high gas flow, Runs 3, 4, 5, 18.

SECTION 6

TRW CHARGED DROPLET

SOURCE AND CONTROL SYSTEM

The charged droplet scrubber was developed by TRW Systems. Instead of charging the particles as in the case of APS electrostatic scrubbers, the TRW charged droplet scrubber charges the water drops. The water flows out of small diameter tubes which also act as electrodes. The water is atomized as it jets from the tubes. Particle collection of this scrubber results from inertial impaction and the electrostatic force that exists between the particle and the water drop.

The TRW Charged Droplet Scrubber was a 3-stage 680 Am^3/min (24,000 ACFM) pilot unit controlling emissions from the exhaust of a coke oven. Figure 27 is a schematic diagram of the control system. The emissions were a side stream from a main stack and enter a 1.5 meter inlet duct at 215°C. The gases were then quenched by a water spray system at the rate of 17.0 to 22.7 liters per minute to lower the gas temperature to 121°C or 93°C, respectively.

The gas then entered an 8.4 kW (11.2 HP) forced draft fan which had a capacity of 680 actual m^3/min (24,000 ACFM) at a ΔP of 10.1 cm W.C. The gases then entered through a duct with straightening vanes leading into the scrubber. The estimated pressure drop of the entire scrubber system was 10.1 cm W.C. and the pressure drop for the electrical system was 1.3 cm W.C. From the scrubber system which had three sections plus a high voltage area the gases exited through the 0.91 meter exit stack. The temperature of the gas at the stack exit was 54-66°C.

The particles from the coke oven exhaust were sticky tar, heavy hydrocarbons, light oil and complex compounds. Cooling

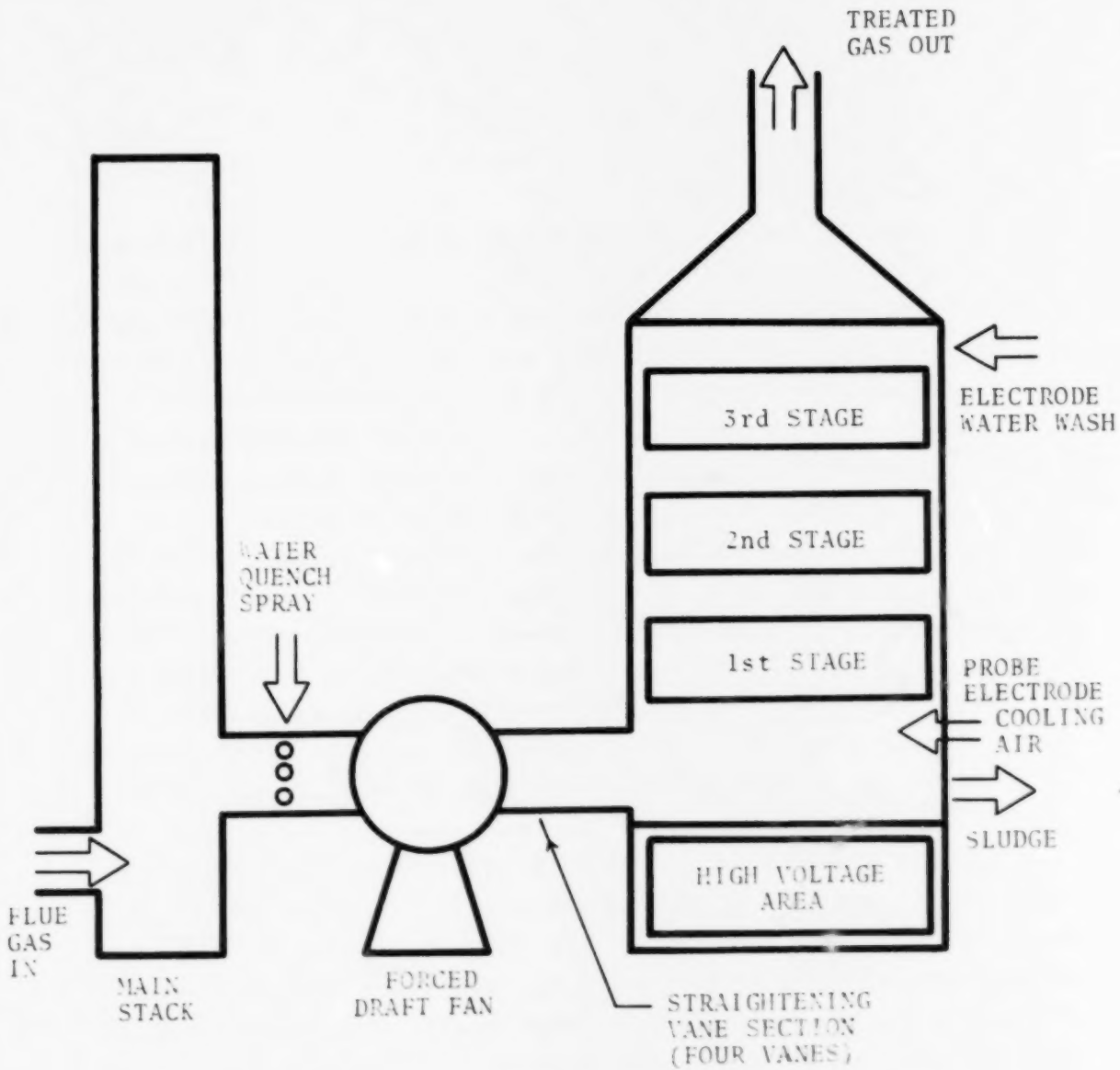

Figure 27. TRW Charged Droplet Scrubber schematic.

air was used on the high voltage electrode which had to be accounted for when analyzing the exit gases.

Scrubber performance is independent of water conductivity in the range of 50 to 1,500 μmhos/cm. Domestic water which was used during the testing period has a conductivity within this range.

TEST METHOD

The performance characteristics of the TRW Charged Droplet Scrubber were determined by measuring the particle size distribution and mass loading of the inlet and outlet gas samples simultaneously.

For the tests performed in October and November 1975, modified EPA type sampling trains with in-stack and ex-stack University of Washington Mark III (U.W.) cascade impactors were used for particle measurements above 0.3 μmA in diameter.

During an impactor run, several inlet and outlet fine particle size measurements were taken alternately with the portable screen diffusion battery. Since the system remained fairly constant during each run, alternate inlet and outlet SDB measurements were considered to approximate simultaneous sampling.

Impactor blank runs were performed periodically to assure that the greased aluminum substrates did not react with the stack gases. A blank impactor run consists of an impactor preceded by two glass fiber filters run at identical sample conditions as the actual sampling runs.

The inlet sample port was located 0.76 meters from the fan outlet in a flow area reducing section with four straightening vanes. The water quench spray section was near the fan inlet. When a velocity traverse was performed on the inlet, eddy mixing and condensation in the pitot tube was evident since some negative velocity heads were measured. The best one point sampling location was taken during the impactor runs. The eddy mixing indicates that the average gas velocity and the gas flow rate (volume/time) are questionable based on the inlet traverse. The outlet port was located

three duct diameters downstream of the nearest disturbance and one duct diameter upstream of the stack outlet. Velocity traverses of the outlet revealed fully developed flow profiles.

OPERATING CONDITIONS

The operating conditions of the TRW Charged Droplet Scrubber for the testing period are shown in Table 9.

TABLE 9. OPERATING CONDITIONS

Condition	Inlet Prior to Quench Sprays	Inlet (1) @ Straightening Vanes Section	Outlet (2) @ Outlet Stack
Temperature, °C	210	107-121	49-63
Velocity, m/sec	---	6.5-7.4	7.0-7.9
Am^3/min	---	637.0-727.3	274.3-311.7
ACFM	---	22,500-25,690	9,690-11,010
DNm^3/min @ 0°C	---	383.2-437.6	200.9-228.3
DSCFM @ 21°C	---	14,580-16,650	7,650-8,690
Vol % H_2O vapor	2-9	7-18	7-15
Static Pressure	-9.3 cm W.C.	+2.5 cm W.C.	+1.2 cm W.C.

Water quench spray	17.0-22.7 ℓ/min
Electrode water rate	45.4-60.6 ℓ/min
Electrode voltage	31,000-38,000 volts
Area for gas flow in scrubber	7.36 m^2
Gas velocity in scrubber (3)	0.62-.71 m/s
Electrode probe cooling air(4)	11.7 std m^3/min @ 21°C
Current	205 mA @ 37 kV, 152 mA @ 32.7 kV

(1) Inlet velocity traverse revealed eddy flow patterns and condensation, e.g., minus velocity heads at some traverse points. This is due to the inlet sample location being in a flow area reduction section with straightening vanes, water condensation in the traverse line due to the quench sprays, and close location to the blower fan outlet. Therefore the data presented for flow are suspect.

(2) More reliable flow data than inlet data.

(3) Based on outlet Am^3/min.

(4) Electrode probe cooling air accounted for as dilution air.

DATA

Cascade Impactor Data

A total of twenty simultaneous inlet and outlet impactor sample runs were performed on the TRW Charged Droplet Scrubber and are summarized in Table 10. The runs were performed for the series of test conditions that TRW had established for their own tests. Table 11 provides a cross reference between the runs and the TRW test matrix.

TABLE 10. TEST RUN SUMMARY

Date	Run No.	Scrubber Velocity (m/s)(2)	Electrode Voltage (kV)	Mass Loadings (mg/DNm^3) Inlet	Outlet	$\overline{Pt}$ %
10/14/75	1	0.62	31	232	35.8	15.4
10/16/75	4	0.71	35	163	61.0	37.5
10/17/75	6	0.62	35	188	11.0	5.8
10/21/75	8	0.71	31	247	29.2	11.8
10/21/75	9	0.71	33	132	41.5	31.4
10/22/75	10(1)	0.71	38	166	84.5	50.7
10/24/75	13(1)	0.62	33	953	56.6	5.9
11/4/75	14	0.71	38	201	23.1	11.5
11/5/75	15	0.71	38	419	35.5	8.5
11/5/75	16	0.71	38	182	22.2	12.2
11/6/75	17	0.62	38	508	23.1	4.5
11/6/75	18	0.62	38	169	21.9	13.0
11/7/75	19	0.71	33	217	25.5	11.7

Runs 2, 3, 5, 7, 11, 12, 20 were not included because of field sampling problems with the weighing balance or sampling equipment train.

(1) For all runs the inlet loading was measured after the quench sprays. For runs 10 and 13 only the inlet was also sampled before the water quench sprays and are noted as runs 10P and 13P.

(2) Scrubber velocity was based on the outlet Am^3/min.

TABLE 11. CROSS-REFERENCE TO TRW TEST MATRIX

RUN NO. IN THIS REPORT	RUN NO. IN TRW TEST MATRIX	TRW CONTROL VARIABLES
1	12	A_0 B_0 C_0 D_1
4	13	A_1 B_1 C_1 D_0
6	14	A_1 B_0 C_1 D_1
8	10	A_0 B_1 C_0 D_0
9	10	A_0 B_1 C_0 D_0
10	15	A_1 B_1 C_0 D_1
13	11	A_0 B_0 C_1 D_0
14	2	A_1 B_1 C_0 D_0
15	7	A_1 B_1 C_1 D_1
16	7	A_1 B_1 C_1 D_1
17	8	A_1 B_0 C_1 D_0
18	8	A_1 B_0 C_1 D_0
19	4	A_0 B_1 C_1 D_0

where the control variables were:

Variable	Symbol	Low Level	High Level
Electrode Voltage	A	A_0 (Runs 1-8, 31,000 volts) (Runs 9-16, 33,000 volts)	A_1 (Runs 1-8, 35,000 volts) (Runs 9-16, 38,000 volts)
Gas Velocity In Scrubber	B	B_0 (0.62 m/sec)	B_1 (0.71 m/sec)
Electrode Water Flowrate	C	C_0 (45.4 ℓ/min)	C_1 (60.6 ℓ/min)
Pre-Cooling Water Flowrate (Water Quench Spray)	D	D_0 (17.0 ℓ/min)	D_1 (22.7 ℓ/min)

Particle concentration, particle size, sampled volumes, and size distributions are tabulated in the Appendix A, Tables A-1 through A-13. Size distributions for the impactor runs are given in Figures A-1 through A-13. A summary of the inlet and outlet size distributions tests is given in Table 12.

Average sample times for the inlet were ten to twenty minutes depending on the mass loading, while the outlet sample times averaged approximately 45 minutes.

The sample data obtained were fairly consistent depending on operation of the scrubber. No data were obtained for runs 2, 3, 5, 7, 11, 12, and 20 because of field sampling problems with weighing balance and sampling train. Other runs were of questionable value because of impactor problems, sampling train problems, entrainment problems, and upset conditions (heavy loading) of the TRW Charged Droplet Scrubber.

Run 1 experienced inlet impactor hole plugging on the 5th and 6th stages of up to 50%. Impactor hole plugging would cause the stage cut diameter to be lower than it would be.

Run 4 experienced heavy loading on the outlet impactor for 15 to 40 minutes total run length. Since the heavy loading was at the end of the run it would cause the penetration to be higher.

For Run 9 the outlet impactor's 6th and 7th stages were very wet indicating condensation of water vapor or hydrocarbon materials.

Run 10 experienced heavy loading conditions during the sampling period. When heavy loading conditions were not simultaneous on inlet and outlet impactor runs faulty penetration data are obtained.

Run 15 is questionable because the inlet 3rd and 5th impactor stages had holes plugged 20-30%. Also the inlet sampling was during heavy loading 1 out of 18 minutes and mild loading (indicating a loading above normal but still not heavy) 3 out 18 minutes while the outlet loading was heavy 9 of 30 minutes and mild 7 of 30 minutes.

Run 18 on the outlet sampling had a heavy loading for 8 of 40 minutes at the end of run. Noting that the inlet sampling ran only 24 mintues and was shut off when the heavy loading occurred on the outlet, one would expect higher penetration than actual.

TABLE 12. INLET AND OUTLET SIZE DISTRIBUTION SUMMARY

Run No.	Inlet		Outlet	
	d_{pg}, μmA	σ_g	d_{pg}, μmA	σ_g
1	1.37	2.7	0.57	2.6
4	0.89	2.0	0.69	1.9
6	0.96	2.0	0.96	2.0
8	0.59	2.1	0.41	2.7
9	0.41	2.6	0.61	1.8
10	2.10	4.3	0.95	2.1
13	1.02	1.9	1.13	2.0
14	1.27	4.2	1.00	2.2
15	1.35	2.1	1.40	2.5
16	0.67	2.5	0.83	2.3
17	1.55	2.2	1.06	2.2
18	1.15	8.0	1.25	2.7
19	1.19	2.8	0.98	2.5

Diffusion Battery Data

Diffusion battery data were taken on December 4 and 5, 1975. Four inlet runs were attempted. Runs 1 and 4 inlets yielded the only usable data. Runs 2 and 3 had to be aborted due to cascade impactor plugging, upset conditions, and blown fuses on the sampling train. Sampling on the outlet yielded no data for the following reasons: Condensation in plastic tubing on the Gardner CNC caused fogging on the upper lens of the Gardner and this problem could not be alleviated.

Figure A-14 in the Appendix contains the inlet size distributions for the two diffusion battery runs that were usable. Since no outlet data were obtained penetrations could not be calculated.

PARTICLE PENETRATION

Particle penetration versus particle size was calculated for the data obtained from the TRW Charged Droplet Scrubber. Figures 28 through 31 represent penetration curves obtained from cascade impactor data for four groups of data sets for low to high electrode voltage and for low to high gas velocity.

Experimental test results on the TRW Charged Droplet Scrubber showed overall collection efficiencies ranging from 94.1% for low gas velocity and low electrode voltage and 94.9% for low gas velocity and high electrode voltage. These results are based on runs that did not have any problems during the testing period such as heavy loading conditions, entrainment, or impactor hole plugging.

The penetration was calculated by fitting the inlet and and outlet particle size data and by the method described in a previous section.

ECONOMICS AND OPERATION PROBLEMS

The Charged Droplet Scrubber tested was a pilot unit. Numberous scrubber upset conditions (heavy loading) were encountered during the sampling period. A high efficiency entrainment separator should be incorporated into the scrubber system because heavy entrainment from the scrubber was visible.

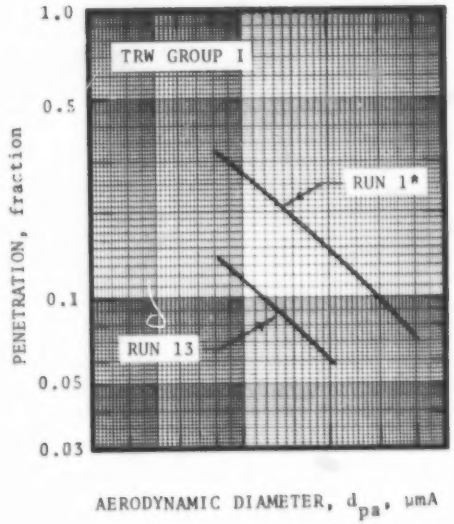

*Impactor 5th & 6th stage holes plugged up to 50%

Figure 28. Particle penetration versus aerodynamic diameter for low electrode voltage and low gas flow rate.

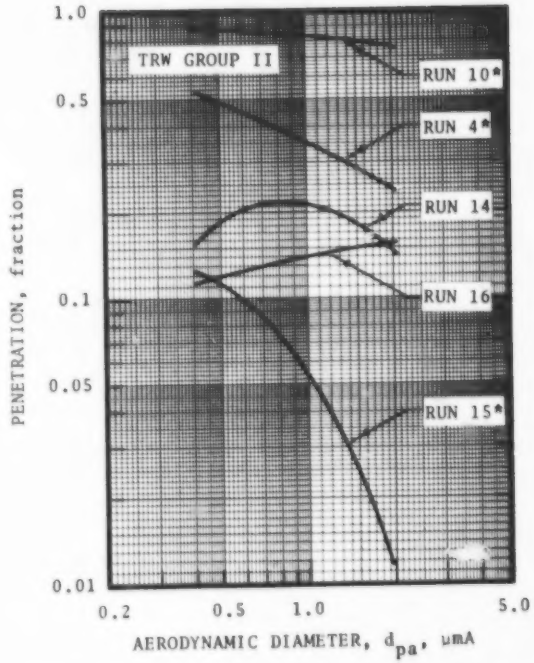

*4 - Heavy loading on outlet 15 of 40 minutes @ end of run.
*10 - Heavy loading conditions while sampling.
*15 - 3rd to 5th impactor stages 20-30% plugged.
Inlet 1 of 18 minutes heavy loading, 3 of 18 mild loading.
Outlet 9 of 30 minutes heavy loading, 7 of 30 mild loading.

Figure 29. Particle penetration versus aerodynamic diameter for high electrode voltage and high gas flow rate

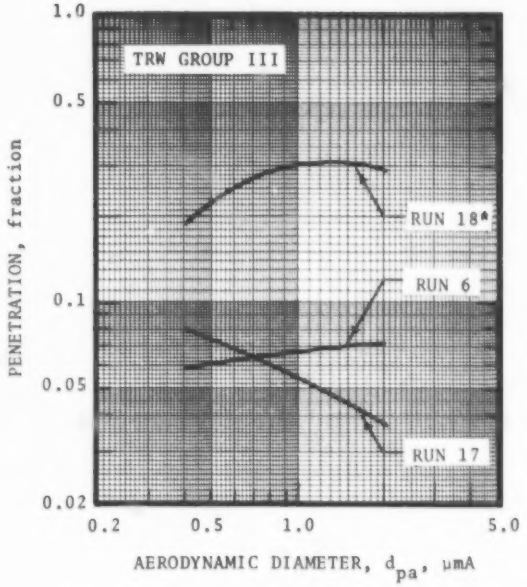

*18 - Heavy loading on outlet sample 8 of 40 min. till end of run - then very heavy loading.

Figure 30. Particle penetration versus aerodynamic diameter for high electrode voltage and low gas flowrate

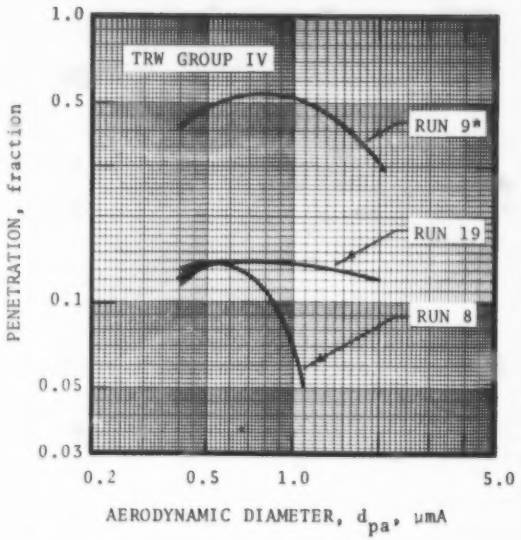

*9 - Impactor 6th and 7th stages very wet

Figure 31. Particle penetration versus aerodynamic diameter for low electrode voltage and high gas flow rate.

Cost data for the TRW Charged Droplet Scrubber were not provided by the manufacturer.

The theoretical power consumption for the electrical power section of the TRW Charged Droplet Scrubber was 25.9 W/(m^3/min) at 37 kV operation and 17.0 W/(m^3/min) at 32.7 kV operation. Power consumption for the fan section was 33.3 W/(m^3/min) based on a fan and motor efficiency of 50% and a total system pressure drop of 10.1 cm W.C.

A venturi scrubber with equivalent overall collection efficiency and cut diameter would have a pressure drop of approximately 100 cm W.C. Based on a fan and motor efficiency of 50%, the power consumption would be 354 W/cm^3/min.

Based on 8,000 hours operation per year and a cost of 3¢ kWhr, the TRW operating cost savings for a 2,830 m^3/min (100,000 CFM) unit would be $203,000/yr.

MATHEMATICAL MODEL

TRW has developed a model for the collection efficiency of their Charged Droplet Scrubber. However, since the model is quite complicated and difficult to apply, it is beyond the scope of this report to make a comparison with the data. Information regarding the model is presented by Lear, et al.(1975).

ECONOMICS

No data were available for predicting the annual costs associated with operating the TRW Charged Droplet Scrubber.

SECTION 7

PERFORMANCE TEST METHOD

The method of approach to the program objectives involved a number of experimental determinations to obtain collection efficiency data, the aquisition of information on system characteristics and behavior, and computations which utilized the performance data and mathematical models. Over the course of the program the methods and apparatus used were generally improved and were modified to suit each specific test situation but the main features were similar and will be described here.

The most important experimental measurements were those regarding particle size and concentration. Cascade impactors were used for particle measurements above 0.3 umA. The Air Pollution Technology portable screen diffusion battery (A.P.T.-S D B) was used for particle measurements from 0.01 μm to 0.1 μm (actual). The apparatus and methods used are outlined below.

1. Gas velocity distribution and parameters had to be measured at the inlet and outlet of the scrubber in order to define the following:
   a. Conditions for isokinetic sampling.
   b. Particle concentration per unit volume of dry gas, which is a consistent basis for comparing inlet with outlet in the computation of efficiency.
   c. Gas flow rate.
   d. Amount of liquid entrainment in the outlet.

Methods to measure these parameters are tabulated below:

Parameter	Equipment	Method
Gas velocity and flow rate	Standard pitot tube or calibrated type "S" pitot tube; differential pressure gauge.	EPA Method 1; EPA Method 2.
Gas temperature	Calibrated thermocouple or mercury filled glass-bulb thermometer.	
Humidity	Thermometers.	Wet and dry bulb temperature measurement on a flowing sample withdrawn from the duct.
Pressure	Inclined water manometer or a pressure gauge.	Measured by means of a static pressure tube inserted in the duct.

2. The most essential part of the scrubber performance tests is the determination of particle size distribution and concentration (loading) in the inlet and outlet of the scrubber. For accurate determination of particle size distribution, a collection mechanism that collects particles and causes neither formation nor breakup of aggregates is necessary. Cascade impactors come close to meeting these requirements.

In a cascade impactor, particles are classified by inertial impaction according to their mass. The larger ones are collected on the plate opposite the first stage and the smallest on the plate opposite the last stage. A.P.T. uses Brink, Andersen, University of Washington Mark III, and a cascade impactor of A.P.T.'s own design for particle size fractionation. These impactors (except Brink) classify particles into seven size groups and are capable of sizing particles down to about 0.1 μm diameter (actual). All impactors were calibrated in the laboratory according to EPA guidelines, see Calvert et al. (1976c) and Harris (1977) on calibration method.

In order to minimize probe losses all tests were made with the impactors in the duct and with the inlet nozzles appropriately sized to give isokinetic sampling. A modified EPA Method 5 train was used to monitor the sample gas flow rate. Figure 32 shows the sampling train arrangement.

In some tests, a pre-cutter was used to remove either the heavy particle loading from inlet samples or the entrained liquid from outlet samples. A round jet impactor with about 8 μmA cut diameter was found to have good characteristics and was adopted for use for both inlet and outlet sampling. The impactors were either given time to reach the duct gas temperature or heated to prevent condensation.

To increase the weighing accuracy, light weight substrates were used on the collection plates. Generally, either greased aluminum foil or a glass fiber filter paper substrate was used. Impactor substrates and back-up filters were weighed with an analytical balance to the nearest tenth milligram (10^{-4}g).

Particle size distribution and loading measurements were conducted simultaneously at the scrubber inlet and outlet. The method minimizes the effects of particle size distribution changes caused by fluctuations in the operation parameters. Since the program objective was to investigate scrubber performance on fine particles, the sampler was held at one location in the duct for the duration of each sampling run. This is an adequate technique for obtaining good samples of particles smaller than a few microns in diameter because they are generally well distributed across the duct.

Blank impactor runs were performed periodically to assure that the greased aluminum substrates did not react with the stack gases or lose weight. A blank impactor run consists of an impactor preceded by two glass fiber filters and run at identical sample conditions as the actual sampling runs.

3. In-stack filter samples were also taken to obtain total particulate loadings and overall collection efficiencies of the system. The sampling train arrangement was the same as the cascade impactor train except the cascade impactor was

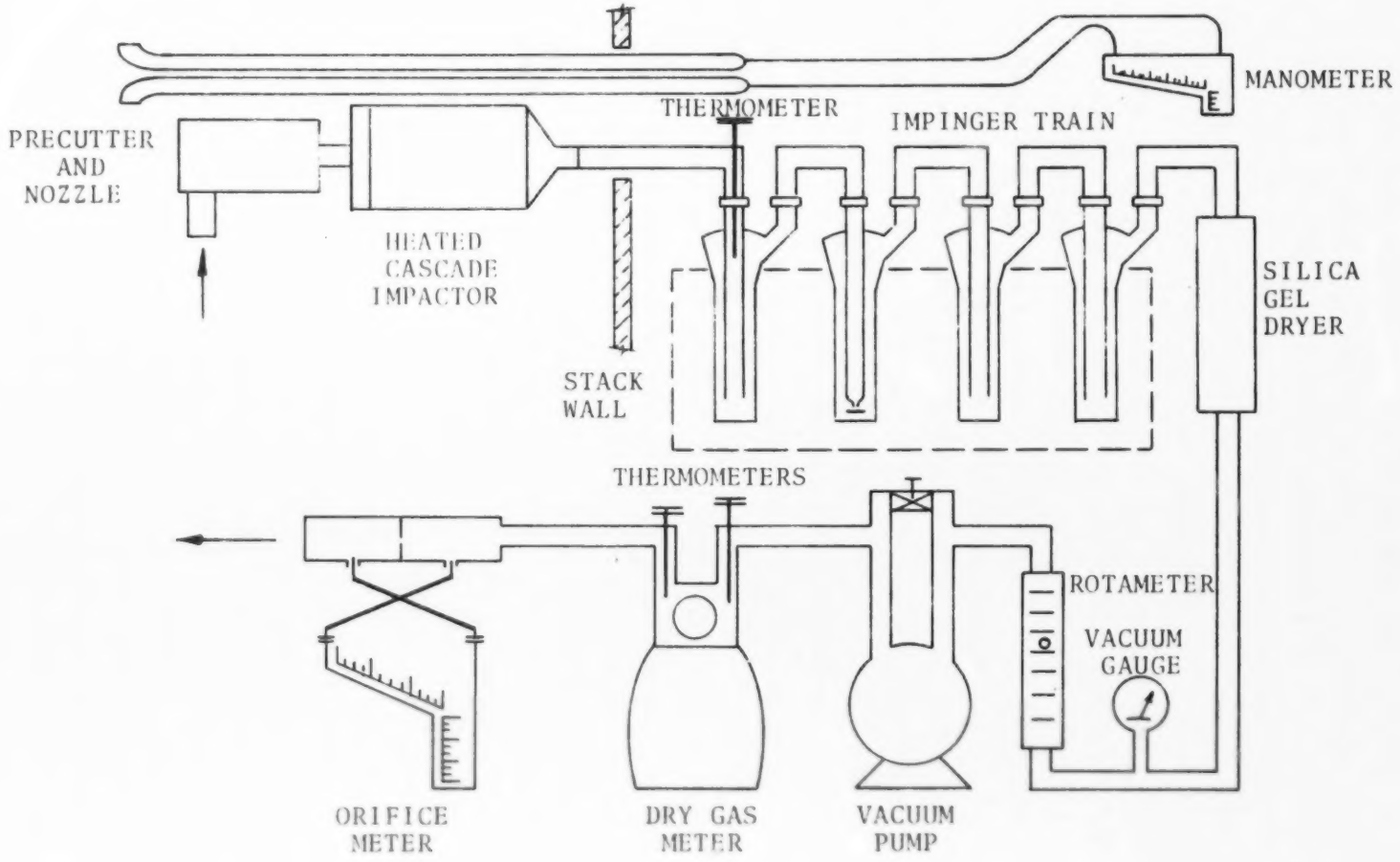

Figure 32. Modified EPA sampling train with in-stack cascade impactor.

replaced with a filter.

4. Inertial impaction devices (cascade impactors) are normally insufficient for measurement of particulates less than 0.3 μm (actual diameter). Fractionation of these particles is best accomplished by diffusional collection devices, or diffusion batteries, usually consisting of closely spaced parallel plates or long, thin tubes. Large quantities of pumps, dilution apparatus, and other battery related equipment are bulky and prove to be cumbersome in field use. For this and other reasons, Air Pollution Technology, Inc. developed a portable screen diffusion battery which is lighter and more mobile than previous devices.

The Screen Diffusion Battery utilizes a series of layered screens intermittently separated for sampling purposes (Figure 33). Size fractionation by the diffusion battery is detected by measurement of overall particle concentrations of the gas stream into and out of a known number of screens using a condensation nuclei counter (CNC). Concentrated aerosol samples are diluted until compatible with the CNC ($\sim 10^6$ particles/cm^3). Screen penetration data are then analyzed to determine size distribution and cumulative mass loading of the particulates in the stream. If desired, cascade impactor and diffusion battery analyses can be combined and an overall characterization of the particulate size distribution (and scrubber penetration) obtained.

Fine particle size measurements with the diffusion battery were not taken simultaneously at the inlet and outlet of the scrubber system. During an impactor run, several inlet and outlet measurements were taken alternately with the S D B Since the system remained fairly constant during each run, alternate inlet and outlet S.D.B. measurements were considered to approximate simultaneous sampling.

Each S D B run consisted of a continuous series of CNC readings. Normally, CNC counts were taken at each diffusion battery stage in order of increasing number of screens and then the process was repeated until three to four sets of

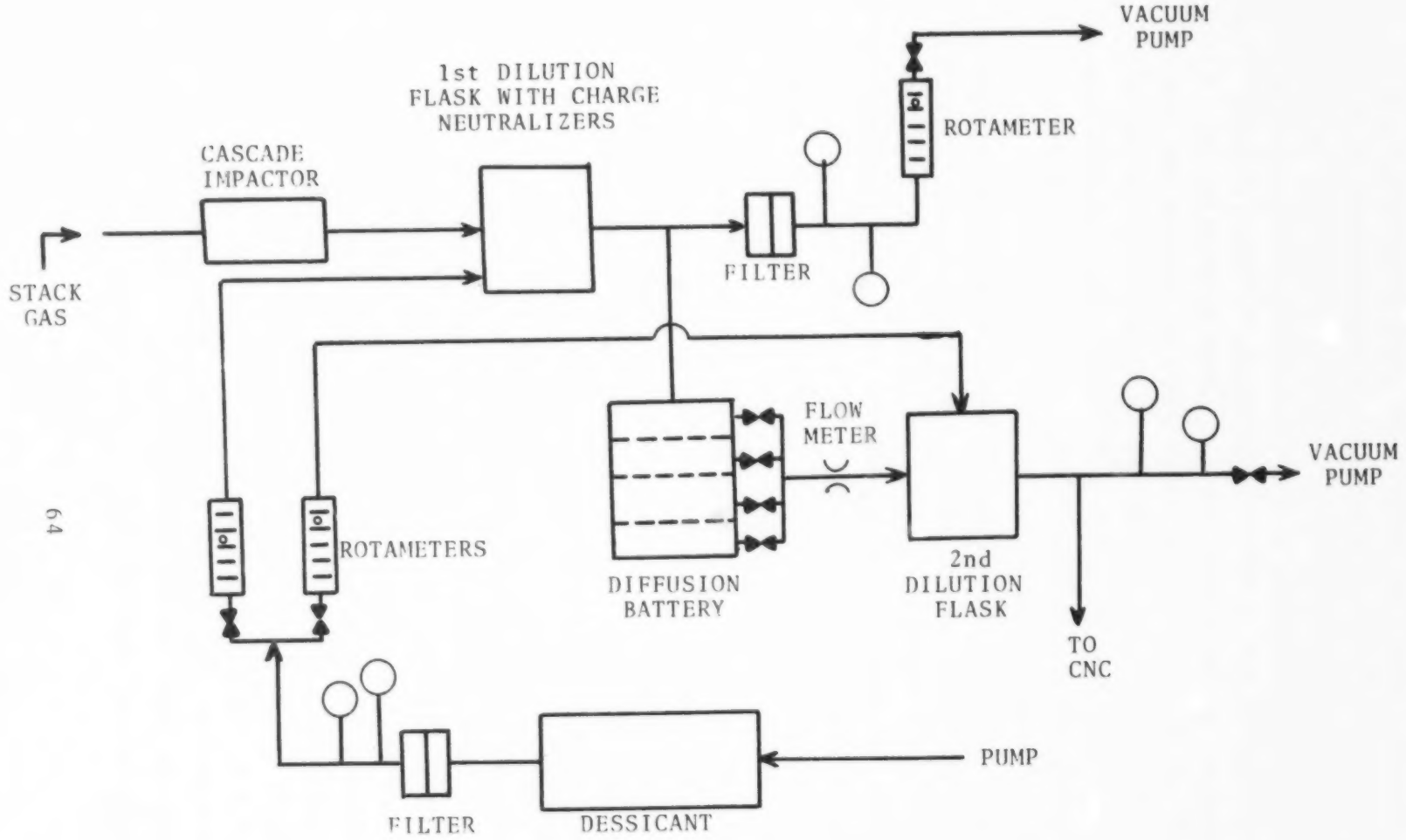

Figure 33. Schematic diagram of diffusion battery system.

readings were obtained. Continuous monitoring of flow, temperatures, and pressures enabled steady operation of the diffusion battery. Conditions in the duct (pressure, gas velocity, temperature, and water vapor content) were obtained during the impactor tests.

The size of particles entering the diffusion battery was limited by using a cascade impactor pre-cutter on the in-stack end of the probe. Isokinetic sampling was not maintained because the particles to be measured were too small to be segregated by inertial effects from bends in the gas stream. The sample stream entering the diffusion battery was immediately diluted with heated, dried, filtered air to control condensation. Two Polonium 210 charge neutralizers were inserted into the flask to eliminate electrostatic effects. A portion of the resultant aerosol was directed through the diffusion battery and the outlet diluted to a concentration measurable by the Gardner CNC. The aerosol from the second dilution flask was sampled with the Gardner CNC. The excess aerosol was exhausted through the vacuum pump. The excess aerosol from the first dilution was passed through an absolute filter and pumped to the atmosphere. The Gardner CNC was calibrated daily against a standard B.G.I. Pollak, Model P, CNC and found to read consistently 33% lower than the Pollak CNC for the concentration range used in the testing.

ERROR ANALYSIS

Sample Bias

It is important to note that the program objective is to investigate scrubber performance on fine particles and, consequently, it is not necessary that the methods used be accurate for large particles. This makes the sampling simpler in the following ways:

1. Isokinetic conditions are not important for fine particles. For example, the error caused by sampling 4 μmA particles at a velocity 50% higher or lower than the gas stream velocity would only be about 2 or 3% of the concentration.

2. The fine particles will be well distributed in the gas stream, except in cases where streams with different particle concentrations have not had time to mix, so single point sampling is generally sufficient. To illustrate, we may note that the Stokes stopping distance of a 3 μmA particle with an initial velocity of 15 m/sec (50 ft/sec) is about 0.04 cm (0.016") and for a 1 μmA diameter particle it is one ninth of that. Since the stopping distance is the maximum a particle can be displaced from a gas stream line by going around a right angle turn, it is obvious that fine particle distribution in the gas stream will be negligibly affected by flow direction changes.

3. The effect of a pre-cutter on the size resolution of a cascade impactor is not significant in the size range of interest, so long as the pre-cutter has a cut diameter larger than several microns.

Diffusion Battery

The Screen Diffusion Battery was calibrated in Air Pollution Technology's (A.P.T) small particle laboratory. An aerosol of known size distribution was generated and passed through the diffusion battery. The total number concentration was measured with a condensation nuclei counter at the battery inlet and outlet of each S D B stage. The penetration of particles (percent) was then calculated and plotted against solidity factors on semi-logarithmic paper. The experiment was repeated with the same aerosol until a smoothed average curve relating number penetration to solidity factor was obtained. From the smoothed curve, a correction factor for the theoretical diffusion battery performance was determined.

The scatter of data points about the smoothed (fitted) calibration curve represents the experimental error in the penetration measurement. This measurement error included meter reading error, accuracy of the CNC, etc. The measurement error was defined in terms of relative error, or the deviation from the averaged penetration value divided by the averaged value.

This procedure was repeated on other aerosols of known size distribution. The maximum relative error was then determined from these experiments for each solidity factor. The maximum relative error the Screen Diffision Battery determined by this method is 10.4% for solidity factors of 13, 26, and 40.

Cascade Impactors

Cascade impactors were used as the principal means of obtaining information about the inlet-outlet size distributions. It was important to understand the sources of error and how the error can be minimized.

The procedural errors include the accuracy of the weighing of the deposits, reading of the test data such as temperature, gas volume, time, and pressures. The errors from the impactor design and construction include wall losses, accuracy and precision in construction of critical components, and particle re-entrainment from the collection surface.

Some of the design and construction limitations can be reduced by procedures such as recovering the wall losses and by sampling at certain flow rates and times to reduce re-entrainment errors and by calibration of the impactor. The experimental data obtained with commercial impactors were reported by Smith et al. (1974). Smith et al (1974) reported that all impactors tested had appreciable wall losses for particle diameters above 10 microns. This error can be reduced by brushing the material from the wall onto appropriate collection disks. The flow velocity through the impactor jets should not be above 65 m/sec to be absolutely certain of avoiding re-entrainment of particles from the collection substrate. The extent of re-entrainment will depend on the properties of the material and the amount of deposit. Lundgren (1967) reported that re-entrainment increased as the collection surface became coated with particles. However, Rao (1975) reported that collection efficiency increased with increased particle load. When the particle weight is over 10 mg, part of the deposit may break away from the surface and migrate within the impactor. The light-weight deposit places

importance on accurate weighing. The analysis of impactor errors was limited to the weighing error and in the calculation of collection efficiency error. The effects of weighing errors on the results of impactor tests have been analyzed by Sparks (1971). An analysis of the weighing error using three different estimations was reported by Fegley et al. (1975). The results indicate that, when the weight of sample per stage is less than 1 mg when weighed with a balance with a precision of 0.05 mg, the error in the fractional mass will be greater than 10%.

SECTION 8

DATA REDUCTION AND COMPUTATION METHOD

CASCADE IMPACTOR DATA ANALYSIS

In a cascade impactor particles are classified by inertial impaction according to their mass. The larger ones are collected on the plate opposite the first stage and the smallest on the plate opposite the last stage.

Once the stage "catches" have been measured, usually by weighing particle collection foils or papers, the data analysis is relatively simple. Generally the objective is to make a plot of particle diameter versus mass percent oversize or undersize and to represent the size distribution in terms of log-normal distribution parameters if possible. Thus, it is necessary to do the following:

1. Add all of the stage and filter collection weights to get the total particle mass collected.
2. Compute either:
   a. Cumulative percent collected as the gas flows through succeeding stages. This is "percent oversize".
   b. Cumulative percent penetrating as the gas flows through succeeding stages. This is "percent undersize".
3. Compute the cut diameters for the impactor stages, taking into account gas viscosity (or temperature) and gas sampling flow rate. The equation is:

$$d_{pac} = K_{p50}^{0.5} \left(\frac{9\ \mu_G\ d_j}{u_j\ x\ 10^{-8}} \right)^{0.5} \qquad (8)$$

where d_{pac} = impactor stage cut diameter, μmA
μ_G = gas viscosity, poise
d_j = jet diameter, cm
u_j = jet velocity, cm/s
K_{p50} = inertial impaction cut parameter, K_p at 50% efficiency

The particle diameter used is called "aerodynamic diameter" and it has the unit of "aerodynamic microns", μmA. This is the effective diameter for particle separation by inertial impaction and it takes into account the effects of particle density and particle "slip" between gas molecules. It is related to the actual physical size of the particle by the following equation:

$$d_{pa} = d_p \left(\rho_p \, C' \right)^{\frac{1}{2}} \qquad (9)$$

where d_{pa} = aerodynamic particle diameter, μmA
d_p = actual particle diameter, μm
ρ_p = particle density, g/cm³
C' = Cunningham slip correction factor, dimensionless

At room temperature for air the Cunningham slip correction factor, C', is given by:

$$C' = 1 + \frac{0.165}{d_p} \qquad (10)$$

Figure 34 is a plot of aerodynamic particle diameter versus particle diameter for various particle densities.

If the particle distribution follows the log-normal law, a straight line will result on log-probability paper. The 50% value of particle diameter is the mass median diameter "d_{pg}" and the geometric standard deviation "σ_g" is given by:

$$\sigma_g = \frac{84.3\% \text{ value of } d_{pa}}{50\% \text{ value of } d_{pa}} \qquad (11)$$

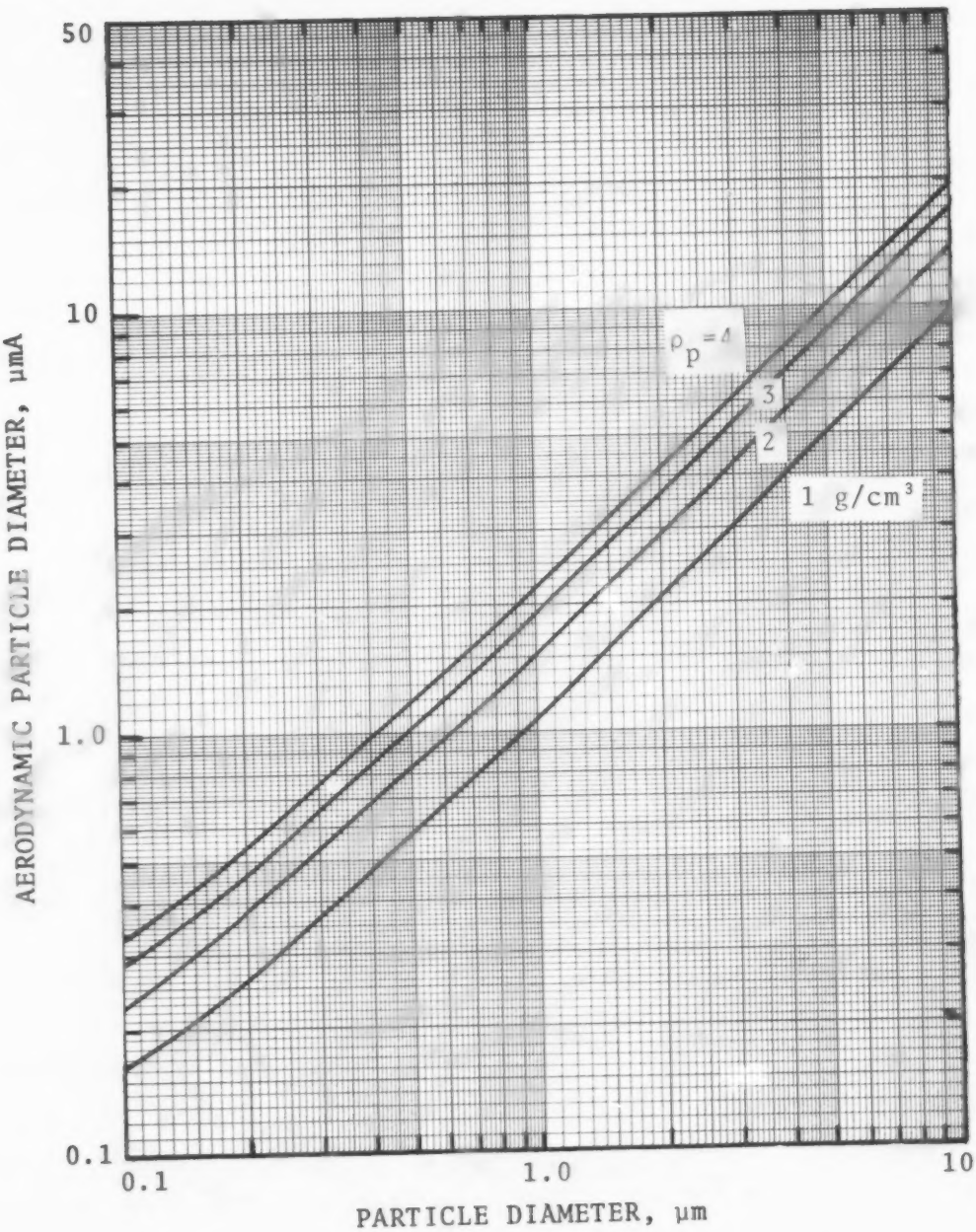

Figure 34. Particle diameter versus particle aerodynamic diameter.

OVERALL PARTICLE PENETRATION

Overall particle penetration is defined as

$$\overline{Pt} = \frac{1}{C_{pt}} \int_0^{C_p} Pt_d \, \bar{d} \, C_p \qquad (12)$$

$$= \frac{\text{mass concentration out}}{\text{mass concentration in}}$$

where $\overline{Pt}$ = overall particle penetration, fraction or percent

Pt_d = penetration for particles with diameter d_p, fraction

C_{pt} = total particle weight, g

C_p = mass of particles, g

The overall particle penetration can be computed using the data from a simultaneous inlet and outlet cascade impactor or filter run.

PARTICLE PENETRATION AS A FUNCTION OF PARTICLE DIAMETER

The particle penetration for particle diameter, d_p, or grade penetration curve is given by

$$Pt_d = \frac{f(d_p)\text{outlet}}{f(d_p)\text{inlet}} = \frac{\left[\frac{\bar{d}C_p}{\bar{d}(d_p)}\right]_{\text{outlet}}}{\left[\frac{\bar{d}C_p}{\bar{d}(d_p)}\right]_{\text{inlet}}} \qquad (13)$$

where Pt_d = particle penetration for particle diameter, d_{pi}, fraction

$f(d_p)$ = particle frequency distribution

$\frac{\bar{d}C_p}{\bar{d}(d_p)}$ = the slope of the cumulative mass versus particle diameter curve at d_p, dimensionless

Particle penetration as a function of particle size is computed from inlet and outlet particle size distributions and concentration data. The major steps involved in the computation are as follow:

1. Reduce cascade impactor data to the form of cumulative particle mass concentration for each impactor cut diameter.

2. Determine the slopes of the cumulative mass distribution curves at several values of particle diameter for

both the inlet and outlet and then compute penetration at each particle diameter.

There are several techniques to determine the slope of the cumulative mass distribution curve. Some of the techniques are discussed below.

1. Graphical technique - Cumulative mass concentration versus aerodynamic particle diameter data may be fitted with a curve by eyeball method. The slopes of the curve at various values of particle diameter are then measured graphically.

2. Curve fitting - Curve fitting to the data points and the measurement of curve slopes by eye involves subjective judgment. To eliminate the judgment errors, it is possible to fit the data with a mathematical function and then evaluate the slope analytically. We have tried fitting the cumulative mass curves with polynomial functions, log-normal distribution functions, and the Weibull distribution

Polynomial Curve Fit

The principle of least squares was used to fit a function of the following form to the data points

$$W_{cum} = a_0 + a_1 d_{pa} + a_2 d_{pa}^2 + ... + a_n d_{pa}^n \qquad (14)$$

where W_{cum} = cumulative mass concentration, g/cm^3

d_{pa} = aerodynamic particle diameter, μmA

"a_0, a_1, a_2, ... a_n" are constants to be determined. A second degree polynomial function will normally fit the data points closely.

Curve smoothing is also required when using a polynomial function because the resulting curve oscillates. The inlet and outlet polynomial curves do not oscillate in the same manner. Therefore, without curve smoothing, the calculated scrubber penetration curve will also oscillate.

Log-normal Distribution

If the inlet and outlet size distributions are nearly log-normal, then a purely mathematical particle penetration is used. The mathematical log-normal penetration is based on the

following:

The distribution of particle sizes is:

$$P(x) = \frac{1}{(2\pi)^{\frac{1}{2}}} \int_{-\infty}^{x} e^{-t^2/2} dt \qquad (15)$$

where $P = \frac{W}{W_t}$, the cumulative mass fraction of sizes smaller than "d_{pa}", and

$$x = \frac{\ln d_{pa} - \ln d_{pg}}{\ln \sigma_g} \qquad (16)$$

The derivative of the distribution function is:

$$\frac{\bar{d}\, P}{\bar{d}\, d_{pa}} = \frac{\bar{d}\, P}{\bar{d}\, x} \frac{\bar{d}\, x}{\bar{d}\, d_{pa}} = \frac{\exp(-x^2/2)}{(2\pi)^{\frac{1}{2}}\, d_{pa}\, \ln \sigma_g} \qquad (17)$$

thus,

$$\frac{\bar{d}\, W}{\bar{d}\, d_{pa}} = \frac{W_t \exp(-x^2/2)}{(2\pi)^{\frac{1}{2}}\, d_{pa}\, \ln \sigma_g} \qquad (18)$$

Using equation (5), the penetration is then:

$$Pt = \frac{(W_t)_{out}}{(W_t)_{in}} \frac{(\ln \sigma_g)_{in}}{(\ln \sigma_g)_{out}} \exp\left(\frac{x^2_{\ in} - x^2_{\ out}}{2}\right) \qquad (19)$$

Weibull Distribution

The Weibull distribution (Lipson & Sheth, 1973) offers 2 advantages over the log-probability distribution. The first is that it has three parameters rather than two. The second is that the cumulative distribution function (CDF) is explicit and does not have to be approximated by multi-termed polynomials.

Cumulative Distribution Function-

$$CDF = 1 - \exp\left[-\left(\frac{d_p - d_{po}}{\Theta - d_{po}}\right)^b\right] \quad (20)$$

where d_p = particle diameter
d_{po} = minimum particle diameter
Θ = characteristic diameter
b = Weibull slope

The CDF has the property that:

$$CDF\ (\Theta = d_p) = 0.632 \quad (21)$$

The median particle diameter occurs when the CDF = 0.5, so:

$$d_{pg} = d_{po} + (\Theta - d_{po})\ (\ln 2)^{1/b} \quad (22)$$

Linear Transformation -

Transformation to a linear form;

$$y = A + B\ x \quad (23)$$

requires that:

$$y = \ln\left[\ln\left(\frac{1}{1-CDF}\right)\right] \quad (24)$$

$$x = \ln\ (d_p - d_{po}) \quad (25)$$

therefore,

$$A = -b\ \ln\ (\Theta - d_{po}) \quad (26)$$

$$B = b \quad (27)$$

and,

$$\Theta = d_{po} + \exp\left(-\frac{A}{B}\right) \tag{28}$$

$$b = B \tag{29}$$

Least Squares Curve Fit -

The minimum particle diameter, d_{po}, is that which results in the highest linear correlation coefficient based on the above linear transformation, when a least squares linear regression is performed on the size distribution data. Note that,

$$0 \leq d_{po} < \text{smallest diameter found in the distribution}$$

Density Function -

The Weibull density function is the derivative of the CDF:

$$f(d_p) = \frac{b}{\Theta - d_{po}} \left(\frac{d_p - d_{po}}{\Theta - d_{po}}\right)^{b-1} \exp\left[-\left(\frac{d_p - d_{po}}{\Theta - d_{po}}\right)^{b}\right] \tag{30}$$

Penetration -

The penetration is the ratio of the cumulative mass loading distribution derivatives,

$$Pt\ (d_p) = \frac{C_{T,out}\ f_{out}\ (d_p)}{C_{T,in}\ f_{in}\ (d_p)} \tag{31}$$

where C_T = total mass concentration or loading
"out" = refers to outlet particle size distribution
"in" = refers to inlet particle size distribution
and $f(d_p)$ = is defined by equation (30)

Minimum Particle Diameter, Physical Interpretation -

"d_{po}" is the smallest diameter of the total distribution. A value other than zero means that the data indicate that there is a minimum particle size. This is physically reasonable

because of the particle formation mechanisms and possible agglomeration and/or particle growth.

Characteristic Diameter, Physical Interpretation -

"θ" is analogous to the geometric mean particle diameter of the log-probability distribution and is therefore an indication of the "average" size of the particles in the distribution. The median particle diameter is directly related to "θ" by equation (22).

Weibull Slope, Physical Interpretation -

"b" is analogous to the geometric standard deviation of the log-probability distribution. It indicates the "spread" of the size distribution. The larger the Weibull slope, b, the more uniform (monodisperse) the particle sizes.

SCREEN DIFFUSION BATTERY DATA ANALYSIS

Screen diffusion battery data consist of particle number concentrations which are obtained after each stage in the diffusion battery. Particle penetrations are calculated from the ratio of the number concentration taken at a given SDB stage to the inlet number concentration. The particle size distribution may then be determined from the penetration data.

Most particle formation processes result in a particle size distribution which is log normal. Log normal size distributions are conveniently represented by two parameters: the number median diameter (d_{pN}) and the standard deviation (σ_g). Typically, process created aerosols fail log normality only at the extremes of large and small particles which represent only a small percentage of the total particulates.

Calvert et al. (1974) describes a method for converting log-normal size distributions to overall penetrations using the relation between particles of a discrete diameter and penetration of those particles through the device.

A log normal particle distribution density function is defined by:

$$f(d_p) = \frac{1}{\sqrt{2\pi}\ \ln \sigma_g} \exp\left[-\left(\frac{\ln d_p - \ln d_{pn}}{\sqrt{2\pi}\ \ln \sigma_g}\right)^2\right] \tag{32}$$

$$= \frac{1}{N} \frac{\bar{d}n}{\bar{d}(\ln d_p)} \tag{33}$$

For particle penetration of the form:

$$Pt = \exp\ (-AS\ d_p{}^B) \tag{34}$$

where Pt = penetration fraction of a particle of a given diameter through S

S = solidity factor, dimensionless

d_p = particle diameter, μm

A,B = constants established by theory and laboratory experimentation

n = number of particles, dimensionless

Calvert, et al.(1972) shows that the overall penetration may be predicted:

$$\overline{Pt} = \frac{1}{N}\int_0^n Pt\ \bar{d}n = \int_{-\infty}^{+\infty} Pt\ f(d_p)\ \bar{d}\ (\ln d_p) \tag{35}$$

$$= \int_{\ln (d_p) = -\infty}^{\ln (d_p) = +\infty} \frac{1}{\sqrt{2\pi}\ \ln \sigma_g} \exp \tag{36}$$

$$\left[-\left(\frac{\ln d_p - \ln d_{pn}}{\sqrt{2}\ \ln \sigma_g}\right)^2 - Ad_p{}^B\right] \bar{d}\ (\ln d_p)$$

$$\text{Setting: } z = \frac{\ln d_p - \ln d_{pN}}{\sqrt{2}\ \ln\ \sigma_g} \tag{37}$$

$$\text{and, } \bar{d}z = \frac{1}{\sqrt{2}\ \ln \sigma_g}\ \bar{d}\ (\ln d_p) \tag{38}$$

then substituting equation (37) and (38) into (36) the result is:

$$\overline{Pt} = \frac{1}{\sqrt{\pi}} \int_{-\infty}^{\infty} \exp\left[-z^2 - AS_{dpn}{}^{B} \exp\ (Bz\sqrt{2}\ \ln\ \sigma_g) \right] dz \tag{39}$$

Since:

$$\ln\ (2) = AS(d_{p_{50}})^B \tag{40}$$

then equation (39) becomes:

$$\overline{Pt} = \frac{1}{\sqrt{\pi}} \int_{-\infty}^{\infty} \left[-z^2 - \ln(2)\left(\frac{d_p}{d_{pn}}\right)^B \exp\left(\sqrt{2}\ z\ B\ \ln(\sigma_g)\right) \right] \bar{d}z \tag{41}$$

Calvert and Patterson (1977) have shown that for particles in the size range of $10^{-3}\ \mu m < d_p < 10^{-1}\ \mu m$ the penetration through the SDB is given by:

$$Pt = \exp\left| -1 \times 10^{-4}\ S\ (u_G\ d_c)^{-0.67}\ d_p{}^{-1.29} \right| \tag{42}$$

where u_G = superficial gas velocity, cm/s
d_c = wire diameter of screen, cm

The overall penetration of particles through the SDB is then given by:

$$\overline{Pt} = \frac{1}{\pi} \int_{-\infty}^{\infty} \exp \left[-z^2 - 1 \times 10^{-4} S (u_G d_c)^{-0.67} d_{pN}^{-1.29} \right.$$

$$\left. \exp (-1.29 z \sqrt{2} \ln \sigma_g) \right] \bar{d}z \qquad (43)$$

Equation (43) may be evaluated for a number of "σ_g" and normalized values of the cut diameter "d_{pc}" as shown in Figure 35. Each stage of the SDB has a corresponding cut diameter, d_{pc}, for a given flow rate. The cut diameter, d_{pc}, is the particle size which is collected at 50% efficiency. The value of the cut diameter, d_{pc}, is determined by substituting 0.5 for "Pt" in equation (42).

For a given flow rate and cumulative solidity, S, each stage of the SDB will have a corresponding cut diameter, d_{pc}, as shown by the dotted lines in Figure 36. The number median diameter, d_{pN}, and standard deviation, σ_g, for the aerosol is determined by plotting the penetration data for each stage on the dotted lines. Figure 36 is for a flow rate of 4.7 ℓ/min through the SDB modules containing 250 mesh screens. The data give a continuous curve when plotted on one graph.

The value of d_{pN} corresponds to the value of "d_{pc}" for Pt = 0.5. For the aerosol which corresponds to the penetration data plotted on Figure 36, the value of d_{pN} = 0.026 μm.

The standard deviation, σ_g, of the size distribution is determined by overlaying Figure 36 with the data on Figure 35. By moving the overlay, with horizontal axes coincident, the curve may be situated within the family of curves and the actual "σ_g" may be interpolated by matching the curvatures.

Non-log normal data must be handled by a graph stripping technique outlined by Sinclair (1972) which entails tedious graphical integration and mathematical conversions. In our experience the data have fallen sufficiently close to log normality that the overlay technique is acceptable.

Conversion of number distribution to mass distribution is necessary in order to put the diffusion battery and cascade impactor data on the same basis. The method used to make this

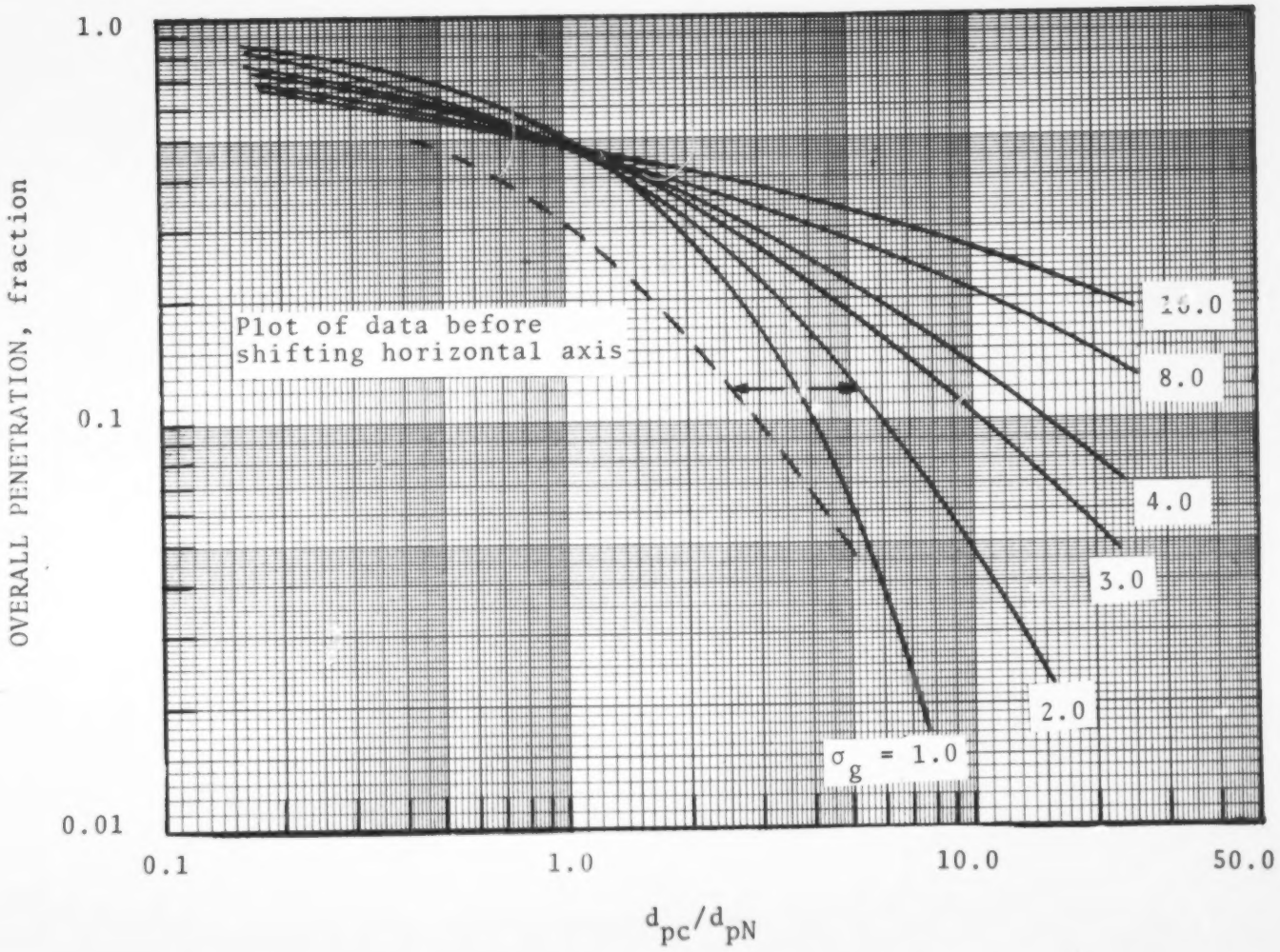

Figure 35. Overall penetration fraction versus "d_{pc}/d_{pN}" with "σ_g" as a parameter.

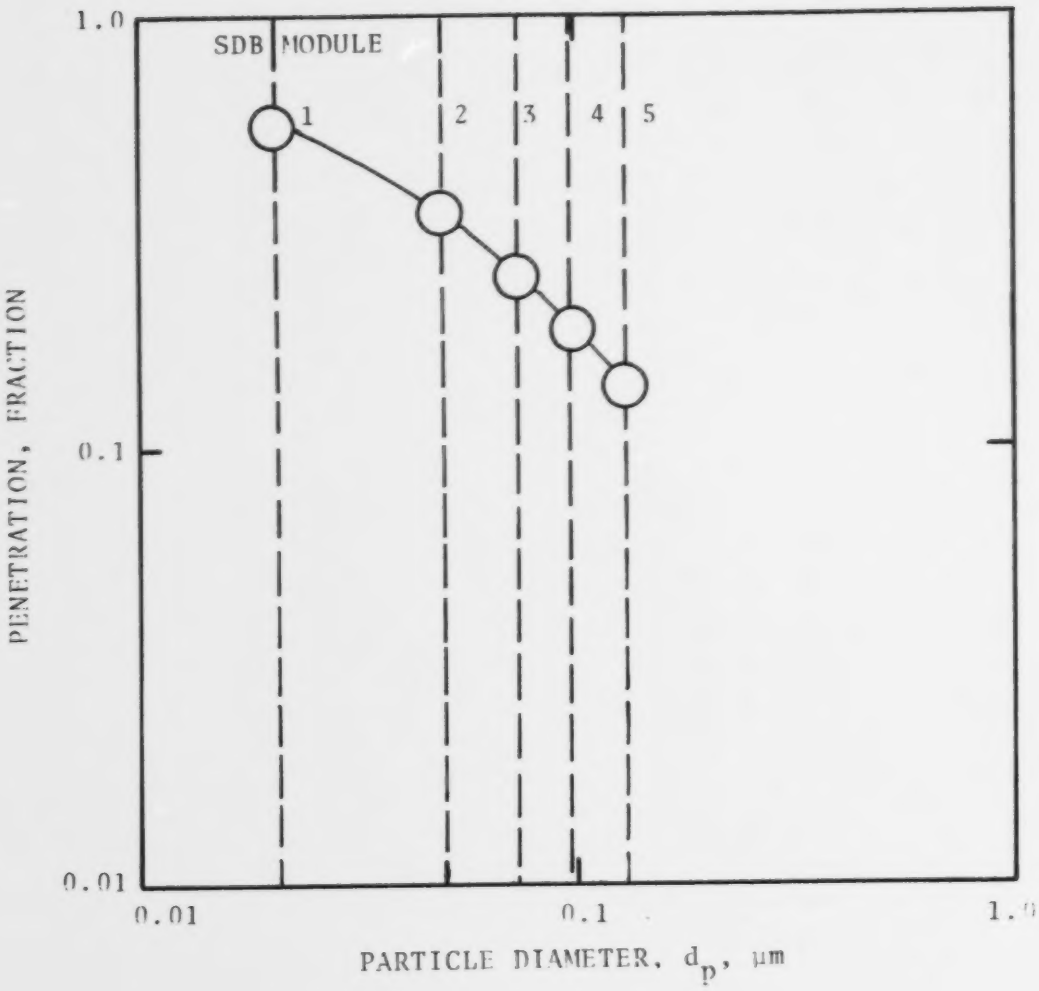

Figure 36. Particle penetration through SDB at Q = 4.7 ℓ/min.

conversion is a graphical integration of the following equation:

$$M_{pi} = \frac{N_{pt}}{100} \int_{o}^{N_{pi}} \frac{dm_p}{dN_p} \, d\left(\frac{N_p \times 100}{N_{pt}}\right) \qquad (44)$$

where N_p = cumulative number concentration of particles smaller than "d_p", no./cm^3

N_{pt} = total number concentration of particles, no./cm^3

d_p = particle diameter, μm

d_{pi} = a specific particle diameter, μm

m_p = mass of particles in the infinitesimal size range ($\bar{d}_p + \bar{d}dp$), g

M_{pi} = cumulative mass concentration of particles smaller than "d_{pi}", g/cm^3

The quantity ($\bar{d}m_p/\bar{d}N_p$) is simply the mass per particle of diameter "d_p". The quantity ($N_p \times 100/N_{pt}$) is the number percent of particles smaller than "d_p". Thus, equation (44) can be evaluated from a plot of mass per particle versus cumulative number percent of particles, both quantities being evaluated at the same particle diameter to provide a point on the plot. The total and cumulative number concentration data are obtained as described previously.

CUT/POWER RELATIONSHIP

When scrubbers are operated at different pressure drops, it is very difficult to evaluate and to compare their performance based only on grade penetration curves. Calvert (1974) has developed a useful correlation called the cut/power relationship for this purpose. The cut/power relationship is a plot of the cut diameter given by the scrubber against pressure drop or power input, as illustrated in Figure 37. Cut diameter is the particle diameter whose collection efficiency is 50%. The solid lines in this graph were calculated theoretically from the design equations presented in the "Scrubber Handbook" and Calvert (1974).

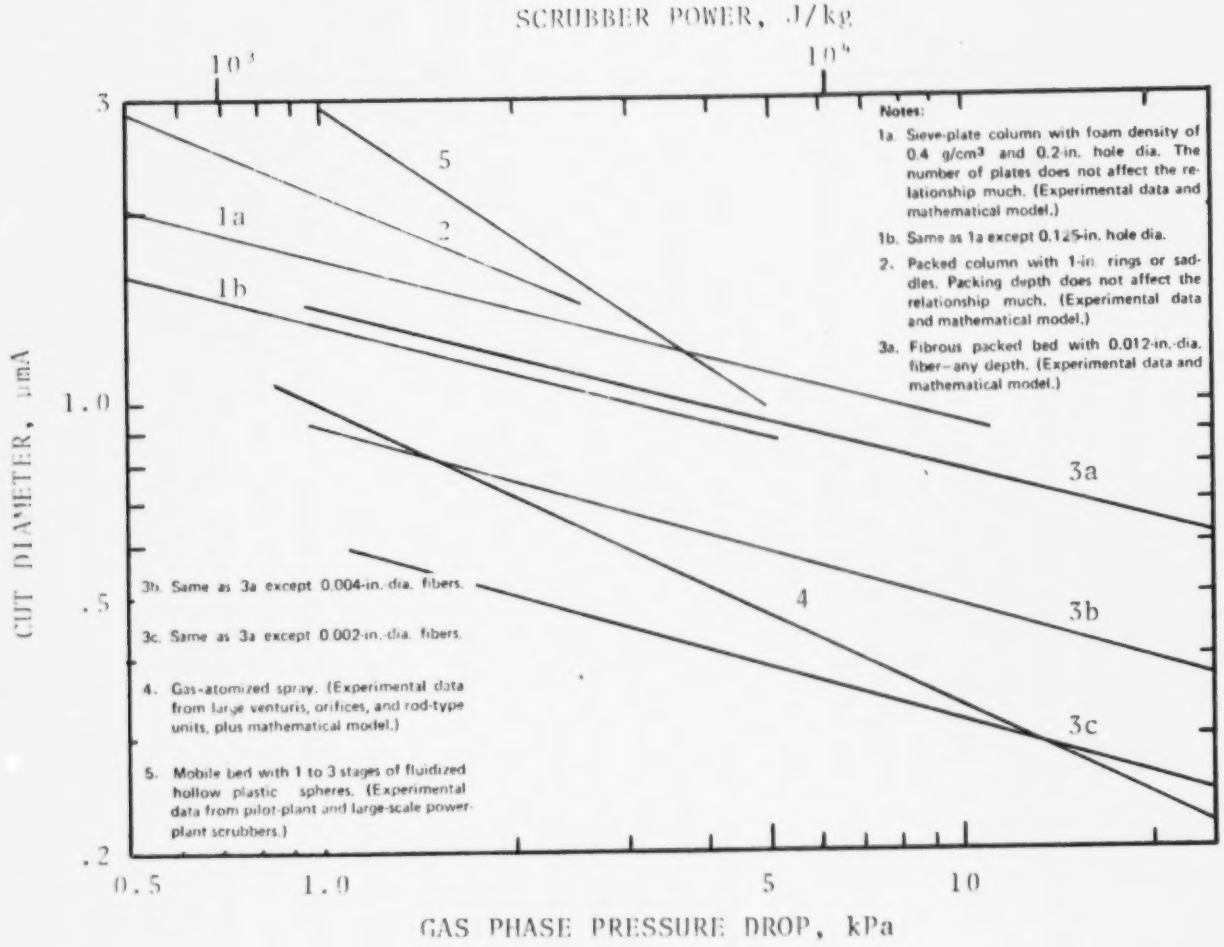
SCRUBBER POWER, J/kg
10^3
10^4
3
1.0
.5
.2
CUT DIAMETER, μmA
0.5
1.0
5
10
GAS PHASE PRESSURE DROP, kPa
1a
1b
2
3a
3b
3c
4
5
Notes:
1a. Sieve-plate column with foam density of 0.4 g/cm³ and 0.2-in. hole dia. The number of plates does not affect the relationship much. (Experimental data and mathematical model.)
1b. Same as 1a except 0.125-in. hole dia.
2. Packed column with 1-in. rings or saddles. Packing depth does not affect the relationship much. (Experimental data and mathematical model.)
3a. Fibrous packed bed with 0.012-in.-dia. fiber—any depth. (Experimental data and mathematical model.)
3b. Same as 3a except 0.004-in.-dia. fibers.
3c. Same as 3a except 0.002-in.-dia. fibers.
4. Gas-atomized spray. (Experimental data from large venturis, orifices, and rod-type units, plus mathematical model.)
5. Mobile bed with 1 to 3 stages of fluidized hollow plastic spheres. (Experimental data from pilot-plant and large-scale power-plant scrubbers.)

Figure 37. A.P.T. cut/power plot.

The cut/power relationship has many useful applications. It may be used to compare and evaluate scrubbers, to make preliminary scrubber selections, or to estimate the minimum pressure drop of a scrubber to attain a required performance level.

Equivalent Cut Diameter

For purposes of comparison it is valuable to have a single parameter which describes the efficiency of a scrubber. The cut diameter has proven to be useful for most scrubbers.

Cut diameter is the particle diameter whose collection efficiency (or penetration) is 50%. It may be read directly from the grade penetration curve.

In cases where the penetration curve does not reach 50%, the cut diameter cannot be determined directly from the curve, but an equivalent cut diameter may be determined. The equivalent cut diameter is the particle diameter which would be required to give the same overall penetration (i.e., over the entire particle size distribution) if the scrubber had the same penetration versus pressure drop characteristics as a venturi scrubber. An alternative is to use the equivalent pressure drop that a venturi would need as a criterion for comparison.

The theoretical cut diameter for venturi-type scrubbers can be calculated using Figure 38. For example, if $\sigma_g = 2.2$ and the overall penetration is 0.087, then using Figure 38, the ratio of cut to mass median diameters is approximately 0.31. For $d_{pg} = 0.95$ μmA and using the above ratio of cut to mass median diameter the theoretical aerodynamic cut size, "d_{pac}" is 0.29. The cut diameter computed by this method is that which would be provided by a conventional high energy (venturi type) scrubber which would give overall penetration equivalent to the subject scrubber.

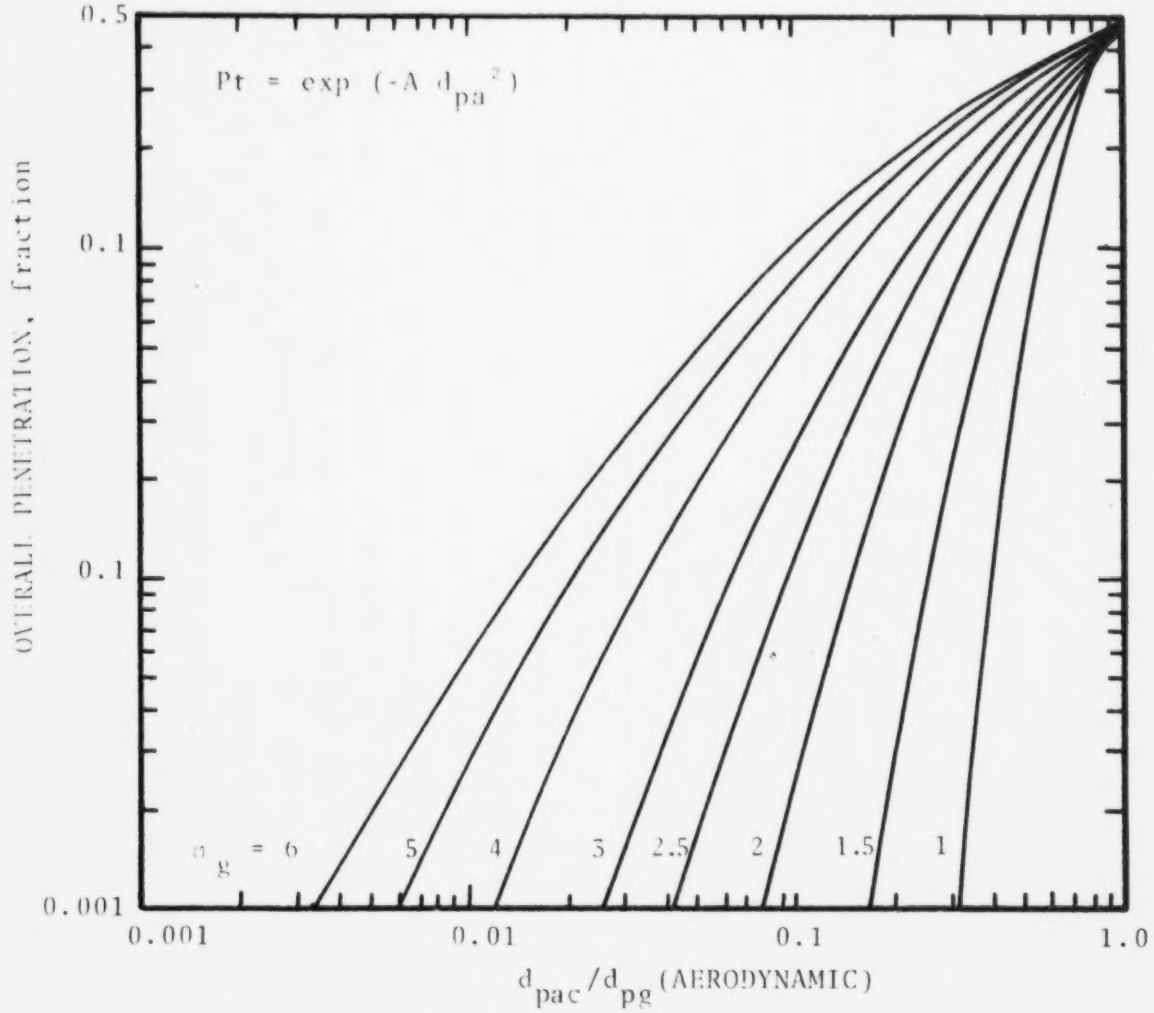

Figure 38. Overall penetration vs. cut to mass mean particle diameter ratio for log-normally distributed particles. (Calvert et al (1972).

SECTION 9
EFFECTS OF CHARGED PARTICLES ON THE EXPERIMENTAL PERFORMANCE OF ELECTROSTATIC CONTROL DEVICES

Recent experiments performed at A.P.T. have shown that cascade impactors may not give accurate size distribution information when measuring charged particles, Patterson et al. (1977). Figure 39 shows that the impaction parameter, K_p, for a given stage of the U. of W. impactor will decrease with charged particles. Using the value of "K_{p50}" determined for uncharged particles will overestimate the size of particles collected.

A more important effect with charged particles which can be seen from Figure 39 is that the collection efficiency does not go to zero for low values of the impaction parameter, but may become constant at 10 to 20%. Therefore, some of the particles which should be collected on the lower stages will be collected on the upper stages. This leads to further overestimation of individual particle size.

The mass distribution will likewise be overestimated such that the larger size fractions will appear to have more mass than is actually there. This can lead to discrepencies between theoretical and experimental performance of control devices. The effect is most noticeable when the inlet dust is electrically neutral and the outlet particles are charged. This situation existed during certain performance test runs on the APS Electrostatic Scrubber and Electro-Tube and the TRW Charged Droplet Scrubber.

The effect of using cascade impactor calibrations based on uncharged particles for determining the performance

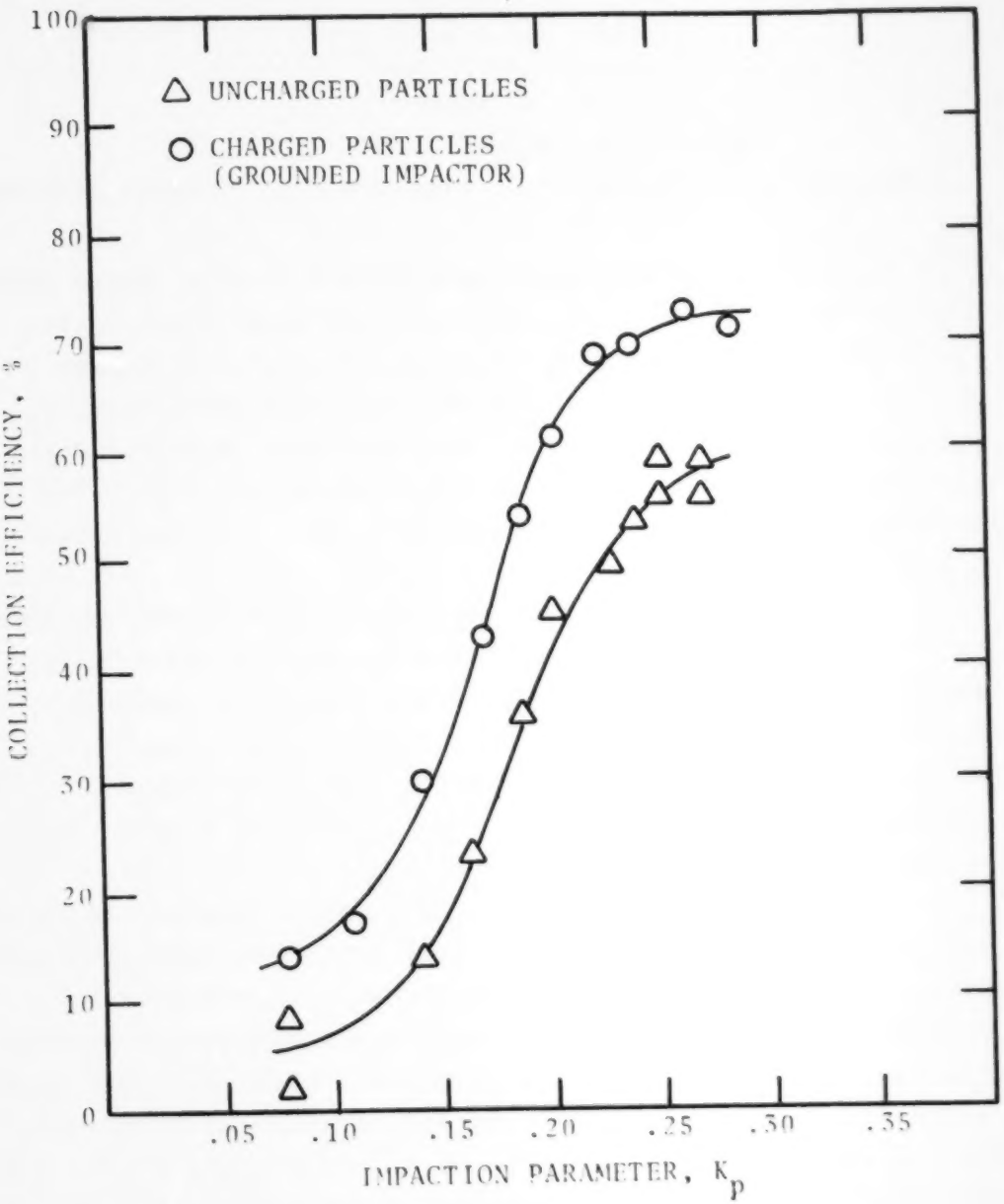

Figure 39. Impaction characteristics with glass fiber filter (0.5 μm PSL).

characteristics of an electrostatic control device was determined with the ESP model of Gooch and Francis (1975). The calculation procedure was as follows:

1. The inlet size distribution was assumed to comprise uncharged particles with a $d_{pg\ IN}$ = 10 μmA and σ_g = 4.0.

2. An outlet size distribution is computed from the theoretical curve shown in Figure 41.

3. The outlet size distribution is converted from that for uncharged particles, curve a, Figure 40 to the recovered size distribution from a cascade impactor assuming charged particles, curve b, Figure 40.

4. The collection efficiency is determined as a function of the particle size using the assumed inlet size distribution and the recovered size distribution as calculated in number 3 above.

Figure 41 shows the theoretical collection efficiency for an electrostatic precipitator, the results of these calculations and some experimental performance data. Therefore the underestimation of the collection efficiency for particles greater than several microns in diameter and the overestimation of the collection efficiency of submicron particles may be the result of inaccurate size distribution determinations of charged particles with cascade impactors.

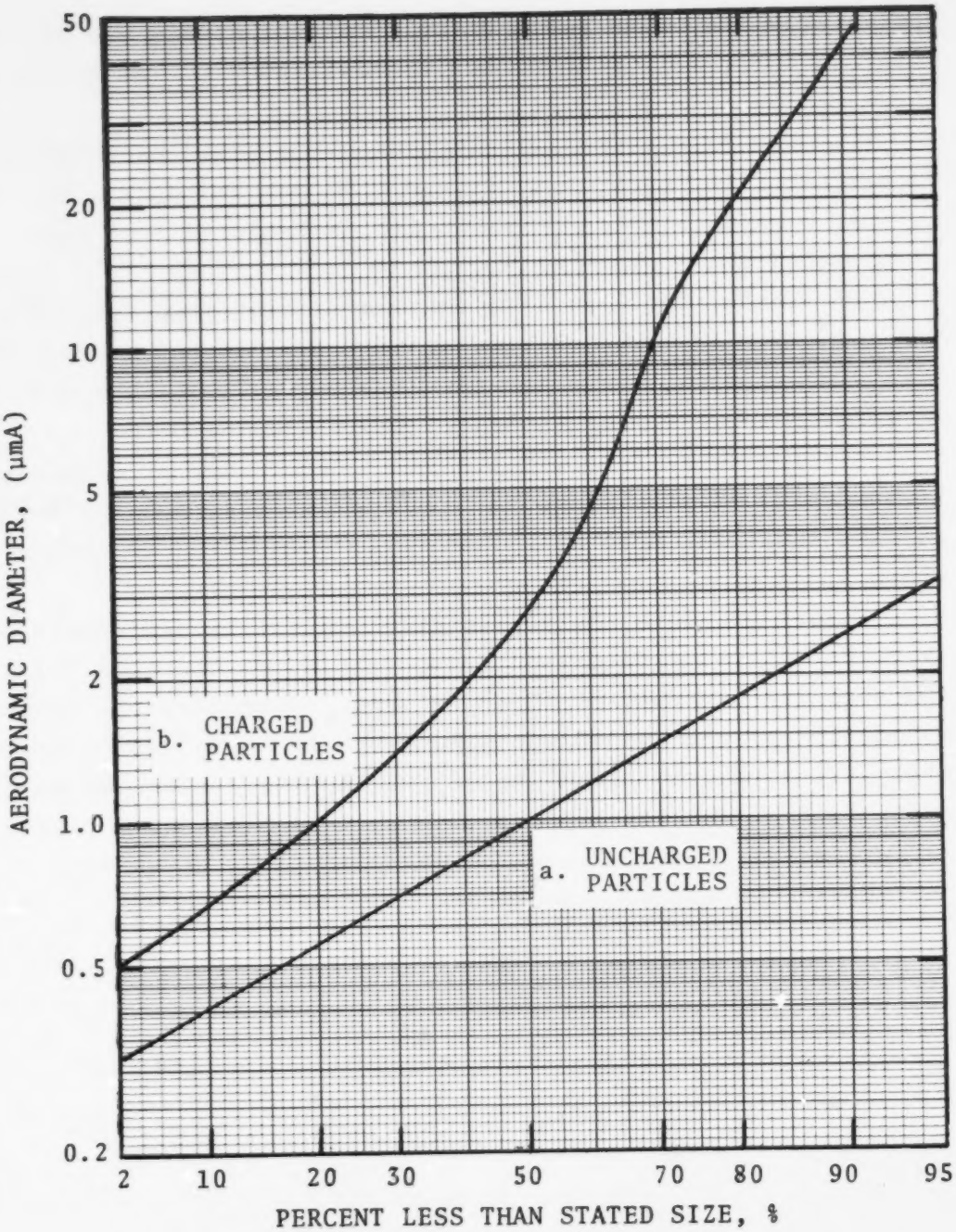

Figure 40. Size distribution of particles exiting ESP when $d_{pg_{IN}}$ = 10 μmA, σ_g = 4.0

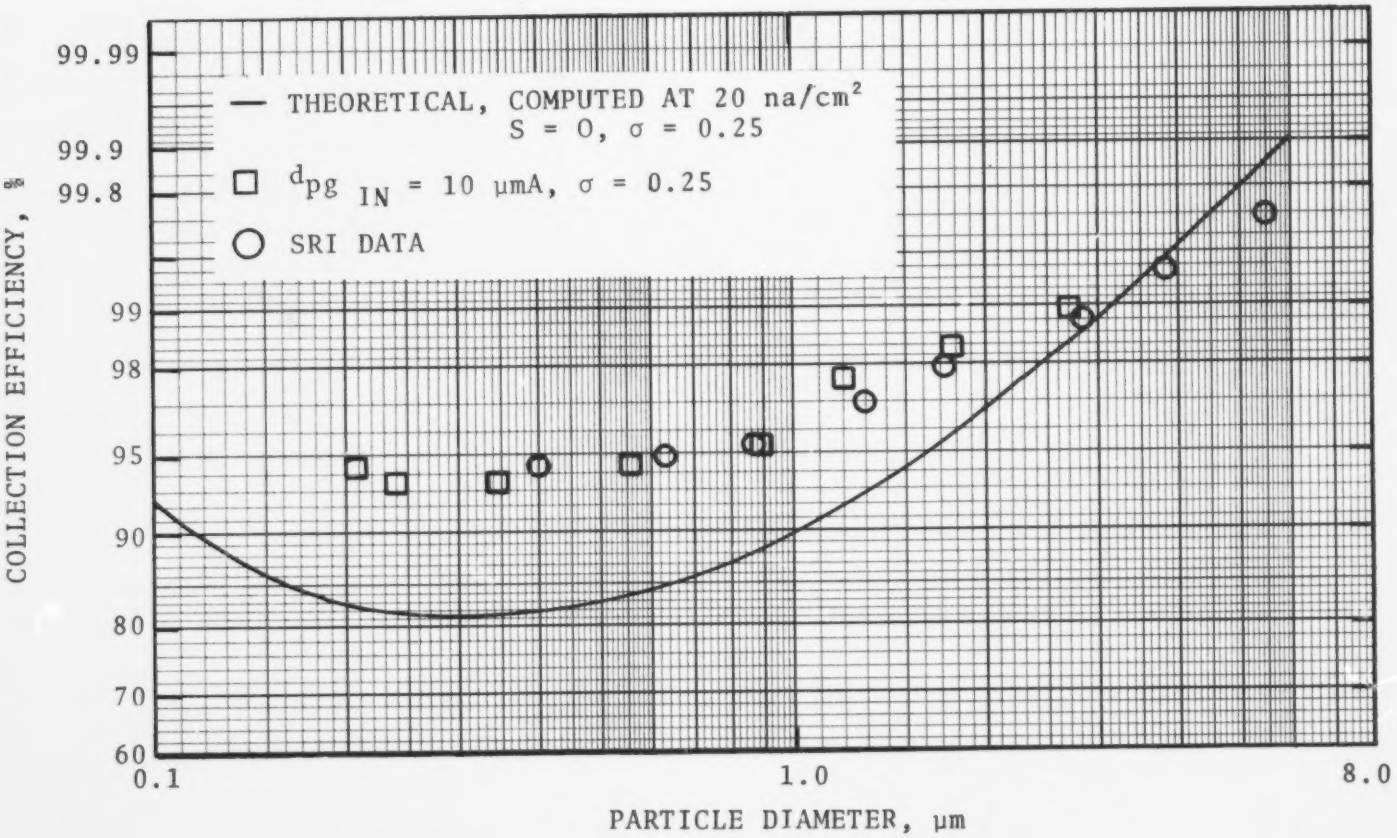

Figure 41. Fractional collection efficiencies for a full-scale precipitator on a coal-fired power boiler. (Gooch et al. (1975))

REFERENCES

Calvert, S., Chapter 46 in "Air Pollution", Stern, A.C. (ed). Third Edition, Academic Press, NY, 1968.

Calvert, S., J. Goldshmid, D. Leith, and D. Metha "Scrubber Handbook" NTIS PB 213-016, 1972.

Calvert, S., J. Goldshmid, D. Leith, and N. Jhaveri, "Feasibility of Flux Force/Condensation Scrubbing for Fine Particulate Collection NTIS PB 227-307, October 1973.

Calvert, S. "Engineering Design of Fine Particle Scrubbers", J. of APCA. 24: 929, 1974.

Calvert, S., J. Rowan, and C. Lake "Johns-Manville CHEAF Evaluation" NTIS PB 256-311, July 1975.

Calvert, S., J. Rowan, S. Yung, C. Lake, and H. Barbarika "APS Electrostatic Scrubber Evaluation" EPA-600/2-76-154a, 1976a.

Calvert, S., C. Christensen, and C. Lake "APS Electro-Tube Evaluation" PB 258-824, 1976b.

Calvert, S., C. Lake, and R. Parker "Cascade Impactor Calibration Guidelines" EPA-600/2-76-118, 1976c.

Calvert, S. and R.G. Patterson "Submicron Particle Size Measurement Particle Size Measurement with a Screen Diffusion Battery", Final Report, EPRI Contract RP 723-1-760205, 1977.

Fegley, M.J., D.S. Ensor, and L.E. Sparks "The Propagation of Errors in Particle Size Distribution Measurements Performed Using Cascade Impactors" Paper 75-32.5 presented at the 68th Annual Meeting of APCA, Boston, MA, June 15-20, 1975.

Harris, D.B. "Procedures for Cascade Impactor Calibration and Operation in Process Streams" EPA 600/2-77-004, January 1977.

Gooch, J.P. and N.L. Francis "A Theoretically Based Mathematical Model for Calculation of Electrostatic Precipitator Performance", J. of APCA. 25: 108-113, 1975.

Lear, C.W., W.F. Krieve, and E. Cohen, "Charged Droplet Scrubbing for Fine Particle Control," J. of APCA. 25: 184-189, 1975.

Lipson, C. and N.J. Sheth "Statistical Design and Analysis of Engineering Experiments", McGraw-Hill, 1973.

Lundgren, D.A. "An Aerosol Sampler for Determination of Particle Concentration as a Function of Size and Time", J. of APCA, 17: 225, 1967.

Oglesby, S. and G. Nichols "A Manual of Electrostatic Precipitator Technology, Part I. Fundamentals" NTIS BP 196-380, 1970.

Patterson, R.G., P. Riersgard, and S. Calvert "The Effects of Charged Particles on Cascade Impactor Calibrations", paper presented at the 70th. Annual Meeting of the APCA, Toronto, June 1977.

Rao, A.K. "Sampling and Analysis of Atmospheric Aerosols", Particle Technology Laboratory, Mechanical Technology Laboratory, University of Minnesota. Publication 269, 1975.

Rei, M.T. and D.W. Cooper "Laboratory Evaluation of the Cleanable High Efficiency Air Filter (CHEAF)", EPA 600/2-76-202, 1976.

Sinclair, D. "A Portable Diffusion Battery" American Ind. Hygiene Assoc. Journal 33: 729-735, 1972.

Smith, W.B., K.W. Cushing, and J.D. McCain "Particle Sizing Techniques for Control Device Evaluations" EPA 650/2-74-102, NTIS PB 240670/AS, October 1974.

Sparks, L.E. Personal Communication, 1971.

APPENDIX A

CASCADE IMPACTOR DATA AND SIZE DISTRIBUTION PLOTS FOR TRW CHARGED DROPLET SCRUBBER

Table A-1. INLET AND OUTLET SAMPLE PARTICLE DATA FOR RUN #1

IMPACTOR STAGE NUMBER	INLET		OUTLET	
	M_{cum} (mg/DNm³)	d_{pc} (μmA)	M_{cum} (mg/DNm³)	d_{pc} (μmA)
Precutter & Nozzle	232	---	35.8	---
1	232	27.3	35.8	23.8
2	232	12.0	35.0	10.4
3	232	5.7	34.7	4.0
4	230	2.3	34.0	2.0
5	180	1.3	33.2	1.2
6	99.8	0.74	27.0	0.64
7	50.8	0.45	20.2	0.37
Filter	42.9	---	15.9	---
Sample Volume (DNm³)	0.134		0.585	

Table A-2. INLET AND OUTLET SAMPLE PARTICLE DATA FOR RUN #4

IMPACTOR STAGE NUMBER	INLET		OUTLET	
	M_{cum} (mg/DNm³)	d_{pc} (μmA)	M_{cum} (mg/DNm³)	d_{pc} (μmA)
Precutter & Nozzle	163	---	61.0	---
1	159	27.4	61.0	23.6
2	159	12.0	60.8	10.3
3	159	4.6	60.6	4.0
4	158	2.3	59.8	2.0
5	157	1.3	58.9	1.2
6	120	0.74	45.4	0.64
7	65.8	0.45	22.9	0.37
Filter	28.9	---	17.2	---
Sample Volume (DNm³)	0.087		0.475	

Table A-3. INLET AND OUTLET SAMPLE PARTICLE DATA FOR RUN #6

IMPACTOR STAGE NUMBER	INLET		OUTLET	
	M_{cum} (mg/DNm³)	d_{pc} (μmA)	M_{cum} (mg/DNm³)	d_{pc} (μmA)
Precutter & Nozzle	188	---	11.6	---
1	187	25.6	10.8	24.3
2	186	11.2	10.6	10.6
3	186	5.3	10.6	4.1
4	186	2.2	10.6	2.1
5	177	1.3	10.0	1.2
6	132	0.69	7.2	0.66
7	67.0	0.42	2.8	0.38
Filter	26.4	---	1.0	---
Sample Volume (DNm³)	0.099		0.602	

Table A-4. INLET AND OUTLET SAMPLE PARTICLE DATA FOR RUN #8

IMPACTOR STAGE NUMBER	INLET		OUTLET	
	M_{cum} (mg/DNm³)	d_{pc} (μmA)	M_{cum} (mg/DNm³)	d_{pc} (μmA)
Precutter & Nozzle	247	---	29.2	---
1	247	21.6	27.5	26.0
2	246	9.5	26.0	11.4
3	245	4.5	25.3	4.4
4	245	1.8	25.3	2.2
5	238	1.1	25.3	1.3
6	194	0.58	24.9	0.70
7	134	0.35	21.0	0.41
Filter	59.0	---	14.2	---
Sample Volume (DNm³)	0.134		0.466	

Table A-5. INLET AND OUTLET SAMPLE PARTICLE DATA FOR RUN #9

IMPACTOR STAGE NUMBER	INLET		OUTLET	
	M_{cum} (mg/DNm³)	d_{pc} (μmA)	M_{cum} (mg/DNm³)	d_{pc} (μmA)
Precutter & Nozzle	132	---	41.5	---
1	119	24.5	41.3	26.6
2	113	10.7	40.6	11.6
3	113	4.2	40.6	4.5
4	113	2.1	40.6	2.3
5	113	1.2	40.6	1.3
6	113	0.66	39.5	0.72
7	95.4	0.40	23.0	0.41
Filter	65.21	---	13.9	---
Sample Volume (DNm³)	0.106		0.438	

Table A-6. INLET AND OUTLET SAMPLE PARTICLE DATA FOR RUN #10

IMPACTOR STAGE NUMBER	INLET PRIME		INLET		OUTLET	
	M_{cum} (mg/DNm³)	d_{pc} (μmA)	M_{cum} (mg/DNm³)	d_{pc} (μmA)	M_{cum} (mg/DNm³)	d_{pc} (μmA)
Precutter & Nozzle	244	---	166	---	84.5	---
1	244	32.1	107	24.7	84.5	26.0
2	244	14.0	105	10.8	83.6	11.4
3	244	5.4	103	5.1	82.8	4.4
4	244	2.7	100	2.1	81.6	2.2
5	244	1.6	100	1.2	76.5	1.3
6	224	0.87	54.7	0.67	48.8	0.70
7	137	0.52	29.6	0.40	22.4	0.40
Filter	57.6	---	27.4	---	16.2	---
Sample Volume (DNm³)	0.045		0.044		0.353	

Table A-7. INLET AND OUTLET SAMPLE PARTICLE DATA FOR RUN #13

IMPACTOR STAGE NUMBER	INLET PRIME		INLET		OUTLET	
	M_{cum} (mg/DNm³)	d_{pc} (μmA)	M_{cum} (mg/DNm³)	d_{pc} (μmA)	M_{cum} (mg/DNm³)	d_{pc} (μmA)
Precutter & Nozzle	1789	---	953	---	56.6	---
1	1678	26.9	945	26.6	54.8	23.2
2	1651	11.8	938	11.7	53.7	10.2
3	1636	4.6	935	4.5	52.0	3.9
4	1569	2.3	923	2.3	50.2	2.0
5	1247	1.3	857	1.3	44.1	1.1
6	477	0.73	644	0.72	29.0	0.63
7	108	0.44	233	0.42	12.5	0.36
Filter	27.7	---	113	---	2.5	---
Sample Volume (DNm³)	0.115		0.088		0.279	

Table A-8. INLET AND OUTLET SAMPLE PARTICLE DATA FOR RUN #14

IMPACTOR STAGE NUMBER	INLET		OUTLET	
	M_{cum} (mg/DNm³)	d_{pc} (μmA)	M_{cum} (mg/DNm³)	d_{pc} (μmA)
Precutter & Nozzle	201	---	23.1	---
1	168	11.1	23.1	17.3
2	156	4.6	22.1	7.6
3	146	2.6	21.0	2.9
4	138	1.4	19.5	1.5
5	126	0.88	16.2	0.85
6	90.8	0.48	10.5	0.47
7	41.4	0.28	4.4	0.27
Filter	5.9	---	1.0	---
Sample Volume (DNm³)	0.051		0.771	

Table A-9. INLET AND OUTLET SAMPLE PARTICLE DATA FOR RUN #15

IMPACTOR STAGE NUMBER	INLET		OUTLET	
	M_{cum} (mg/DNm³)	d_{pc} (μmA)	M_{cum} (mg/DNm³)	d_{pc} (μmA)
Precutter & Nozzle	419	---	35.5	---
1	410	8.4	35.2	18.8
2	399	4.2	33.5	8.2
3	382	2.4	31.4	3.2
4	360	1.3	27.2	1.6
5	195	0.81	21.6	0.92
6	84.5	0.45	12.3	0.51
7	36.8	0.26	4.9	0.29
Filter	7.4	---	1.8	---
Sample Volume (DNm³)	0.054		0.554	

Table A-10. INLET AND OUTLET SAMPLE PARTICLE DATA FOR RUN #16

IMPACTOR STAGE NUMBER	INLET		OUTLET	
	M_{cum} (mg/DNm³)	d_{pc} (μmA)	M_{cum} (mg/DNm³)	d_{pc} (μmA)
Precutter & Nozzle	182	---	22.2	---
1	177	10.1	22.2	18.0
2	174	4.2	21.8	7.9
3	168	2.4	21.2	3.1
4	163	1.3	20.0	1.5
5	149	0.80	17.6	0.89
6	108	0.44	12.9	0.49
7	58.0	0.25	7.4	0.28
Filter	5.5	---	1.4	---
Sample Volume (DNm³)	0.036		0.933	

Table A-11. INLET AND OUTLET SAMPLE PARTICLE DATA FOR RUN #17

IMPACTOR STAGE NUMBER	INLET		OUTLET	
	M_{cum} (mg/DNm³)	d_{pc} (μmA)	M_{cum} (mg/DNm³)	d_{pc} (μmA)
Precutter & Nozzle	508	---	23.1	---
1	476	9.4	23.0	18.6
2	467	4.8	22.2	8.1
3	456	2.7	21.1	3.2
4	433	1.5	19.1	1.6
5	214	0.90	15.9	0.91
6	119	0.50	10.3	0.50
7	50.2	0.29	4.1	0.29
Filter	9.3	---	1.4	---
Sample Volume (DNm³)	0.054		0.876	

Table A-12. INLET AND OUTLET SAMPLE PARTICLE DATA FOR RUN #18

IMPACTOR STAGE NUMBER	INLET		OUTLET	
	M_{cum} (mg/DNm³)	d_{pc} (μmA)	M_{cum} (mg/DNm³)	d_{pc} (μmA)
Precutter & Nozzle	168	---	21.8	---
1	129	11.3	21.8	19.2
2	126	4.7	21.0	8.4
3	121	2.7	19.8	3.2
4	116	1.5	17.5	1.6
5	111	0.89	14.3	0.94
6	103	0.49	9.8	0.52
7	78.4	0.28	5.2	0.30
Filter	24.5	---	1.1	---
Sample Volume (DNm³)	0.061		0.943	

Table A-13. INLET AND OUTLET SAMPLE PARTICLE DATA FOR RUN #19

IMPACTOR STAGE NUMBER	INLET		OUTLET	
	M_{cum} (mg/DNm^3)	d_{pc} (μmA)	M_{cum} (mg/DNm^3)	d_{pc} (μmA)
Precutter & Nozzle	217	---	25.5	---
1	170	8.7	25.5	19.5
2	166	4.4	24.6	8.5
3	160	2.5	23.7	3.3
4	151	1.4	21.9	1.7
5	135	0.83	19.0	0.96
6	77.5	0.46	13.3	0.53
7	50.3	0.27	6.3	0.30
Filter	15.0	---	2.1	---
Sample Volume (DNm^3)	0.074		0.663	

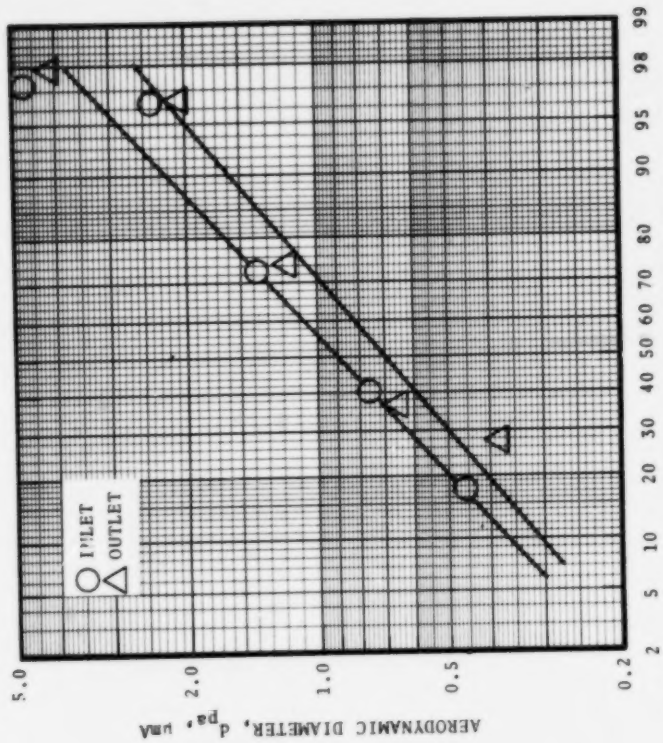

Figure A-2. Inlet and outlet size distribution for run 4.

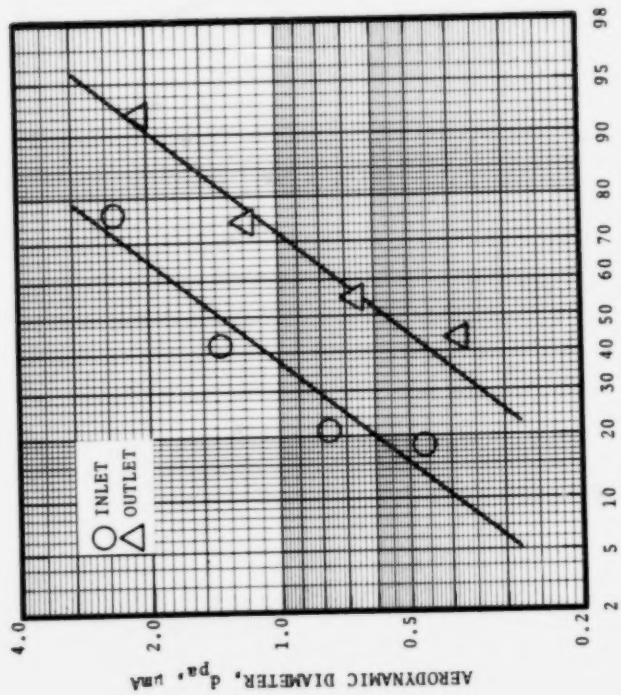

Figure A-1. Inlet and outlet size distribution for run 1.

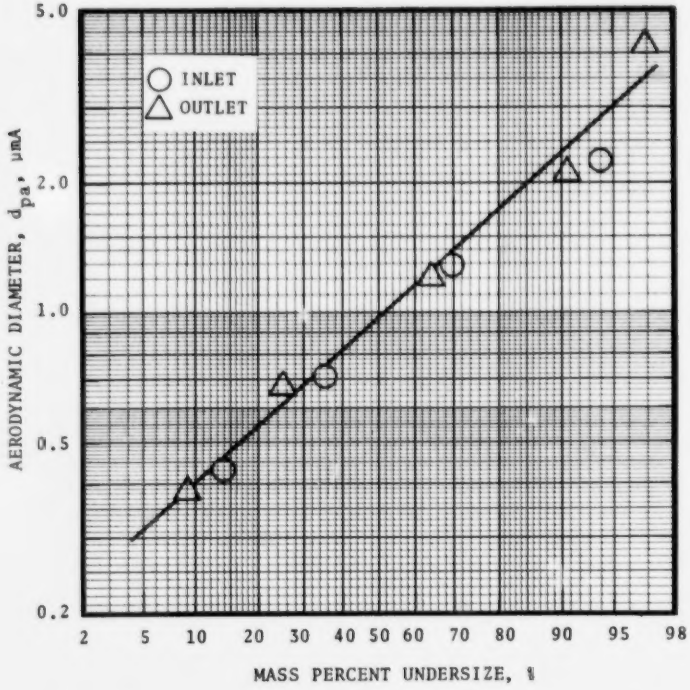

Figure A-3. Inlet and outlet size distribution for run 6.

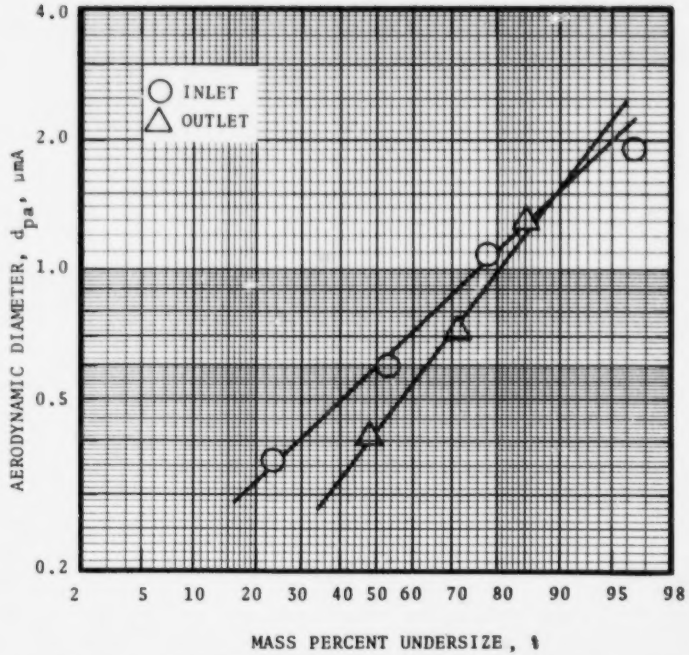

Figure A-4. Inlet and outlet size distribution for run 8.

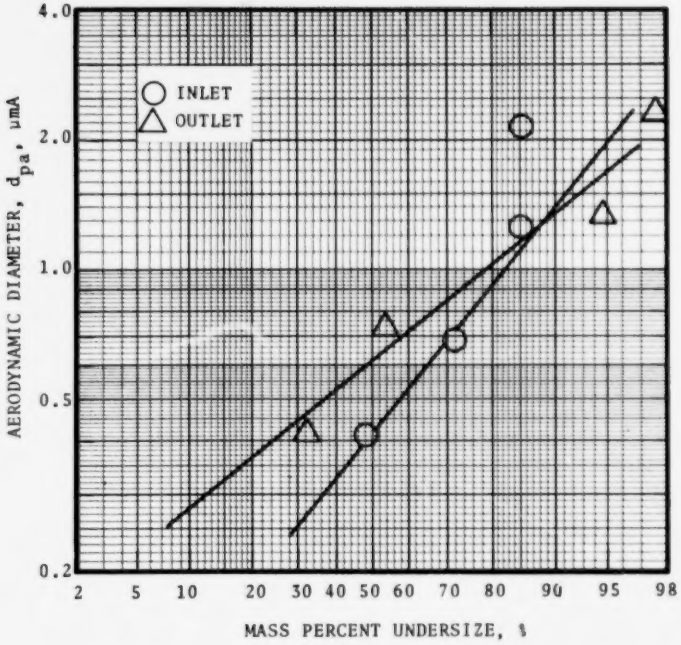

Figure A-5. Inlet and outlet size distribution for run 9.

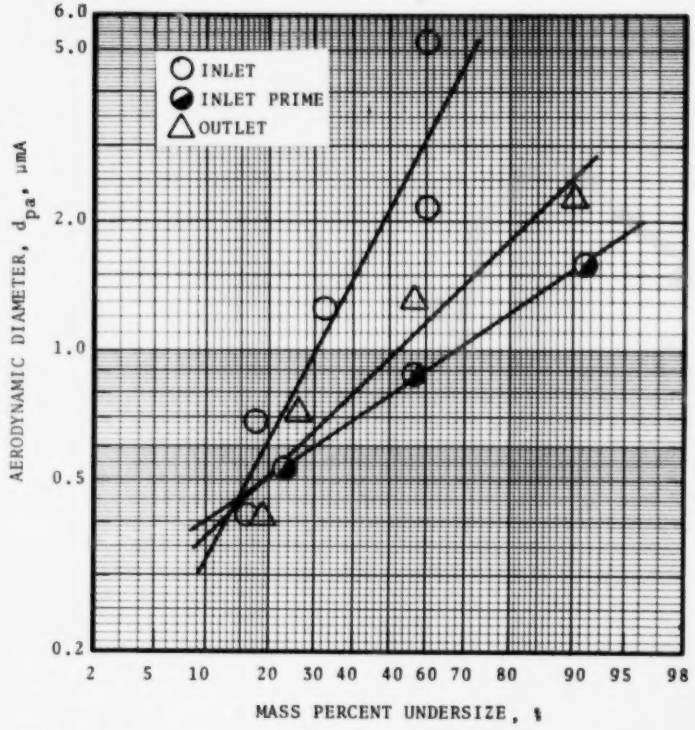

Figure A-6. Inlet and outlet size distribution for run 10.

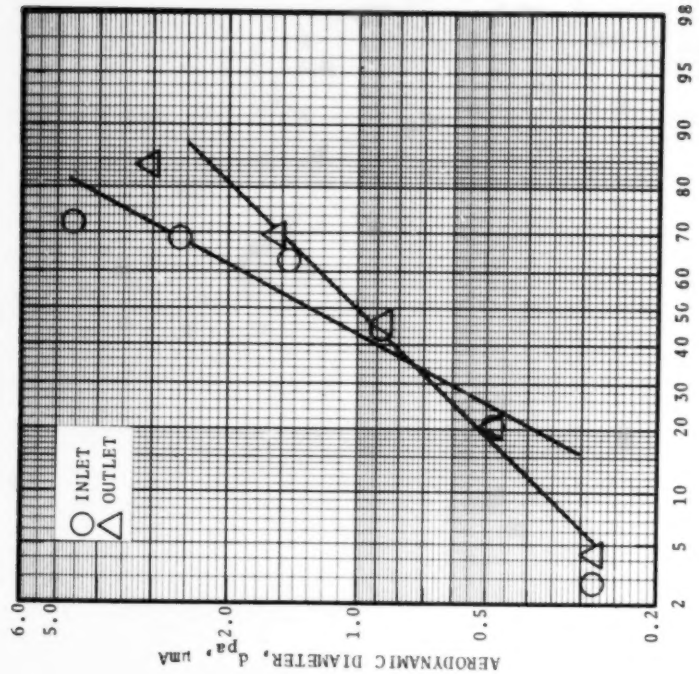

Figure A-8. Inlet and outlet size distribution for run 14.

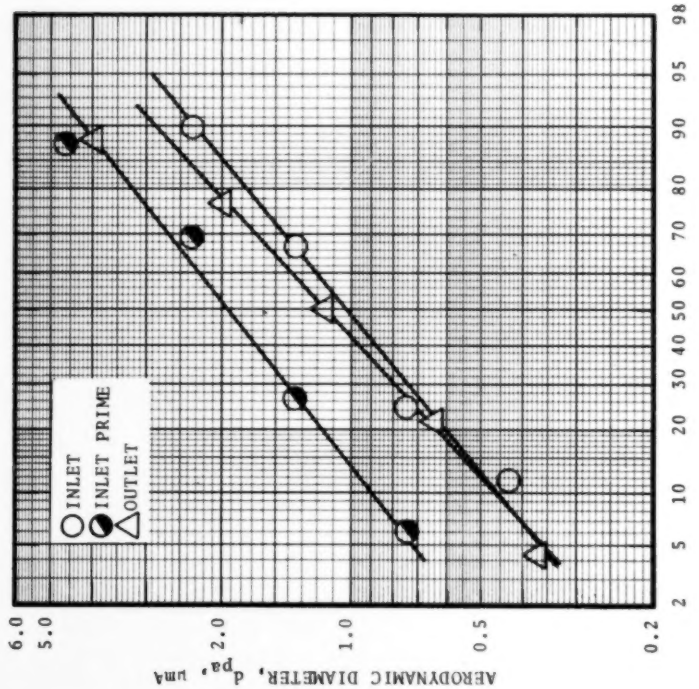

Figure A-7. Inlet and outlet size distribution for run 13.

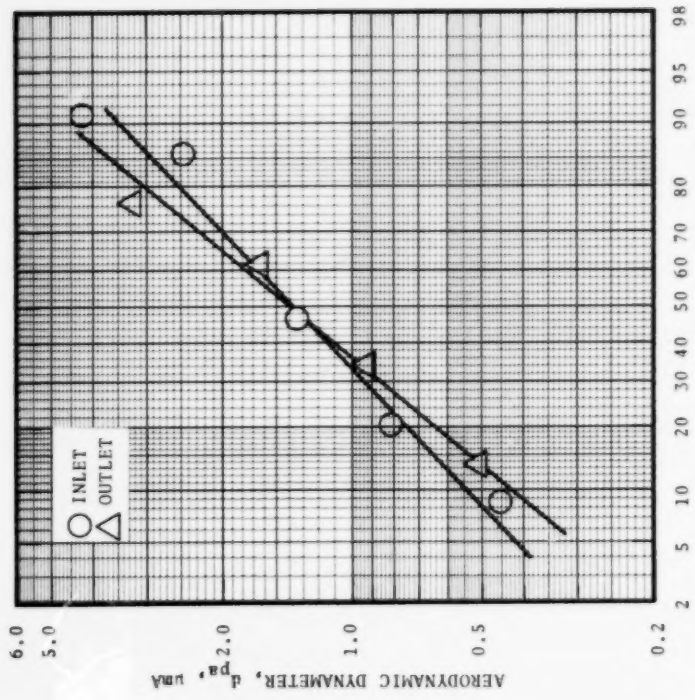

Figure A-9. Inlet and outlet size distribution for run 15.

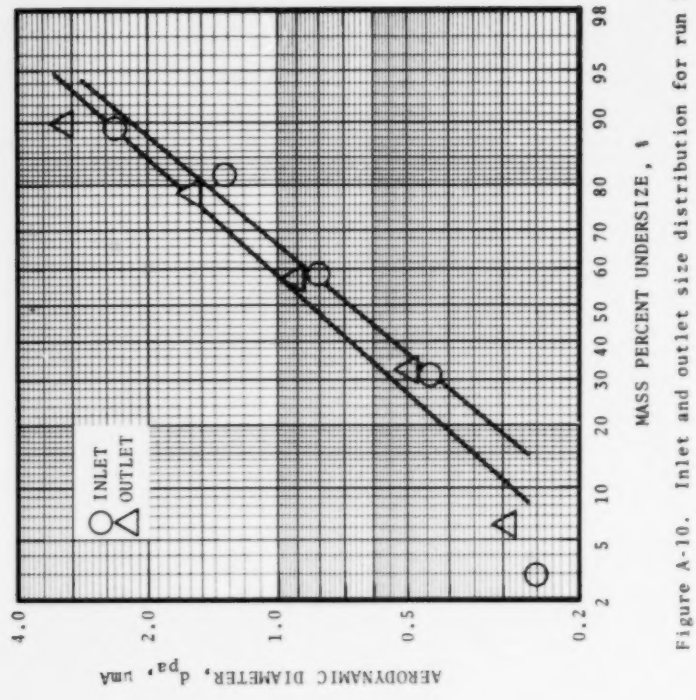

Figure A-10. Inlet and outlet size distribution for run 16.

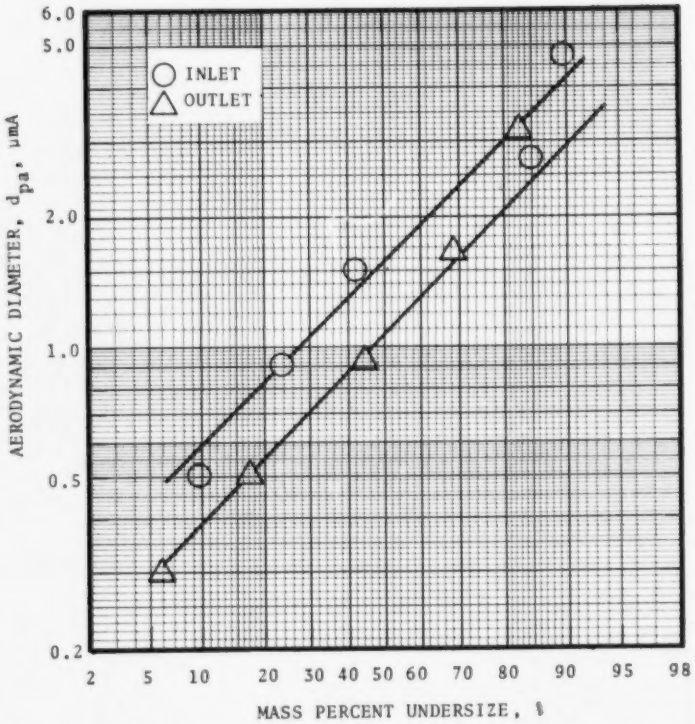

Figure A-11. Inlet and outlet size distribution for run 17.

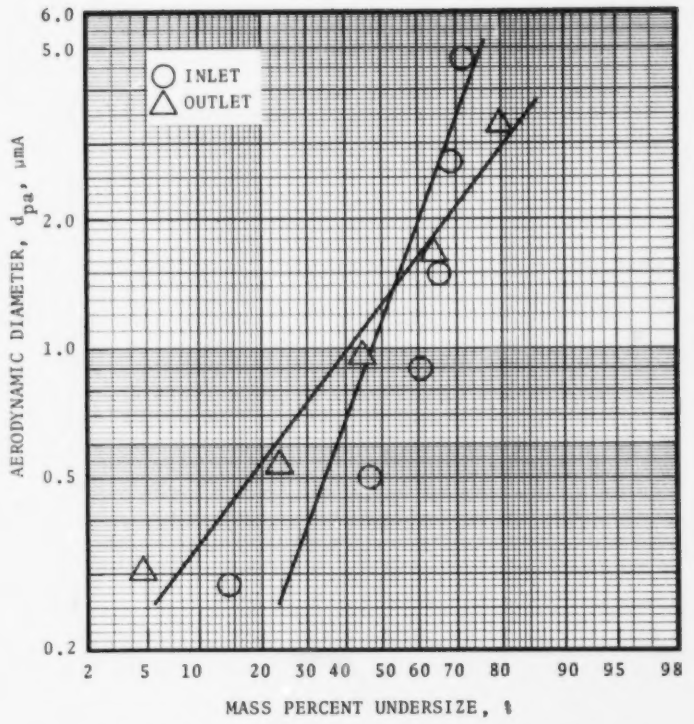

Figure A-12. Inlet and outlet size distribution for run 18.

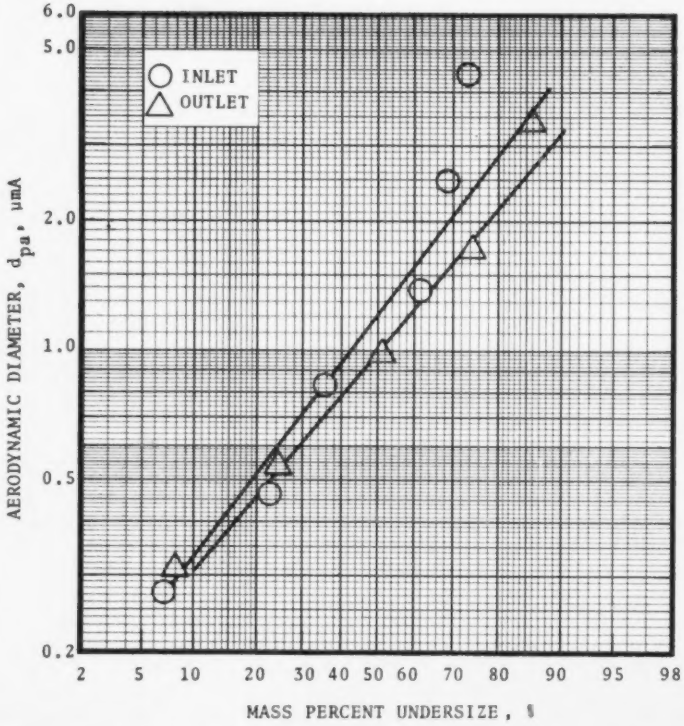

Figure A-13. Inlet and outlet size distribution for run 19.

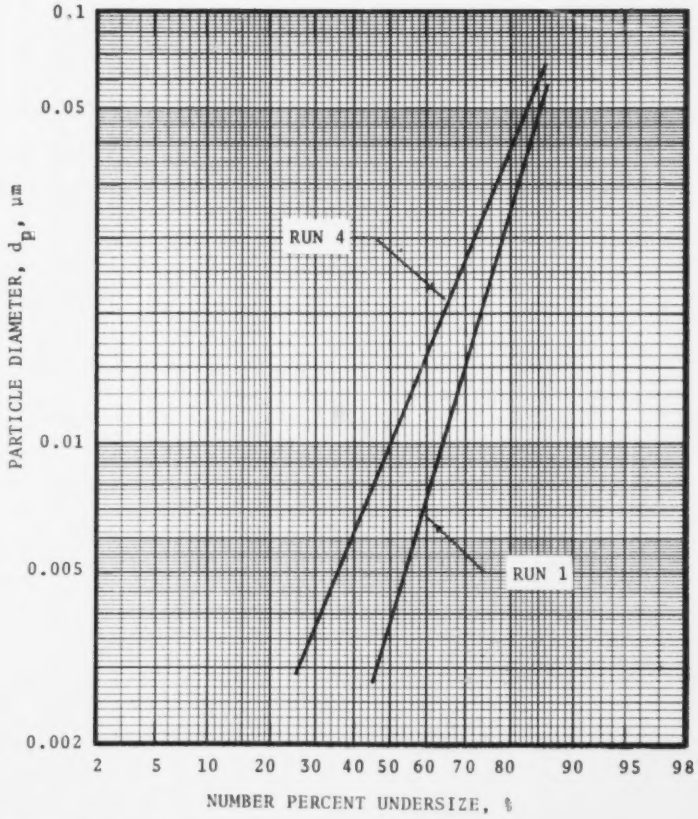

Figure A-14. Diffusion battery data for inlet run 1 & 4.